STUDENT LAUNCH COMPETITION
2021-2022

CAL POLY POMONA
Preliminary Design

November 1, 2021

California State Polytechnic University, Pomona
3801 W Temple Ave, Pomona, CA 91768
Department of Aerospace Engineering

Table of Contents

List of Acronyms

AoA = Angle of Attack

AGL = Above Ground Level

AIAA = American Institute of Aeronautics and Astronautics

APCP = Ammonium Perchlorate Composite Propellant

AR = As Required

CAR = Canadian Association of Rocketry

CDC = Center for Disease Control and Prevention

CDR = Conceptual Design Review

CNC = Computer Numerical Control

CPP = Cal Poly Pomona

FAA = Federal Aviation Administration

FAR = Friends of Amateur Rocketry

FN = Foreign National

FRR = Flight Readiness Review

GPA = Grade Point Average

GPS = Global Positioning System

JPL = Jet Propulsion Laboratory

LRR = Launch Readiness Review

LTE = Long-Term Evolution

LV = Launch Vehicle

MATLAB = Matrix Laboratory

MESA = Mathematics Engineering Science Achievement

MOSFET = Metal–Oxide–Semiconductor Field-Effect Transistor

MSDS = Material Safety Data Sheet

NAR = National Association of Rocketry

NASA = National Aeronautics and Space Administration

NFPA = National Fire Protection Association

NSL = NASA Student Launch

PDC = Program Database

PDR = Preliminary Design

PLA = Polylactic Acid

PPE = Personal Protective Equipment

PPM = Pulse Position Modulation

PVA = Polyvinyl Alcohol

PVC = Polyvinyl Chloride

PWM = Pulse Width Modulation

RAC = Risk Assessment Codes

RAL = Rocket Assembly Laboratory

RCF = Refractory Ceramic Fiber

RFP = Request for Proposal

RSO = Range Safety Officer

RTM = Requirements Traceability Matrices

SBUS = Serial Communication Protocol

SCRA = Southern California Rocket Association

SHPE = Society of Hispanic Professional Engineers

SIM = Subscriber Identification Module

SOW = Statement of Work

SWE = Society of Women Engineers

STEM = Science, Technology, Engineering, and Mathematics

TRA = Tripoli Rocketry Association

UAV = Unmanned Aerial Vehicle

UFP = Ultra-Fine Particle

UGV = Unmanned Ground Vehicle

UMBRA = Undergraduate Missiles and Ballistics Rocketry

USB = Universal Serial Bus

USLI = University, NASA Student Launch Initiative

VOC = Volatile Organic Compound

List of Figures

List of Tables

1.0 Summary

1.1 Team Summary

Team Name: California State Polytechnic University, Pomona
Organization: Undergrad Missiles Ballistics and Rocketry Association (UMBRA)
Mailing Address: 3801 W Temple Ave, Pomona, CA 91768
Team Mentor: Rick Maschek TRA Level 2 Certification #11388
Team Mentor Contact Info: rickmaschek@rocketmail.com | (760) 953-0011
Documentation of the team's hours for the PDR can be found in **Appendix A**, and totals to **1193** hours as a team.

1.2 Launch Vehicle Summary

The Launch Vehicle team has decided to use G-12 fiberglass for the fuselage. The overall architecture of the launch vehicle has been systematically determined by evaluating the pros and cons of each alternative. The official target apogee for our launch vehicle is 5,100 ft, and this will be achieved by utilizing our leading motor choice, an Aerotech L-2200G. The launch vehicle consists of three sections; the first section consists of the nose cone, ballast, payload, payload retention/ deployment system, main chute, dry mass is 18.11 lbm, and length is 53.5 in. The second section of the launch vehicle consists of the avionics bay, dry mass 7.53 lbm, and its length is 19 in. The third section of the launch vehicle consists of the drogue chute, motor retention rings, motor casing, fins, dry mass is 19.11 lbm, and its length is 39 in. The recovery system consists of the avionics bay which houses the main altimeter, redundant altimeter, GPS, and four copper charge wells, as well as our 10 ft main chute and our 2 ft drogue chute.

1.3 Payload Summary

Payload Title: Palantir

The payload mission this year is to locate the launch vehicle after it has landed, on a gridded aerial image of the launch field without the use of a GPS. The payload will be a dead weight style payload and will be utilizing a multi-layer 3D printed design to house all the necessary components. The components housed in the payload include an IMU, barometric pressure sensors, raspberry pi, 2,400 mAh battery, voltage boost module, and a LoRa Module. The total weight of the payload is approximately 0.8 lbm with a length of 4 in and a diameter of 5 in. Using the mentioned components, the payload will track the launch vehicle's trajectory from the launchpad and will be able to communicate the final landing location to the ground station via the LoRa module at a frequency of around 900 MHz.

2.0 Changes Made Since Proposal

Table 2.1: Launch Vehicle Changes

Change made	Summary	Justification
Air Frame Diameter	Diameter was reduced to 6 in from 7.5	It is easier to source components for 6 in LVs than 7.5 in LVs and the desired apogee is more attainable with a thinner diameter
Air Brake Design	The number of fins for the air brake design was reduced from 3 to 2	It was realized that 3 fins may cause flow issues during deployment, but 2 fins can be oriented, so they are not in direct line of the other fins at the aft end of the Launch vehicle
Target Altitude	Target altitude has increased from 5,000 ft to 5,100 ft	The reduced diameter and weight of the air frame has allowed for a higher apogee and to help meet the descent time requirement
Fin thickness	Fin thickness was increased from 0.093 in to 0.186 in	Fin flutter analysis showed that the previous fins would fail during flight, so thicker fins that survived fin flutter analysis were chosen
Ballast weight	Ballast weight is now being incorporated; weight was increased from 0 lb to 2 lb	Stability analysis showed additional weight was required to meet the stability margin requirement.
Stability Margin	Stability margin increased from 2.02 to 2.05	Fin flutter analysis proving fin survivability and leading motor choice has increased the static stability margin
Total Launch Vehicle Length	Total length decreased from 117.5 in to 111.5 in	AV bay length oversight was corrected from 12 to 9 in, nosecone reduced from 37.5 to 34.5 in

Table 2.2: Payload System Changes

Change made	Summary	Justification
Payload size	The size of the payload was reduced to a 5-in diameter cylindrical Capsule	To reduce weight and size while having enough room for each component, the stated size for the cylindrical capsule fits the criteria needed
Design of payload	The first design of the payload was a drone but now it is designed as a cylindrical Capsule	To reduce weight significantly, designing the payload as a cylindrical Capsule was the best option
Payload components	With the payload no longer being a drone, the cylindrical Capsule components necessary are much less than the previous design	The payload as a drone had many extra components, with it now being redesigned, the list of components is much smaller reducing the total weight of the payload
Design of Payload Integration system	No longer a need for a jettisoned self-leveling barrel to prepare for drone launch. Instead, the system simply extrudes out from the launch vehicle by a small distance	Payload is no longer a drone and doesn't need to be ejected from the rocket to create a stable launch platform. To guarantee communication between the base station and payload computer is not hindered the PLI system is separated from the launch vehicle
Payload Integration Components	Payload integration no longer needs linear actuators, accelerometer, or altitude sensor	PLI no longer needs to lock and unlock payload, negating the need for linear actuators. PLI must be remotely triggered, negating the need for onboard sensors to autonomously deploy

Table 2.3: Recovery System Changes

Change made	Summary	Justification

Avionics Bay Bulkhead Diameter	The Avionics bay bulkhead diameter originally would have been 7.5 in diameter but has since been reduced to a 6 in diameter	To fit in the new airframe diameter the AV bay had to be downsized to function properly, electronic components remain the same
Avionics Bay Length	The original avionics bay length was set to a total of 12 in including two 0.5-in bulkheads but has since been decreased to a total length of 10 in	With the need for more space in other systems, the AV bay was downsized to its minimum length

Table 2.4: Project Plan

Change made	Summary	Justification
Budget	The team must find an additional source of funding, along with the newly established GoFundMe to meet our necessary budget for the launch vehicle and travel to Huntsville.	Northrop Grumman will no longer fund the CPP NSL project due to an already allocated budget earlier in the year for school projects across the nation.

3.0 Launch Vehicle Design

3.1 Mission Statement

The launch vehicle will ascend to 85 ft/s and obtain a stability of 2.0 at rail exit via a solid rocket propellant motor. During the coast period, air brakes will deploy and slow the launch vehicle to its target apogee of 5,100 ft followed by a drogue deployment at apogee, then a main deployment at an altitude of 600 ft followed by a landing with less than 75 ft-lb of kinetic energy. The payload will then be deployed followed by landing location data being transmitted back to the launch site.

3.2 Alternative Launch Vehicle Architectures

3.2.1 Airframe Dimension Alternatives

For our launch vehicle this year, our team is considering using a 6-in inner diameter or a 7.5-in inner diameter fuselage. The benefits of each will be highlighted below in section 3.2.5.

3.2.2 Fin Alternatives

The fins were deemed to be G-10 fiberglass material as mentioned in the proposal milestone of the design. The fins shown in **Figure 3.2.2-1** are from the same manufacturer, Public Missiles, for which they have to offer. The naming convention of the fins are as follows: “size letter - fin number”. The size letter would indicate the size of the fin, while the fin number would indicate the general shape of fin. The various shapes of the fins which are shown below were analyzed.

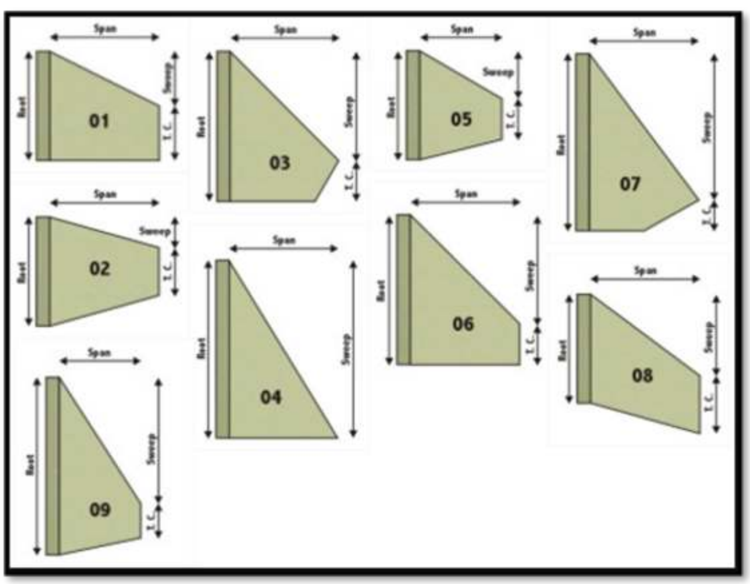

Figure 3.2.2-1: Various Fin Shapes

The size group of the fins under consideration were in the "C" size group according to Public Missiles. The key dimensions of the fins are shown in **Table 3.2.2-1**. The simulation used the leading motor candidate that will be mentioned in section 3.4. The main trait that is shared among the fins is the thickness of 0.186 in. The fins are compared by modeling each fin in OpenRocket to simulate the apogee altitude and stability margin. The apogee altitude ranges from 5,393 ft to 5,735 ft. Along with the stability margin ranging from 1.97 to 3.42. Most of the fins meet the stability margin requirement of 2.0 but note that having a high stability margin doesn't necessarily mean a very stable rocket. The stability margin is expected to increase at rail exit and early flight as well. A high stability margin can mean that the rocket will be over stable. An over stable rocket tends to overcorrect and oscillate wildly in response to a crosswind. The team decided to have the "C-09" fin as our leading candidate in response to this, as well as to give more margin with the apogee altitude. The launch vehicle is anticipated to become heavier as we proceed further in the design which will lower the altitude to the target apogee.

Table 3.2.2-1: Fin Dimensions w/ Stability Margin & Altitude

Fin Dimensions w/Openrocket Results (PUBLIC MISSILES)							
Type/Style	**Thickness (in)**	**Root Chord (in)**	**Tip Chord (in)**	**Span (in)**	**Sweep Distance (in)**	**Stability Margin (cal)**	**Altitude (ft)**
C-01	0.186	6	3	6	3	**3.19**	**5,442**
C-02	0.186	6	2.6375	6	1.6875	**3.10**	**5,393**
C-04	0.186	10	0	6	10	**2.87**	**5,685**
C-05	0.186	6	2.25	4.5	2.625	**1.97**	**5,607**
C-06	0.186	9	2.5	6.5	6.5	**3.42**	**5,518**
C-08	0.186	6	3.125	6	4.5	**3.21**	**5,515**
C-09	0.186	10	2	4.625	7.125	**2.05**	**5,735**

3.2.3 Cone Selection

A few different cone designs were considered for the launch vehicle with Madcow Rocketry currently being the leading candidate to source G-12 fiberglass nosecones from. In **Table 3.2.3-1,** lists the various nose cone shapes available for a 6-in inner diameter airframe. The factors that were considered are the weight and the coefficient of drag as shown below.

Table 3.2.3-1: Cone Selection Options

Cone	Weight with Coupler	Coefficient of Drag Approximation
4:1 Ogive	5.5 lb	0.66
5:1 Ogive	5.5 lb	0.66
5.5:1 LV-Haack	5.5 lb	0.33

Given that each of the nosecones available are all the same estimated weight and the nosecone will not be used to contain subsystems, the main factor in deciding which cone to use would be the coefficient of drag, which in this case the LV-Haack minimizes drag, and thus is the primary candidate for the launch vehicle cone selection.

3.2.4 Subsystem Organization

Placement of each section of the rocket is placed based on weight and functionality. A requirement of a static margin of 2.0 is required, as well as a desire to bring the center of gravity forward or closer to the tip. With a software called Openrocket, after inserting approximate weights for each section, it is determined that the rocket has a static margin of 2.05. As seen in the figure below, **Figure 3.2.4-1,** our architecture is designed as follows: cone, payload, main chute, avionics bay, drogue chute, air brakes, then finally, the motor. The payload is placed in front to avoid any possible damage done by the motor firing and to place the center of gravity forward as it weighs the heaviest of all the sections at 12.5 lb. The main chute and the avionics bay are placed together weighing 7.5 lb total. The drogue chute, air brakes and the motor are placed next weighing a total of 12.6 lb. After conducting research, the team had found that the airbrake could be placed nearly anywhere along the rocket body. The placement is just dependent on the space available and weight placement for stability purposes.

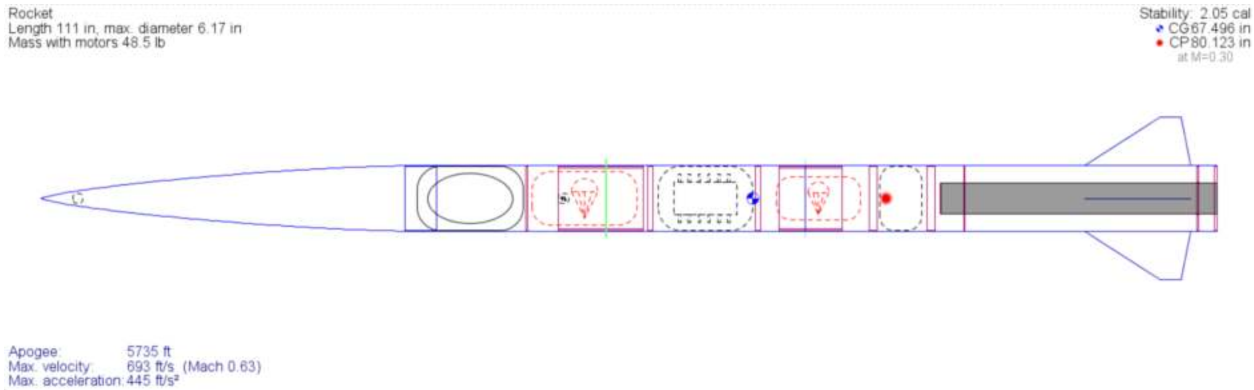

Figure 3.2.4-1: Openrocket Simulation

3.2.5 Benefits and Drawbacks of Alternative Launch Vehicle Architectures

The rocket's dimensions were originally driven by the size the payload needed to fit the quad helicopter and concluded an inner diameter of 7.5-in was needed. With a big inner diameter, there were also many more options to integrate and deploy the payload but after running early simulations, our rocket was unable to reach the minimum apogee required of 4,000 ft even when lowering the weight of subsystems within our architecture. This is highlighted in **Figure 3.2.5-1**. At this point, the apogee was the new design driver and to fix this problem, the rocket's inner diameter needed to be lowered to 6-in. This smaller diameter reduced drag and allowed for more rocket motor selections which in turn increased our apogee. A 6-in inner diameter also allowed us to access easier pre-made parts such as our nose cone thereby making our rocket easier to rebuild for testing.

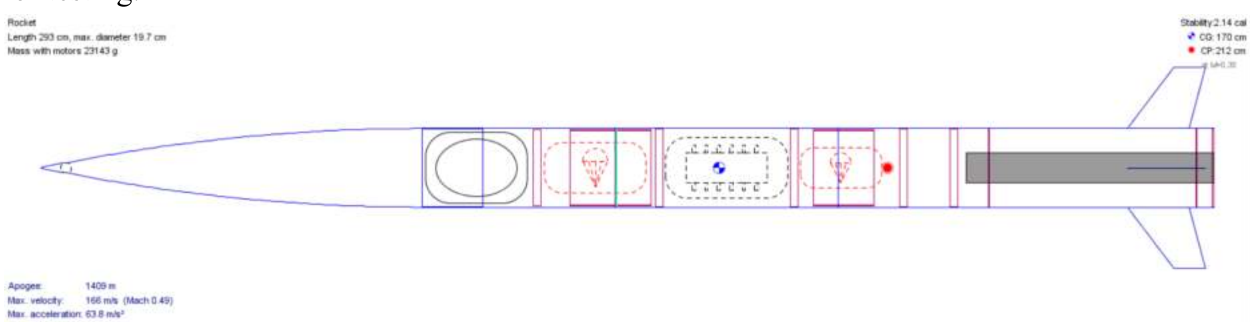

Figure 3.2.5-1: 7.5-in Openrocket Simulation

3.2.6 Location of Separation Points & Energetic Materials in LV

The location of each separation point is highlighted in order in **Figure 3.2.6-1.** After the rocket reaches the target apogee of about 5,100 ft, the drogue chute will be deployed by separating at the green line at 72.5 in from the nose tip. This is between the drogue chute and the air brakes sections. The drogue chute will slow the launch vehicle to a decent rate of about 75 ft/s. When the rocket reaches an altitude of about 600 ft, the main chute will be deployed at the red line in between the payload bay and the main chute sections, 53.5 in from the tip. When the launch vehicle has landed, the cone will pop off at the blue line to allow the payload to exit and receive a better signal. A small explosive or black powder will be used to separate and eject the red and green line highlighted in the figure below while a mechanical mechanism will be used to separate the cone from the payload, separating at 34.5 in from the tip. The current leading candidate AeroTech L2200G motor will be used to launch our vehicle.

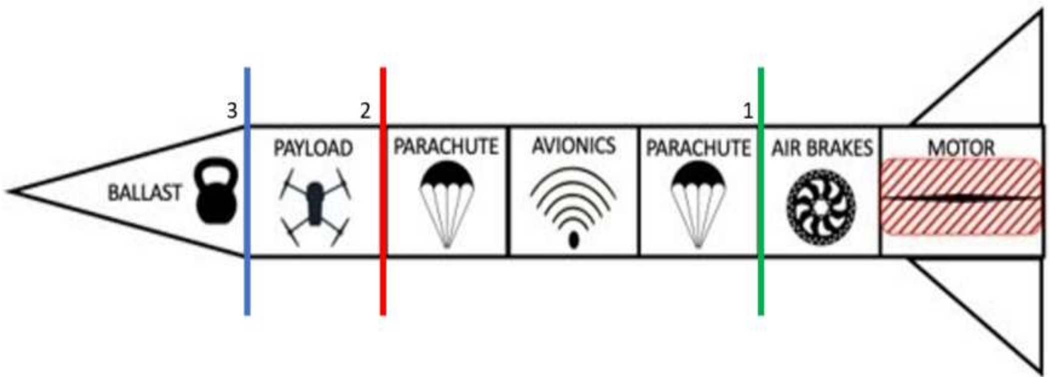

Figure 3.2.6-1: Order of Separation

3.3 Leading Launch Vehicle Architecture

3.3.1 Leading Launch Vehicle Subsystems Overview

The Launch Vehicle Subsystems comprises two major sections: Motor Retention Design and Air Brakes System. The following sections will detail each subsystem's overall design and critical components.

3.3.2 Motor Retention Design

A motor mount was designed to keep the motor secured in place. The motor mount restricts the motion of the motor in all 6 degrees of freedom. An outer cylindrical tube will house the motor keeping it centered within the airframe. The upper end of the tube will be capped preventing the motor from slipping upwards towards the nose of the rocket. A bulkhead will be placed directly above the capped end to provide redundancy. The lower end of the tube has two caps to prevent the motor from slipping upwards towards the nose and downwards towards the base of the rocket.

The cylindrical tube housing the motor will be secured to the rocket by attaching it to the inside of the airframe via centering rings. Centering rings will be secured to the housing tube via JB Weld. The JB Weld will perform well at the high temperatures the firing of the motor will expose the housing tube and centering rings to. The centering rings will be epoxied to the inside of the airframe to hold the entire system in place. **Figure 3.3.2-1** below is the CAD drawing of the motor mount.

Figure 3.3.2-1: Motor Mount Design with Capped Ends and Centering Rings

3.3.3 Fin Mount Design

A fin mount was designed to ensure that the rocket fins are installed properly to the rocket. The fin mount will be installed on the exterior of the air frame. Four slits located on the fin mount will allow the fins to be inserted and positioned in the desired location: 90 degrees from each other. Once in place, the fins will be epoxied to the air frame. **Figure 3.3.3-1** below is a CAD drawing of the fin mount.

Figure 3.3.3-1: Fin Mount Design with Slits

3.3.4 Air Brakes Design Alternatives

In **Figure 3.3.4-1**, three separate designs emerged as candidates for the airbrake system. The first design option 1 is a disc with retracted blades stacked in line with the rocket body, and a servo motor drives a central gear to equally extrude the blades, thereby increasing drag. A system of linkages is controlled. The second option is achieved by a servo motor and stacked in line with the rocket body, and the servo changes the position of the central linkage to equally extrude two uniform plates to increase drag. Option three is like the deployment of a rain umbrella, a central plate with linkages attached to 3 curved plates is driven by a piston. The piston moves down to equally deploy these 3 plates to varying positions and increase the drag on the body.

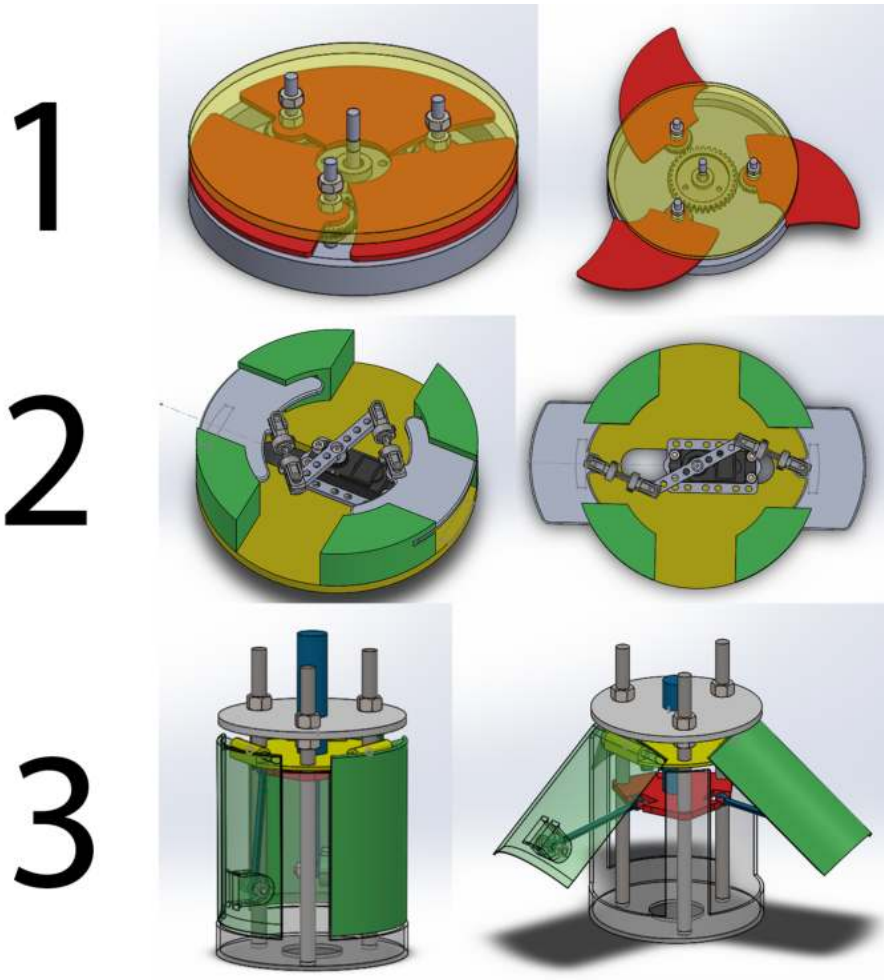

Figure 3.3.4-1: Variations of Air Brakes

Iterating through the positives and negatives of each potential design yielded a list of overarching key criteria necessary for a successful airbrake system. These characteristics were condensed and evaluated by measure of importance, and then adapted to create a trade study heuristics chart to quantitatively determine the best option available.

Table 3.3.4-1: Airbrake Design Trade Matrix

Utility Value (1-5)		Option 1		Option 2		Option 3	
Criteria	Weight	Utility Value	Weighted Value	Utility Value	Weighted Value	Utility Value	Weighte d Value
Manufacturing	4	3	12	4	16	2	8
Drag	4	4	16	4	16	5	20
Size	2	5	10	5	10	1	2
Weight	3	3	9	4	12	2	6
Control	5	4	20	4	20	3	15
Cost	1	2	2	3	3	2	2
Durability	5	3	15	4	20	2	10
Weighted Total		86		**97**		63	

After trade study completion, option 2 aligned the most with the goals of the design. Simplicity of manufacture, minimal parts and cost, and ease of revision to the control surfaces to elicit favorable properties like laminar flow made this design very appealing as well.

Software: The control scheme used to govern the operation of the airbrake will revolve around increasing drag after engine cut off to shorten maximum altitude. A Raspberry Pi 3 board will regulate the deployment of the plates, with coefficients of drag for different deployment configurations being experimentally determined via wind tunnel prior to launch. The computer will take altitude, velocity, and acceleration measurements in real time from onboard instrumentation, and will calculate the acceleration necessary to hit 0 velocity at target altitude. The computer will then use drag formulas to determine the right deployment percentage for the plates and augment the deceleration of the rocket, with recalculations running in an infinite loop to retract and protrude the plates as necessary.

3.3.5 Benefits and Drawbacks of Airbrake Design Alternatives

The most important criteria we are looking at are durability and control. Durability is important because it is a requirement that the launch vehicle must be reusable. The control criteria in **Table 3.3.4-1** means the ability for the air brakes to aid in reaching the target altitude and ease of coding the system. Control is just as important because it is also a requirement to hit a certain target altitude. Option 1 and Option 2 are best suited to meet these two requirements since they are flat, take up less space, and have fewer moving parts. Option 3 has long thin parts that can buckle if enough axial force is applied. Option 3 has the benefit of providing the most drag when fully extended since it provides the most surface area exposed to oncoming wind compared to options 1 and 2. Option 3 however takes up the most space, not as durable, heavier, and complex to build. Option 1 and 2 are similar but option 2 is the primary design as will be discussed in the section below. Both 1 and 2 uses a servo and gear mechanism to deploy the brakes out of the rocket and has the benefit of being easy to build, weighs less, and durable. Shear analysis is needed to ensure the plates don't bend or shear off when exposed to wind.

3.3.6 Primary Airbrake Design

The leading candidate for our airbrake design is option 2 shown in **Figure 3.3.6-1**. Compared to option 1, this is superior in that this will not disrupt the airflow for the fins thereby increasing stability for the rocket as it is slowed down. The parts for this design are also pre-built and sourced from existing shops. The green part is the only part that must be 3D printed. This allows us to run tests more easily by easily making multiple copies if needed. Parts can also be easily replaceable if a failure occurs. Multiple servo options are also available and easily replaceable if more torque is needed.

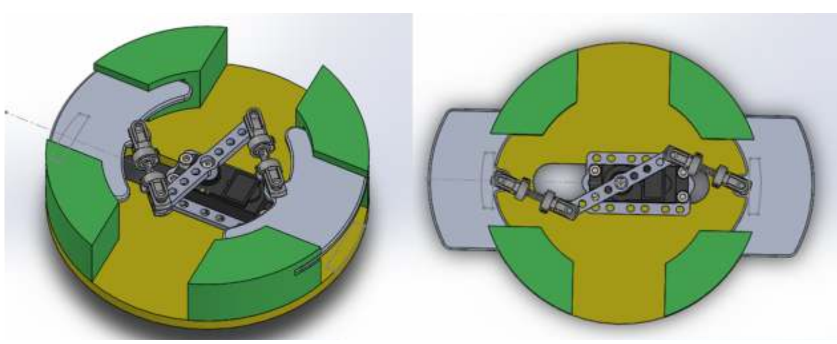

Figure 3.3.6-1: Primary Airbrake Design

3.3.7 Airbrakes Component Selection

As will be mentioned in greater detail in section 5.2.4, the four material types being considered for the airbrake system are PLA, AL 6061, AL 5052, and Al 7075. The benefit of having PLA as a material choice is that it will be cheaper and can be printed in house. All the aluminum variations will have the benefit of deflecting less and being reusable due to its more robust properties compared to PLA. Although more expensive, it is a requirement for the Launch vehicle to be reusable and after repeated use, it is expected that PLA will have permanent deformation after repeated use even if it survives multiple launches. Cost and structural analysis are further explained in the section below. A trade study is also shown to indicate our leading material type in section 5.2.

Another component we considered alternatives for is the microcontroller. Our team plans on varying the exposed area of the fins to vary drag that will in turn, help the rocket reach a more precise apogee. This year our team looked at the Raspberry Pi 4 or Raspberry Pi 3, Arduino Uno, and Elegoo Uno r3. Arduino and Elegoo have the benefit of being cheaper and having members of our team more familiar with the language. The Arduino IDE allows us to quickly fix and debug and quickly upload any changes to the system. Arduino is also open source allowing easy navigation of making a proper air brake system. The raspberry Pi is more expensive but allows us to play with features that a computer is capable of. With the Pi, we can use a wider range of programming languages like Python, Java, and HTML. We can also use C++ and C or any similar languages that run on the Arduino. The hardware design files, and the firmware of Raspberry Pi are not open source, however. This year, our team opted for the Raspberry Pi 3. The Raspberry with its wider features and flexibility allows us to not only develop a code to adjust our altitude but allows us to retrieve more data when testing early models allowing us to make better adjustments. Members of our team are also very familiar with this microcontroller and an extra one is already made available for us to use.

Figure 3.3.7-1: Microcontrollers Left to Right - Arduino Uno R3, Elegoo Uno R3, Raspberry Pi 3

Table 3.3.7-1: Trade Matrix of Microcontroller Selection

Utility Value (1-10)		Option 1		Option 2		Option 3	
		Arduino Uno R3		Elegoo Uno R3		Raspberry Pi 3/4	
Criteria	**Weight**	**Utility Value**	**Weighted Value**	**Utility Value**	**Weighted Value**	**Utility Value**	**Weighted Value**
Flexibility	4	5	20	5	20	9	36
Cost	1	5	5	4	4	6	6
Availability	2	9	18	9	18	6	12
Ease of Use	3	9	27	9	27	7	21
Weighted Total		**70**		**69**		**75**	

As Shown in the table above, flexibility and ease of use are weighted the most. Flexibility refers to the I/O and its broad capabilities. The Raspberry Pi weighs the most here since it is basically a computer. The Raspberry Pi 3 tends to go out of stock quicker relative to the Arduino and Elegoo so that is why its utility value is less in this category. The cost needs to be considered but it is found that all these microcontrollers' costs are about the same with slight differences. The size was also looked at, but they are also almost the exact same dimensions. Although a little harder to use, the flexibility and capabilities of the Raspberry Pi is the leading candidate for controlling the air brakes system.

Another Component our team looked at is servos. These will be used to turn the gear in the middle of the rocket. The three main servos we looked at are HS-645MG Servo-Clockwise (HS), Feedback 360 Degree - High Speed Continuous Rotation Servo (High-speed), and the 30:1 Metal Gearmotor 37Dx68L mm 12V with 64 CPR Encoder (Gearmotor). Although considered earlier in the design for its small size and light weight of 0.0875 lb, The High-speed servo became quickly obsolete as we found that the 360° rotation was not required for our needs. With a peak torque of only 30.5 oz-in, it was quickly overshadowed by the other two alternatives. A torque of 30.5 oz-in was estimated to not be capable of fighting the friction between the fins, the friction between the bracket it sits on, and the winds encountered during cruise after burnout. The Gearmotor has a peak torque of 190 oz-in which is more than capable of solving this issue. However, the cons that the Gearmotor has is it weighs the most at 0.4 lb. It also takes up the most space and requires a 12V power source which is undesirable as it takes up more space and weighs the rocket down even more. Lastly, the HS is the primary component as it is the middle ground between these two. It is as small as the High-speed and only weighs 0.12 lb. It also has a peak torque of 133.13 oz-in at 6V which is estimated to be enough. A lubricant or roller system will also be implemented to help with friction. With a smaller battery, the whole system is designed to be optimized for size and weight with the proper torque required.

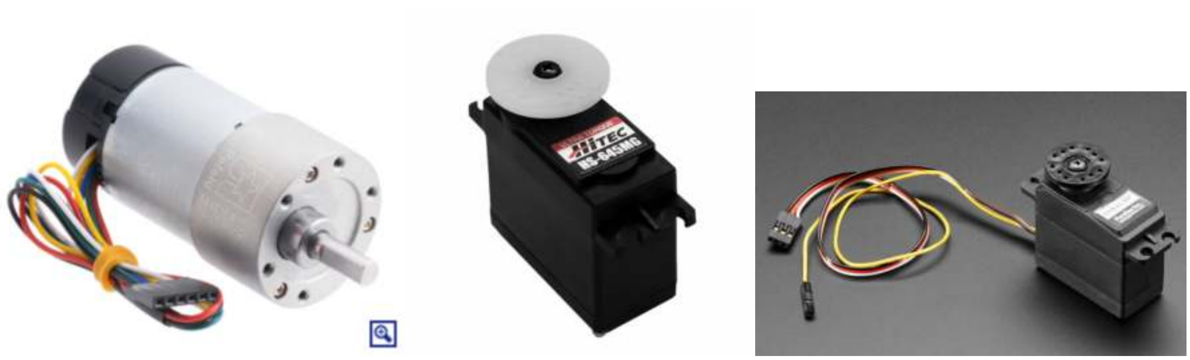

Figure 3.3.7-2: Servos Left to Right - Gearmotor, HS, High-speed

Table 3.3.7-2: Trade Matrix of Servos

Utility Value (1-10)		Option 1		Option 2		Option 3	
		Gearmotor		HS-645MG		HighSpeed	
Criteria	**Weight**	**Utility Value**	**Weighted Value**	**Utility Value**	**Weighted Value**	**Utility Value**	**Weighted Value**
Size	2	3	6	8	16	8	16
Torque	3	9	27	7	21	3	9

Weight	1	5	5	7	7	8	8
Weighted Total		**38**		**44**		**33**	

3.3.8 Launch Vehicle Dimensional Drawing

As shown in **Figure 3.3.8-1**, the cone is 37.61 in long, the payload and where half the main chute will be located is highlighted in blue and will be 24.00 in long. The next section highlighted orange shares a space with the main chute, avionics bay as well as the drogue chute and is 19.00 in in length. The air brakes are where the pink section is and is 4.26 in long and lastly the yellow section containing the L2200G AeroTech motor is 36.00 in long. The inner diameter of the rocket is 6.00 in with an outer diameter of 6.17 in making the fuselage 0.17 in thick. The C-09 fin configuration has a thickness of 0.186 in with a root chord of 10.00 in, tip chord of 2.00 in, a span of 4.625 in and a sweep distance of 7.125 in. Additional measurements are highlighted in the figure below.

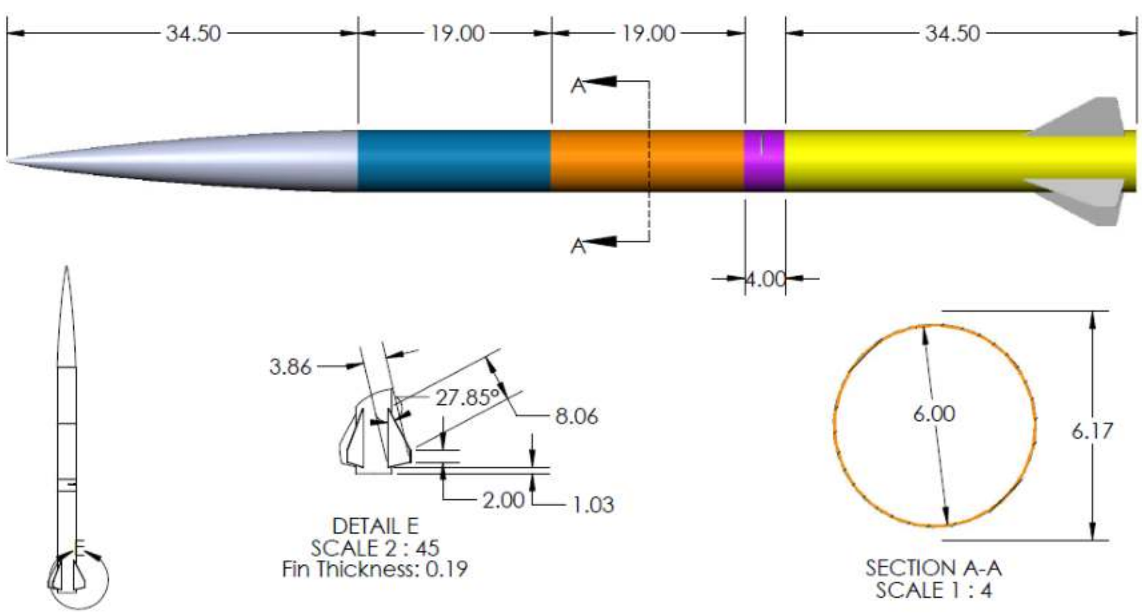

Figure 3.3.8-1: Launch Vehicle Dimensions

3.3.9 Launch Vehicle Subsystem Estimated Masses

The Launch Vehicle masses include cone mass, payload mass, avionics mass, motor/air brake masses, and rocket motor mass.

Tables 3.3.9-1 through **3.3.9-5** show the masses for each Launch Vehicle subsystem. These values are used in Open Rocket Simulation and hand calculation analysis to verify the final masses the rocket will have.

Table 3.3.9-1: Payload Bay Masses

Payload Bay Masses		
Payload & PLI	6.6139	lbm
Bulkhead	0.62391	lbm
Airframe	3.7534	lbm
Main Parachute	2	lbm
Top Coupler	0.9436	lbm
Total Mass	**13.9343**	**lbm**

Table 3.3.9-2: Avionics Bay Masses

Avionics Bay Masses		
Airframe	6.6139	lbm
Avionics	.6239	lbm
Bottom Coupler	3.7534	lbm
Wooden Bulkheads (2)	2	lbm
Total Mass	**7.3811**	**lbm**

Table 3.3.9-3: Motor/Air Brake and Drogue Masses

M/A Brake and Drogue Masses		
Airframe	5.5997	lbm

Bulkheads (2)	1.2258	lbm
Centering Rings (2)	1.5141	lbm
Fins (4)	.7011	lbm
Motor Tube	1.1993	lbm
Motor Casing	.1001	lbm
Drogue Chute	1.4991	lbm
Total Mass	**11.8613**	**lbm**

Table 3.3.9-4: Rocket Motor Masses

Rocket Motor Masses		
Loaded Mass	10.5447	lbm
Burnout Mass	4.9935	lbm

Table 3.3.9-5: Cone Masses

Cone Masses		
Total Mass	**9.2427**	**lbm**

3.3.10 Launch Vehicle Design Justification

With the mass estimated from the subsystems, the 6 in diameter airframe is the better design choice given that the airframe weight is much more ideal than using the 7.5 in diameter airframe.
Table 3.3.9-1 shows the apogee difference between using a 7.5 in airframe design versus a 6 in design. Both designs utilize an Aerotech L2200G which is one of the most powerful motors available and appropriately scaled fins and nose cones.

Table 3.3.10-1: Design Apogee Prediction

Airframe Diameter (in)	Approximate Wet Mass (lbm)	Predicted Apogee (ft)
6	48.5	5,735

7.5	55.8	4,445

The minimum apogee for the competition is 4,000 ft, using the 6 in diameter airframe allows more motors to choose from since the predicted apogee is well above the minimum requirement given current mass estimates. Subsystems are organized with the heaviest subsystems as close to the cone as possible, moving the CG as far forward as possible thus increasing stability.

Given previous experience in this competition, one of the biggest challenges is finding as many things as possible during the mission that one can control. Using air brakes in the launch vehicle design allows for some control over the launch vehicle apogee in flight rather than having to rely on specific wind conditions.

The fin mount design and manufacturing process will be like last year's design with one minor modification. Last year the launch vehicle had very little body roll and no structural failures, however during landing the motor section of the launch vehicle would always land on the motor retainer, since the engine overhang was 1 in, the motor retainer was the furthest protruding structural object. To correct this, there will be no engine overhang from the airframe, thus the motor section of the rocket will instead land on the airframe, a much sturdier structure, rather than landing on the motor mount

3.4 Motor Alternatives

Three motors were under consideration for the design of the launch vehicle. The three being the Cesaroni L-1115, Aerotech-L2200G, and the Aerotech L-2375W. The Cesaroni L-1115 has an average thrust of 251.6 lbf. This results in a simulated apogee of 5,508 ft with a stability margin of 2.10. The cost of the motor is $306.84 and is available under multiple online resources. The loaded weight of the motor is 9.71 lbm and a burnout weight of 4.25 lbm. The Aerotech L-2200G has an average thrust of 696.9 lb. This results in a simulated apogee of 5,735 ft with a stability margin of 2.05. The cost of the motor is $322.99 and is available under multiple online resources. The loaded weight of the motor is 10.54 lbm and a burnout weight of 4.99 lbm. The Cesaroni L-2375W has an average thrust of 551 lb_f. This results in a simulated apogee of 5,555 ft with a stability margin of 2.16. The cost of the motor is $347.89 and is available under multiple online resources. The loaded weight of the motor is 9.17 lbm and a burnout weight of 4.06 lbm.

These three motors were under consideration because they all are viable options within the criteria set forth in **Table 3.4-1.** The criteria are the predicted apogee, stability, cost, availability, and weight. Each criteria have their weighted values based on what the team deems most important to the design of the launch vehicle. The most important criteria are the predicted apogee because for the launch vehicle being able to overshoot the target apogee will allow there to be margin. This margin is key because the team anticipates the launch vehicle to become heavier as the design process continues. The least important criteria are the cost of the motors because all three motors are relatively priced similarly. From the results of the conducted trade study prove the AeroTech 2200G to be the current leading candidate for the design.

Table 3.4-1: Motor Trade Matrix

Utility Value (1-10)		Option 1		Option 2		Option 3	
		Cesaroni L-1115		Aerotech L-2200G		Cesaroni L-2375W	
Criteria	**Weight**	**Utility Value**	**Weighted Value**	**Utility Value**	**Weighted Value**	**Utility Value**	**Weighted Value**
Predicted Apogee	5	7	35	9	45	8	40
Stability	4	8	32	8	32	9	36
Cost	1	9	9	9	9	9	9
Availability	4	9	36	9	36	9	36
Weight	2	6	12	7	14	7	14
Weighted Total		**124**		**136**		**135**	

4.0 Recovery Subsystem

4.1 Avionics

4.1.1 TeleMetrum V3 by Altus Metrum

The TeleMetrum V3 by Altus Metrum is a dual deployment altimeter with an integrated GPS. The TeleMetrum's barometric sensor is accurate up to 100,000 ft and can store multiple flights with its onboard memory. The setup is simple due to the user interface via micro-USB port where the board can be configured. Ignitors can be fired manually using Altus Metrum's AltosUI. This allows for ground testing of the separation events via black powder charges. Main parachute deployment can also be configured through AltosUI.

The TeleMetrum was selected due to the integrated GPS which provides the team with real-time tracking when combined with the TeleDongle RF interface. The advantage of this is that it will serve as both a GPS and an altimeter which allows us to save space in the AV bay. The TeleDongle allows for the ground station computer to collect live data as well as to conduct ground testing. The one downside to TeleMetrum is the price. At $400 including the TeleDongle, this is the most expensive option for altimeters. However, the pros outweigh the cons of this device which makes it the best choice amongst the other options.

Figure 4.1.1-1: TeleMetrum V3

4.1.2 RRC3

The RRC3 by MissileWorks is a highly programmable altimeter with a module for telemetry and a barometric sensor accurate up to 40,000 ft. The board is efficiently priced at $75 plus $25 for a USB Interface Module. In addition to this, the RRC3 also has a simple and easy setup as it is ready to fly out of the box and is pre-programmed to deploy the main parachute at 600 ft. Additionally, MissileWorks includes the MissileWorks Data Acquisition and Configuration Software which allows for a high degree of programmability and data recovery with graphs.

The RRC3 was considered due to its relatively cheap price in comparison to the TeleMetrum with similar functions at a vastly lower price. However, in a direct comparison with the TeleMetrum, there were clear disadvantages that overrode its price advantage. First off, there wasn't a built-in GPS module on the board which would have required an additional GPS module that would create additional complexity and risks of failure while also decreasing the price advantage the RRC3 had over the TeleMetrum. Because of this, the GPS functionality built into the TeleMetrum valued it over the RRC3 for our main altimeter selection.

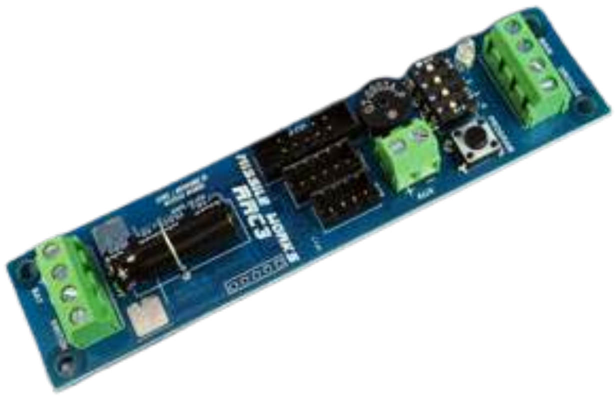

Figure 4.1.2-1: RRC3

4.1.3 Raven4

The Raven4 by Featherweight electronics is a high-performance altimeter priced at $160 and capable of performing many different tasks with high-rate data (+/- 0.3% error), flexible outputs, training exercises, and air starts. Before mounting the Raven4, it can perform a flight simulation. When it comes to data, it provides up to 8 minutes of high-rate 20 Hz data, plus an additional 45 minutes of low-rate data per flight. It is also another highly programmable altimeter that can utilize both a 100 Gs barometer and altimeter for data and deployment. Setup for the Raven4 is minimal as it is ready to fly out of the box and can be used immediately after a power source is attached.

The Raven4 was considered due to its numerous functions and performance to ensure quality data and proper deployment. However, the Raven4 still pales in comparison to the TeleMetrum as just as the RRC3, there is no built-in GPS on board. An additional GPS tracker module could be purchased from Featherweight Electronics at a steep price of $352, which overshadows the TeleMetrum's price of $300. With no built-in GPS and similar functions to the TeleMetrum, the TeleMetrum was still valued over the Raven4 as the main altimeter.

Figure 4.1.3-1: Raven4

4.1.4 Eggtimer Proton

The Eggtimer Proton by Eggtimer Rocketry features Wi-Fi capabilities and an advanced flight computer with dual deployment, six outputs for data logging, a 120 Gs accelerometer, barometric sensor, and flexible deployment and arming modes to handle any flight scenario and record data up to 60,000 ft. Each channel can be used for a variety of purposes as there is no dedicated channel such as “Drogue" or “Main". The Proton costs $70 on the Eggtimer website with optional add-ons such as a Telemetry Module for $20 and the Eggtimer Wi-Fi switch for $20. However, one major drawback of the Proton is that it is not ready out of the box, meaning the team would have to solder the altimeter together.

The Eggtimer Proton was considered due to its high capabilities at a low price compared to most altimeters and being able to be wirelessly armed. The TeleMetrum was still chosen over the Proton because of its manufacturing process, as members on the avionics team are not skilled enough in soldering such small components, and due to COVID-19, we want to minimize physical contact as much as possible.

Figure 4.1.4-1: Eggtimer Proton

4.1.5 RRC2+

The RRC2+ by Missile Works is shown in **Figure 4.1.5-1** it is a less advanced version of their RRC3 altimeter that the team had considered for the main altimeter. The altimeter is dual-deployment and can record up to 40,000 ft. It is reasonably priced at $47.95 without any additional or required upgrades. Its setup is simple with a plug-and-play mentality only requiring a battery connection, parachute leads, and mounting onto the sled. The board reports data through a combination of beeps and can be programmed with simple configurations on the four dip switches.

The RRC2+ was considered due to its cheap pricing and solid performance. Priced lower and easier to set up than the other boards, the RRC2+ had many positives. However, the main drawback was its programmability and data logging which was significantly less advanced than the other boards. The simple dip switches to the program were not comparable to the computer interfaces on the other altimeters and the flight data reported through beeps was inferior to the computer interfaces with graphs and actual data logging included with other altimeters. For these reasons, the RRC2+ was not selected for selection for the team's redundant altimeter.

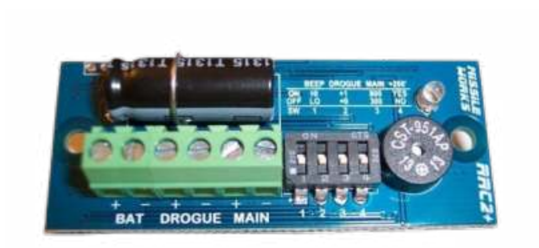

Figure 4.1.5-1: RRC2+

4.1.6 StratoLoggerCF

With the requirements given and the research completed into each of the altimeters, the team decided that the best altimeter would be the StratoLoggerCF from (PerfectFlite). This altimeter has been proven to be the most reliable and respected altimeter in production from websites such as Hararocketry. On top of the recommendation, when compared to the other altimeters, the Stratologger has superior programmability including keeping programmable presets and main deployment altitudes. Additionally, in comparison with all altimeters, the Stratologger has the most refined user interface. With all these considerations, the StratologgerCF would be the most effective altimeter to serve as a redundant in case the TeleMetrum would fail.

The StratologgerCF was selected in comparison to all other altimeters because of its low price, customization, reliability, and user interface. Although it may have fewer features than altimeters such as the EasyMini, the low cost for reliable performance outweighs any other redundant altimeter selected for consideration.

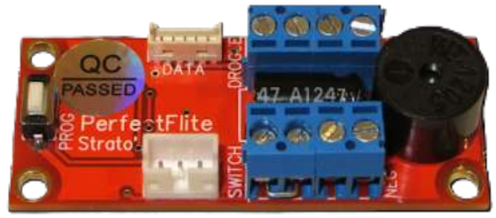

Figure 4.1.6-1: StratologgerCF

4.1.7 EasyMini

The EasyMini by Altus Metrum is an advanced altimeter with many of the same features as a full altimeter but at the price and size of a redundant one. The board is dual deployment and can record up to 100,000 ft. At a price of $80, is the most expensive redundant altimeter but does have a very simple setup with the standard setup of attaching a battery, main and drogue parachute, and has a terminal for a key switch. Altus Metrum provides their AltOS to program and report data with a variety of settings for launch and advanced graphs with velocity, altitude, and most important data points.

Regarding the team's selection, the EasyMini was highly rated and came close to being selected as the redundant altimeter. The board had the most advanced programmability and flight data reporting due to Altus Metrum's AltOS. This program would allow the team to get valuable data such as altitude and velocity and program the altimeter with increments of main parachute deployment and other settings. However, the board's con is the higher price when compared to the other redundant altimeters. As a redundant altimeter would most likely be used during the subscale launches, the team needed to have multiple copies for the full scale in case of a failure during the subscale launch. The StratologgerCF by PerfectFlite is currently sold out. If the StratologgerCF would remain sold out, the team would select the EasyMini by Altus Metrum as the redundant altimeter.

Figure 4.1.7-1: EasyMini

4.1.8 Eggtimer TRS

The Eggtimer TRS by Eggtimer Rocketry is a dual-deployment altimeter with GPS tracking features. The range of operation is 26,000 ft and can be doubled if the 70 cm ham version is purchased instead. Multiple flights can be recorded using an SD card placed in the Openlog data logger.

The Eggtimer TRS was considered since it features GPS functions at a lower cost point than the other devices. The cons to this device are that the board requires soldering during the setup process, and it is rated as a notoriously difficult board to solder according to the Eggtimer website. Damage or short circuits to the board could occur during the setup process, and this could jeopardize the team's mission, which is why the Eggtimer was not chosen.

Figure 4.1.8-1: Eggtimer TRS

4.1.9 RTx/GPS Telematics

The RTx Telematics system by Missile Works is a GPS tracking device that has an operational range of up to 160,000 ft. Setup is plug and play with no soldering required. Applications like uCenter can stream live data with the use of the USB IO Dongle. This paired along with Missile Works mDACS application would allow for data to be transferred easily. Multiple flights are also recorded via the onboard memory. There is an optional LCDT module that allows the ground station to have the LCD display locate the rocket rather than a computer.

The RTx Telematics was considered because it offers GPS tracking in real-time. Missile Works offers this system as a pair that comes with the receiver and GPS for the price of $329 which is less than the TeleMetrum. However, there are no dual deployment features which means an additional altimeter would be necessary to meet our current parachute design. The cost of this additional altimeter would ultimately eliminate the money saved from purchasing the RTx Telematics system. This would also mean three devices would be necessary to complete the team's mission which also introduces the need for an additional battery.

Figure 4.1.9-1: RTx/GPS Telematics

Tables 4.1-1, 4.1-2, and **4.1-3** below are the pros and cons for the main and redundant altimeters and GPS options.

Table 4.1-1: Main altimeter Pros/Cons

Altimeter	Pros	Cons
TeleMetrum V3	- Built-in GPS - Reliable - Dongle - Easy setup - AtlasOS - Telemetry - Extremely programmable	- High price ($300 TeleMetrum + $100 TeleDongle) - Large Antennae requires a larger AV bay
RRC3	- Low Price ($75+$25) - Easiest Setup - MWDACS program - Good brand	- Fewer features than TeleMetrum - Would require a GPS
Raven4	- Good software - Solid and reliable - Test exercises in the program - Easy Setup - Variety of data collected - Owner of the brand is responsive on forums - LED visuals	- Nothing overly special to stand out - No GPS features - May require extra wiring if the PowerPerch is not bought
Eggtimer Proton	- Low Price ($70) - Highly customizable with modules - Wi-Fi capabilities - Remote arming	- Setup Time - Soldering - Possibility of failure due to manufacturing process - Simplistic program with

		minimal features

Table 4.1-2: Redundant Altimeter Pros/Cons

Altimeter	Pros	Cons
RRC2+	- Quick setup time - Simple and Reliable	- Reports data in beeps - Lacking in customization
StratoLoggerCF	- Praised for Reliability - Highly programmable with presets - Computer Interface for Data - Dual deploy - LED visuals	- Slightly longer setup time - Needs additional accessories for full capability - Not as customizable - Out of stock
EasyMini	- Reliable Brand (Altus Metrum) - Computer Interface for Data	- High Price ($80) - Slightly longer setup time

Table 4.1-3: GPS Pros/Cons

GPS	Pros	Cons
TeleMetrum V3	- Dual deployment functions - Ground testing with software - Easy Setup	- High price ($300 + $100 TeleDongle) - Large Antennae requires a larger AV bay
Eggtimer TRS	- Dual deployment functions - Low price ($90 +$25 receiver)	- Requires soldering - Long setup time
RTx/GPS Telematics	- Simple setup - LCD screen option for maneuverability	- High price ($329 + $25 Dongle) - No dual deployment features

4.2 Avionics Leading Components

The leading components for the avionics are the TeleMetrum V3 and the StratologgerCF, as shown in **Figures 4.2-1** & **Figure 4.2-2**. The TeleMetrum is the main altimeter that offers active tracking and dual deployment. The primary reason the TeleMetrum was selected was due to the integrated GPS functions. This allows the team to eliminate the need for an additional device in the AV bay. A StratologgerCF will be implemented to provide redundancy in the event the TeleMetrum fails.

The StratologgerCF was chosen due to its cheap price and simple setup. The Stratologger also offers flight data for the altitude, temperature, and battery voltage. **Tables 4.2-1 and 4.2-2** below display the trade matrices conducted for the leading altimeters.

Figure 4.2-1: TeleMetrum V3

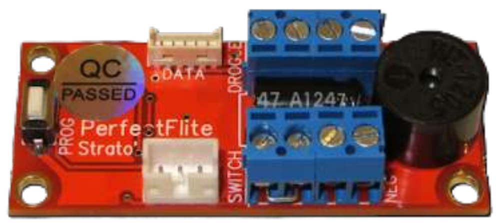

Figure 4.2-2: StratologgerCF

Table 4.2-1: Main Altimeter Trade Matrix

Utility value (1-10)		Option #1		Option #2		Option #3		Option #4	
		Telemetrum v3 (Altus Metrum)		RRC3 (Missile Works)		Raven 4 (Featherweight Electronics)		Eggtimer Proton (Eggtimer Rocketry)	
Criteria	**Weight**	**Utility Value**	**Weighted Value**	**Utility Value**	**Weighted Value**	**Utility Value**	**Weighted Value**	**Utility Value**	**Weighted Value**
Cost	2	3	6	6	12	5	10	8	16
Labor	1	6	6	9	9	8	8	2	2
Manufacturing	2	7	14	7	14	7	14	2	4
Reliability and Redundancy	4	8	32	7	28	7	28	5	20
Programmability	2	9	18	7	14	8	16	5	10

Flight Data	4	9	36	7	28	7	28	6	24
Weighted Total		**112**		**105**		**104**		**76**	

Table 4.2-2: Redundant Altimeter Trade Matrix

Utility value (1-10)		**Option #1**		**Option #2**		**Option #3**	
		RRC2+ (MissileWorks)		**StratoLoggerCF (PerfectFlite)**		**EasyMini (Altus Metrum)**	
Criteria	**Weight Value**	**Utility Value**	**Weighted Value**	**Utility Value**	**Weighted Value**	**Utility Value**	**Weighted Value**
Cost	2	8	16	7	14	4	8
Labor	1	8	8	6	6	6	6
Manufacturing	2	7	14	6	12	7	14
Reliability and Redundancy	4	6	24	8	32	7	28
Programmability	2	6	12	7	14	7	14
Flight Data	4	4	16	6	24	7	28
Weighted Total		**90**		**102**		**98**	

4.3 Redundancy Plan

In terms of redundancy, the TeleMetrum will be wired to a black powder charge above and below the AV bay in altimeters, a StratologgerCF will be used as a second altimeter and will be used as redundancy in case the TeleMetrum fails for any reason. Due to the possible interference between the main and redundant altimeters, the team decided to implement a shielding plan to prevent signal interference. This plan would consist of copper tape around each electronic device with the antenna of the TeleMetrum extruding outside of the tape to provide a telemetry and GPS downlink. Additionally, copper tubes would cover the steel bolts that hold the AV bay together.

4.4 AV Bay Design

The design of the avionics bay features the TeleMetrum and Stratologger mounted on the 3D printed removable sled. **Figures 4.4-1** and **4.4-2** below display the general layout of the avionics bay. These altimeters will be on independent circuits as shown in **Figure 4.4-3** below which displays the schematics for the TeleMetrum and Stratologger altimeters. Both altimeters will have independent power supplies as well as independent key switches. These key switches will be accessible outside of the rocket's airframe to allow for external arming of the recovery electronics. The 3D printed sled will allow access to the recovery electronics outside of the threaded rods and will hold two bulkheads and sled in place. The copper tape will be utilized to shield the recovery electronics from electromagnetic interference.

The avionics bay will have four charge wells, each will house a single black powder charge. The placement of the charge wells can be seen in **Figures 4.4-1 & 4.4-2.** Two of the charge wells are placed on the top bulkhead and two on the bottom bulkhead. Terminal blocks will be placed on the top and bottom bulkheads. These terminal blocks will allow the connections to be made between the e-match wire and the spiral wire from the altimeters. The e-match will be inside the charge wells to ignite the black powder during the recovery events. U-bolts will be mounted to the top and bottom bulkheads to allow quick links to be connected from the shock cords.

Figure 4.4-1: Isometric View of AV Bay

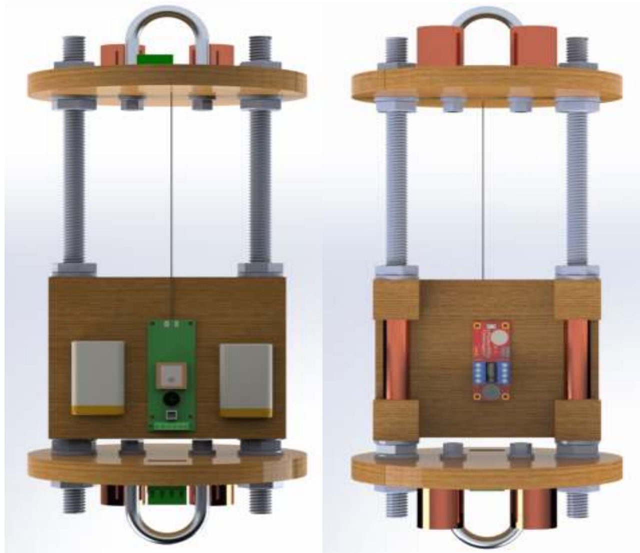

Figure 4.4-2: Front and Back View of AV Bay

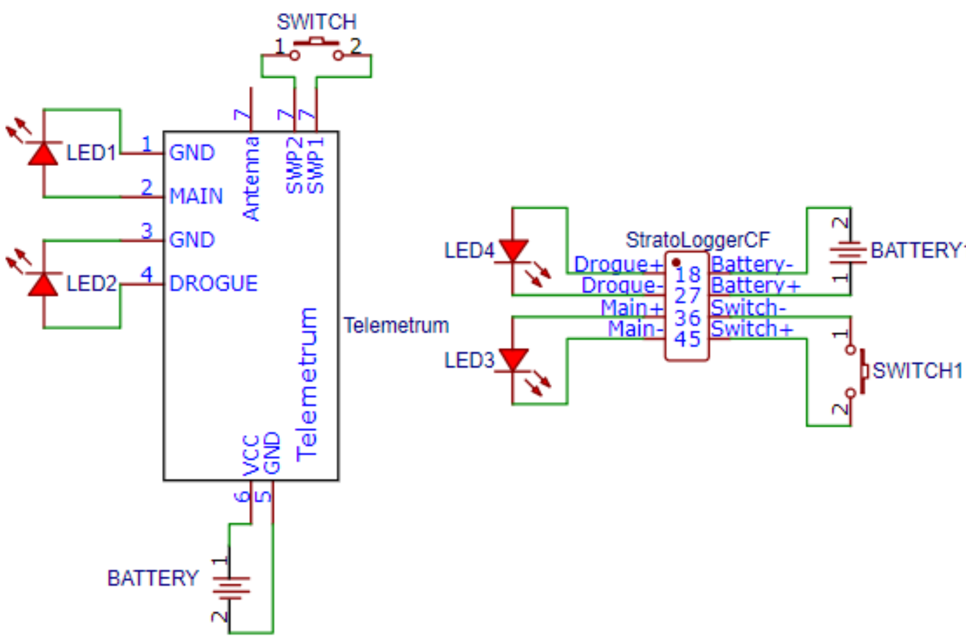

Figure 4.4-3: Electrical Schematics for TeleMetrum V3 and StratologgerCF

Regarding the frequency of the TeleMetrum the downlink of telemetry and GPS signals, the team has opted to select the default frequency of 434.550 MHz to simplify the setup times. However, the team understands that by necessity, the frequency may need to be changed before launch to avoid signal interference with other teams. In this scenario, the team would alter the altimeter's transmission frequency through AltOS before launching at the request of the launch supervisors.

The altimeters would require considerable amounts of power throughout the standby time on the pad, launch, and recovery. To account for this, the team determined the current consumption of the TeleMetrum and StrattoLoggerCF, the intended main and redundant altimeters, to be a total of 150mA and 1.5mA respectively. The team has selected a pair of 1200mAh lithium polymer batteries to be sufficient in powering the AV bay. One li-po battery and mechanical arming switch are dedicated for each altimeter. With a milliamp-hours capacity of 1200, the main battery provides up to 8 hours of power while the redundant battery would last up to 800 hours of power. This would account for standby time before launch, the launch itself, and the recovery of the rocket. On a side note, Altus Metrum indicated that specific batteries may include an integrated current limiting circuit that could result in the battery shutting down after the igniter circuit fires. Therefore, the team will select batteries without the integrated current limiting circuit or remove them if possible. To test this, the team will conduct ground tests on the batteries using the fire igniter selection in the AltOS interface outside and inside a vacuum chamber to test the battery's reliability.

4.5 Parachutes

4.5.1 Spring Ejection System

This method uses a high-powered spring that is compressed and placed underneath the parachute canister. The parachute would be capped tightly with a lid to keep the spring from expanding prematurely. Upon the time of release, the parachute lid would be removed using a small pyrotechnic or a triggered mechanism. The parachute would then be pushed out completely using the potential energy stored in the spring. The spring would be about $70-$90 including any additional parts needed for the ejection process. It could cost significantly more if a custom spring is needed instead.

If this option is chosen, the parts would have to be ordered/made separately and then assembled. The spring would be purchased beforehand while the spring canister would be made to order or could be 3D printed to fit the body tube accurately. The setup of the system is simple, the spring just must remain compressed until the time for parachute release. The release would trigger through a small pyrotechnic or mechanism as previously mentioned. This method would have a quick and easy setup. The spring would have to be pushed down and locked in compression and then the parachute would have to be folded shortly after. This process should only take a few minutes to complete.

The one reason why this method should be used is its simple and straightforward design. The main reason this method should not be chosen is that it takes up a lot of space in the rocket. There are a lot of components that go into this design, and it would require too much space, not leaving room for other equally important parts. Additionally, this method is somewhat unreliable since there is a chance that the spring could trigger prematurely and eject the parachute earlier than intended.

Figure 4.5.1-1: Ejection Spring

Table 4.5.1-1: Spring Ejection Pros and Cons

Spring	
Pros	**Cons**
• Complexity: Simplest of the 3 ejection methods • Safety: Safest of the 3 ejection methods with least chance of injury or damage by an explosion versus black powder and CO_2 • Performance: Least powerful but with less chance for error (misfire: black powder, leak: CO_2)	• Weight: Heavier than both black powder and CO_2 • Size: Largest of the 3 ejection methods • Cost: More than black powder, but less than CO_2 ○ Could cost more if a custom spring is needed • Reliability: Could easily activate at an inopportune time, could be hard to reset for multiple attempts

4.5.2 Black Powder Ejection System

Black powder is another method to achieve parachute deployment. This ejection system is relatively simple to set up, this is done by packing the wells with the appropriate amount of black powder. The wells are first secured to the bulkhead with epoxy, and the black powder is packed inside the wells with insulation material placed on top to ensure that the black powder is shielded from the outer components. Ejection is then achieved through the ignition of an e-match that is placed inside the canisters. The first e-match will be ignited at apogee to trigger the drogue parachute, then a second e-match will be ignited to eject the main parachute.

The charges are about $12 for a pack of 12 and the canisters are around $5. There is additional black powder in the team's inventory, so this option could be cost-free. Considering there is stored black powder in the team's inventory, and with the addition of a few parts, this setup is quite simple. On launch day, the black powder wells will need to be packed as soon as the avionics bay is initiated. The wells will be properly packed and can remain idle for more than 2 hours on launch day.

Black powder is a great option because it saves space which is ideal for the team's rocket that has limited space. Another great factor is that it is an easy design with great redundancy by wiring two ejection charges just in case the first one fails. The reason not to go with this design is because of a safety issue with the handling of black powder. Another issue that can arise is the potential to damage the parachute from the explosion, this can be prevented using a fireproof sheet that can be placed inside to shield the parachute from the explosion.

Figure 4.5.2-1: Black Powder Canisters

Table 4.5.2-1: Black Powder Ejection Pros and Cons

Black Powder	
Pros	**Cons**
• Weight: More than black powder but less than spring • Performance: Powerful • Size: Smaller than spring but needs more room than black powder • Safety: Safe less chance of explosion or fire so less chance of injury or damage • Reliability: Simple method of switching CO_2 tanks	• Complexity: The most complex device setup • Reliability: CO_2 tanks aren't refillable needing more tanks for multiple attempts adds to cost • Cost: Most expensive method with necessary components and CO_2 tanks •

4.5.3 CO_2 Pressure Ejection System

This method holds compressed gas (CO_2) in a cylinder cartridge. When the parachute needs to be released, a high-energy compression spring with a puncture device is released using a small pyrotechnic charge (E-match). This puncturing device creates the largest possible hole in the CO_2 cartridge, which releases the CO_2 at a very high velocity. This release pressurizes the parachute container, allowing the parachute to eject at a high velocity.

The cost for a CO_2 ejection device kit is about $190. This includes everything that is needed for two CO_2 ejection systems, including four of each of the 8 gram and 12-gram canisters. If more canisters are needed, each 8 gram and 12-gram canisters cost about $2 each.

CO_2 ejection systems are sold commercially. There is the option of buying everything separately, or in kits. It would be more convenient to order a kit, as it includes everything needed to have a functioning system. It would be possible that more than one CO_2 cartridge is needed, which is also sold separately. If this ejection method is chosen, a kit would be purchased and any needed extra parts from Fruity Chutes.

The benefit of this setup is that the package comes with all the parts necessary for this method. It also requires fewer explosive parts, as opposed to a black powder ejection charge. This allows for a much cleaner release that doesn't put the rocket body structure at risk. It is also a very lightweight method of ejection, which could save space and reduce weight. The disadvantages are that this method is quite expensive. The cartridges aren't refillable, so if more than 8 are needed for testing and launch, then more cartridges would have to be purchased, which will drive up costs even more so. Also, to meet the team's needed requirements using this option, it would make the setup more complicated because more parts are necessary. To maintain the required safety factor, this would require many more steps and parts to make it possible.

Figure 4.5.3-1: CO_2 Ejection Mechanism

Table 4.5.3-1: CO_2 Gas Ejection Pros and Cons

CO_2	
Pros	**Cons**
• Weight: Lightest of the 3 ejection methods • Performance: The most powerful method • Reliability: Easy to reset for multiple uses • Size: Most compact of the 3 ejection methods • Cost: The most affordable option	• Complexity: Relies on a spark to ignite so misfire is possible • Safety: Least safe of the 3 ejection methods with the highest chance of injury or damage by an explosion to both persons and the rocket and its components, especially the parachutes

4.6 Parachute Sizing Calculations

4.6.1 Drogue and Main Parachute Calculations

For the calculation of the main parachute, we started off by using the drag equation which is presented as follows:

$$F_d = \frac{1}{2}\rho\, v^2 C_d A$$

Where:
F_d = drag force
ρ = air density
C_d = drag coefficient
A = parachute area
v = velocity

When rearranged, this formula gives the area of the parachute which in turn can be manipulated once more to solve for the radius of the parachute. Finally, we can calculate the diameter of the parachute. Furthermore, considering that the launch vehicle will reach the terminal velocity at some point (acceleration is equal to 0), velocity is set to 0; only the drag and weight are along the y-axis.

The equation will look like this:

$$mg = \frac{1}{2} r C_d A v^2$$

Rearrange and write in terms of A:

$$A = \frac{2mg}{rCdv^2}$$

Then, plug in the values and solve for the area. Afterwards, use the following formula to find the diameter:

$$D = \sqrt{\frac{4A}{\pi}}$$

Since the spill hole must be accounted for, it must be subtracted from the diameter that was calculated. Considering that the spill hole is about 20% of the diameter, calculations can be made accordingly:

$$Diameter\ \ with\ spill\ hole\ \ = D \times 0.2$$
$$Actual\ Diameter = Diameter - Diameter\ with\ spill\ hole$$

From the calculations for the main parachute, the diameter is expected to be 10 ft, with a spill hole of 1.9 ft in diameter. These steps were also used to calculate the size necessary for the drogue parachute. The drogue parachute was calculated to be about 2 ft in diameter, with a spill hole of 0.4 ft in diameter. All calculations were verified via MATLAB and OpenRocket.

4.6.2 Drift Calculations

To calculate the drift, each value was converted from miles per hour to miles per second. The result was then multiplied by the previously calculated decent time leaving the drift in miles. This result was then converted to ft.

$$Drift \ = V_w t$$

All these equations were calculated by hand and then verified by using a code written in MATLAB. The results are shown in **Table 4.6.2-1.**

Table 4.6.2-1: Drift Calculations

Section	0 mph	5 mph	10 mph	15 mph	20 mph
Nose Cone	0 ft	657.934 ft	1,315.868 ft	1,973.824 ft	2,631.737 ft
Payload	0 ft	657.934 ft	1,315.868 ft	1,973.824 ft	2,631.737 ft
Motor	0 ft	657.934 ft	1,315.868 ft	1,973.824 ft	2,631.737 ft

$$Drift \ = \ [(\frac{V}{3{,}600 \ sec}) \times Total \ Time] \times 5{,}280 \ ft$$

$$Drift \ at \ 0 \ \ mph \ winds \ = \ [(\frac{0}{3{,}600 \ sec}) \times (89.72 \ sec)] \times 5{,}280 \ ft \ = \ 0 \ ft$$

$$Drift \ at \ \ 5 \ \ mph \ winds \ = \ [(\frac{5}{3{,}600 \ sec}) \times (89.72 \ sec)] \times 5{,}280 \ ft \ = \ 657.934 \ \ ft$$

$$Drift \ at \ 10 \ mph \ winds \ = \ [(\frac{10}{3{,}600 \ sec}) \times (89.72 \ sec)] \times 5{,}280 \ ft \ = \ 1{,}315.868 \ ft$$

$$Drift \ at \ 15 \ mph \ winds \ = \ [(\frac{15}{3{,}600 \ sec}) \times (89.72 \ sec)] \times 5{,}280 \ ft \ = \ 1{,}973.824 \ \ ft$$

$$Drift \ at \ 20 \ mph \ winds \ = \ [(\frac{20}{3{,}600 \ sec}) \times (89.72 \ sec)] \times 5{,}280 \ ft \ = \ 2{,}631.737 \ ft$$

4.6.3 Descent Time Calculations

To calculate descent time for every section of the rocket, MATLAB is used to find the velocity, which is:

$$v \ = \sqrt{\frac{2KE}{m}}$$

Where:

KE = Kinetic Energy
m = mass of heaviest section

Once the velocity was calculated, the following equations were used to find the descent times. This is the descent time after the drogue parachute is deployed, which is at apogee until the main parachute is deployed.

$$T_{drogue} = \frac{A - H_{main}}{80}$$

Where:
A = apogee height
H_{main} = main parachute release height

This equation is divided by 80 because 80 ft per second is the highest acceptable descent velocity for a drogue chute. After calculating T_{drogue}, find the descent time from the main parachute deployment until the rocket lands using the following equation:

$$T_{main} = \frac{H_{main}}{v}$$
$$T_{total} = T_{main} + T_{drogue}$$

Once these two are calculated, find the total descent time by adding them together. Following this process, a total descent time of 89.72 seconds is calculated, with the main deployment height of 600 ft. This time meets the landing time requirement of being under 90 seconds from apogee until the rocket lands. All these equations were calculated by hand and then verified by using a code written in MATLAB.

Descent Time Drogue:

$$Drogue\ Time = \frac{(5{,}100\ ft - 500\ ft)}{80\ ft/s} = 57.5\ sec$$

To find the descent time for the main parachute, compute the velocity of each section in the rocket.

$$Section\ 1\ Velocity = \sqrt{\frac{2(Max\ KE)}{8.6676\ Kg}} * 3.281 = 15.893\ \text{ft/s}$$

$$Section\ 2\ Velocity = \sqrt{\frac{2(Max\ KE)}{9.0901\ Kg}} * 3.281 = 15.519\ \text{ft/s}$$

$$Section\ 3\ Velocity\ =\ \sqrt{\frac{2(Max\ KE)}{2.5401\ Kg}} * 3.281\ =\ 29.358\ \text{ft/s}$$

Main Parachute Time: (Where Vmax = min velocity)

$$\frac{Main\ Deployment}{Vmax} = \frac{500\ ft}{15.519\ ft/s} = 32.22\ sec$$

Total Descent time:

$$Drogue\ time\ +\ Main\ time\ =\ Total\ Descent\ Time$$

$$57.5s\ +\ 32.22s\ =\ 89.72\ sec$$

4.6.4 Kinetic Energy Calculations

For kinetic energy to be calculated, the formula had to be rearranged to solve for the max velocity of each section. This was done by first assuming a kinetic energy value of 75 ft-lb or 101.69 Joules which is the max value for kinetic energy that cannot be exceeded. For each section, the max velocity was taken and the highest acceptable velocity to descend at was determined from these values.

$$v_{max}\ =\ \sqrt{\frac{2 * KE}{m}}$$

Where:
v_{max} = Max velocity
KE = kinetic energy
m = mass of section

Next, the kinetic energies for each section after the drogue parachute's ejection were calculated using the standard equation for kinetic energy. Finally, the kinetic energies for each section after the main parachute's ejection were calculated using the standard equation for kinetic energy shown below. The same calculations are done for the sections after the main separation.

$$KE\ =\ \frac{1}{2}mv_{max}^2$$

Where:
KE = Kinetic energy of section
m = mass of section
v_{max}= Max velocity of the section

Table 4.6.4-1: Kinetic Energy After Drogue Release

Section of Rocket	Kinetic Energy ($lb_f - ft$)
Section 1 - Nose Cone	1,900.3061
Section 2 - Payload	1,992.9153
Section 3 - Motor & Motor Casing	556.892

Table 4.6.4-2: Kinetic Energy after Main Release

Section of Rocket	Kinetic Energy ($lb_f - ft$)
Section 1 - Nose Cone	71.512
Section 2 - Payload	74.997
Section 3 - Motor & Motor Casing	20.957

All these equations were calculated by hand and then verified by using a code written in MATLAB. Velocity for each section is:

$$V1 = \sqrt{\frac{2 \times 101.686\, Joules}{8.66769\, kg}} \times 3.281 = 15.8927\, \frac{ft}{s}$$

$$V1 = \sqrt{\frac{2 \times 101.686\, Joules}{9.0906\, kg}} \times 3.281 = 15.5187\, \frac{ft}{s}$$

$$V1 = \sqrt{\frac{2 \times 101.686\, Joules}{2.5401\, kg}} \times 3.281 = 29.358\, \frac{ft}{s}$$

$$V_{max} = 15.5187\, \frac{ft}{s}$$

Kinetic energy after drogue separation is:

$$Drogue\ KE1 = \frac{\frac{1}{2} \times (8.66769\, kg) \times (\frac{80}{3.28084})^2}{1.356} = 1{,}900.31\, lbf$$

$$Drogue\ KE2 = \frac{\frac{1}{2} \times (9.0901\ kg) \times (\frac{80}{3.28084})^2}{1.356} = 1,900.31\ lbf$$

$$Drogue\ KE3 = \frac{\frac{1}{2} \times (2.5401\ kg) \times (\frac{80}{3.28084})^2}{1.356} = 1,900.31\ lbf$$

Kinetic energy after main separation is:

$$Main\ KE1 = \frac{(0.5) \times (8.66760\ kg) \times (\frac{21.5821}{3.28084})^2}{1.356} = 71.51\ lbf$$

$$Main\ KE2 = \frac{(0.5) \times (9.0901\ kg) \times (\frac{21.5821}{3.28084})^2}{1.356} = 74.99\ lbf$$

$$Main\ KE3 = \frac{(0.5) \times (2.5401\ kg) \times (\frac{21.5821}{3.28084})^2}{1.356} = 20.96\ lbf$$

4.7 Optimal Component Summary

4.7.1 Ejection Method

The lead choice for the rocket's ejection method is black powder. Black powder is a simple yet reliable ejection method that uses black powder packed into charge wells that are ignited by an e-match to create a small, controlled detonation. The black powder is packed inside the wells with insulation material placed on top to ensure that the outer components are shielded from the black powder, this is done to help ensure at the ignition of the charge no black powder is on a component that could catch fire. The initial black powder charge via an e-match will be ignited at apogee, followed by a second charge that will eject the main parachute.


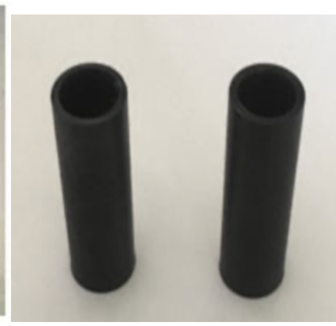

Figure 4.7.1-1: Black Powder Capsules & Figure 4.7.1-2: Charge Wells

Black powder was determined to be the best ejection system. This is because of its affordability, size, and setup. It is the most affordable option, costing around $12, while a CO_2 ejection system can cost $190, and a spring ejection system can cost around $80. Because each black powder capsule costs around $5, buying multiple for the redundancy plan is also affordable. Black powder does have its disadvantages, which includes that it can be an explosive hazard that can risk lighting the parachute on fire. This hazard is easily minimized; By placing a fire blanket between the parachute and motor, this will greatly reduce any damage the parachutes may take from the black powder ejection.

4.7.2 Redundancy

The rocket parachutes will have multiple black powder packs each with its own e-match. Multiple black powder packs ensure that if one fails by not igniting there are multiple attempts, increasing the chances of a successful deployment of the parachutes.

4.7.3 Drogue Parachute

The leading choice for the rocket's drogue parachute is the 30 inches compact elliptical parachute - 3.3lbf at 20fps. The cost of the chosen 30 inches compact elliptical-shaped drogue parachute is $77.41 and is being purchased from Fruity Chutes. The elliptical parachute has a high coefficient of drag (C_d) at about 1.6 which is ideal for decreasing the rocket's descent speed after apogee, while also allowing the rocket to have enough speed to descend within the 90 second time window. Furthermore, the elliptical parachute is designed to have better stability at high speeds, while also taking up the least amount of space when packed into the rocket. Overall, the elliptical parachute is the best drogue parachute choice for its C_d, stability, and low packing volume.

Figure 4.7.3-1: Drogue Parachute

4.7.4 Main Parachute

The leading choice for the main parachute is a 120 inches toroidal parachute from Rocketman parachutes. This parachute will cost around \$315.00 if purchased from Rocketman parachutes. The toroidal parachute is being chosen because of its high C_d value of 2.2. This will allow for a slow descent time as well as reduce the force in which the rocket lands, reducing any possible damage. Additionally, the toroidal parachute is compact and takes up minimal space inside the rocket making packing easy and quick while also leaving room for other important components of the rocket.

Figure 4.7.4-1: Main Parachute

5.0 Launch Vehicle Mission Performance

5.1 Official Target Altitude

For the 2021-2022 competitive year, the target apogee will be 5,100 ft AGL. This is a very achievable apogee given current weight estimates for the launch vehicle and its subsystems combined with the capabilities of the selected motor candidates. The current leading motor candidate, the Aerotech L2200G is predicted to propel the launch vehicle to an apogee above 5,700 ft which gives some margin for error in mass approximations and is close enough to the target apogee of 5,100 ft to allow the air brakes to slow the launch vehicle.

5.2 Flight Profile Simulations for Main Architecture

5.2.1 Flight Profile Predictions Vs. Time

The below figures show the flight profile predictions plotted against time in an OpenRocket simulation. In **Figure 5.2.2-1** shown below, the simulation shows the predicted altitude of the rocket during the flight. The apogee is approximately 5,700 ft at 18.5 seconds. The total flight time resulted in about 107 seconds. The altitude between drogue chute deployment and main chute deployment is relatively linear, indicating a constant terminal velocity had occurred.

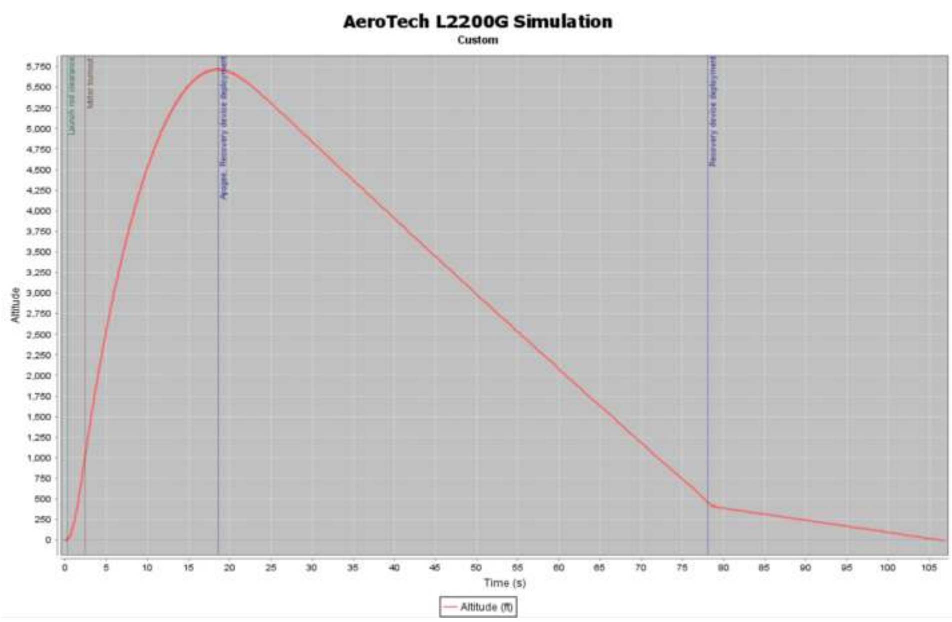

Figure 5.2.1-1: Altitude vs. Time

Figure 5.2.1-2 shows the maximum velocity the rocket reaches, which is around 690 ft/s at motor burnout. The rocket reaches terminal velocity during descent between the drogue parachute and main parachute deployment, which can be observed as about 80 ft/s. The jump in the graph from

-80 ft/s to -14.5 ft/s at around 85 seconds indicates the velocity around the time of the main parachute deployment. After the main parachute deployment, velocity decreases to about 14.5 ft/s until landing.

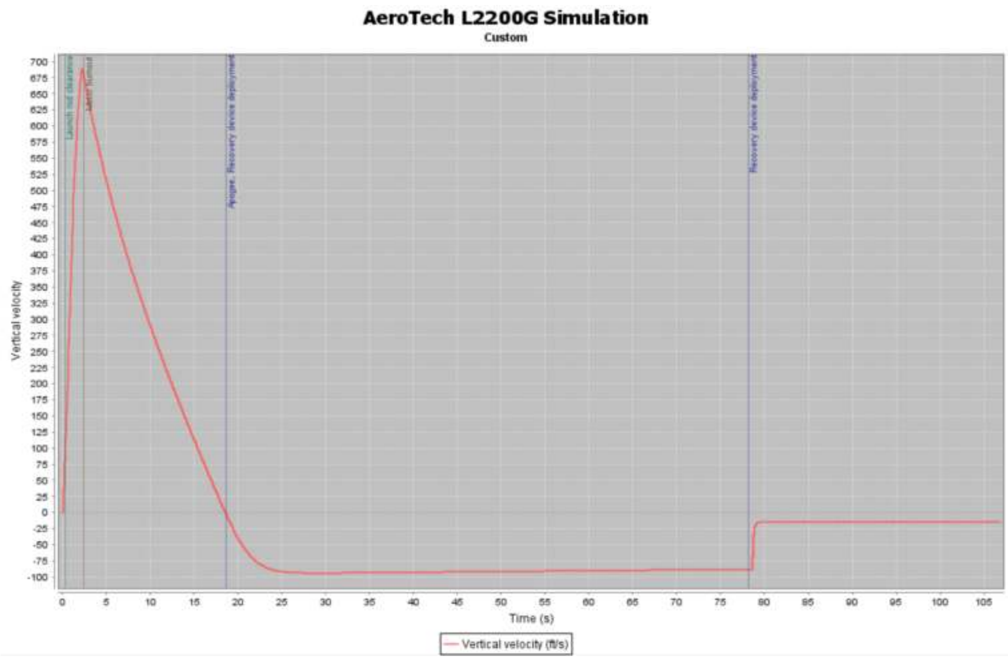

Figure 5.2.1-2: Vertical Velocity vs. Time

The graph in **Figure 5.2.1-3** shows that the maximum acceleration occurs around 0.8 seconds, reaching around 450 ft/s^2. We can observe that the acceleration reaches 0 m/s^2 between the deployment of the drogue parachute and the main parachute, indicating that the launch vehicle has reached terminal velocity. The acceleration spikes up to 1,000 ft/s^2 when the main parachute is deployed at around 78.2 seconds. The jagged plot after this point indicates the turbulence the rocket will experience from falling as multiple connected sections.

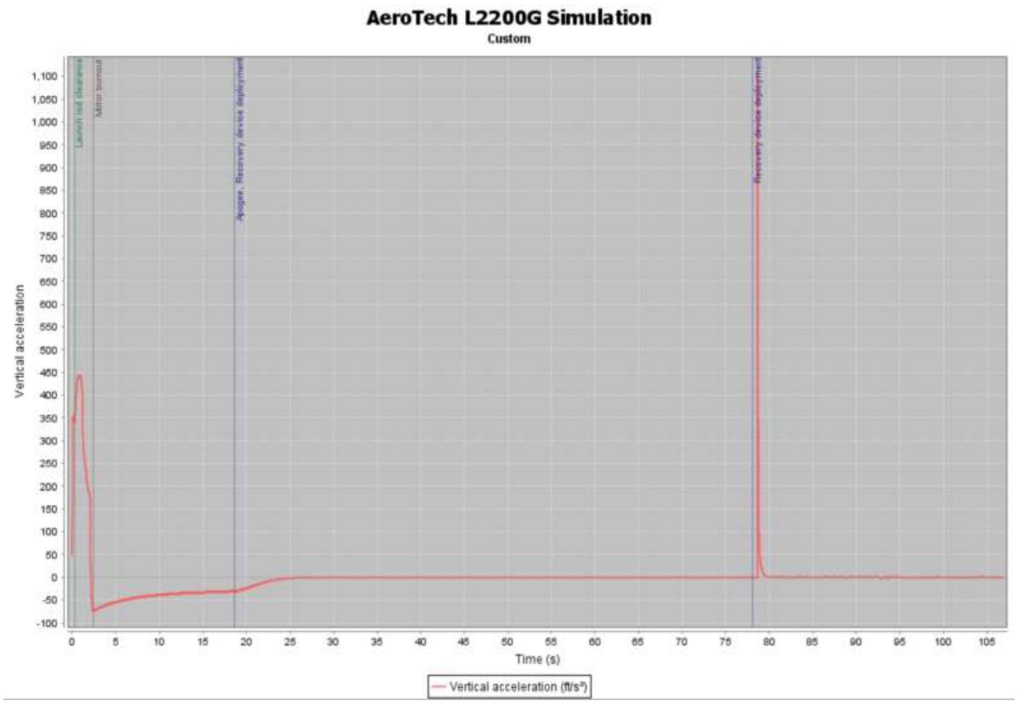

Figure 5.2.1-3: Vertical Acceleration vs. Time

5.2.2 Motor Thrust Curve

For our leading motor candidate AeroTech L2200G, we developed an OpenRocket model of the rocket and motor. As shown in the Motor Thrust vs. Time curve in **Figure 5.2.2-1**, the motor has a peak thrust of 670 lbf. Notable events occur, such as liftoff at 0.04 seconds, launch rail exit at 0.159 seconds, and motor burnout at 2.45 seconds.

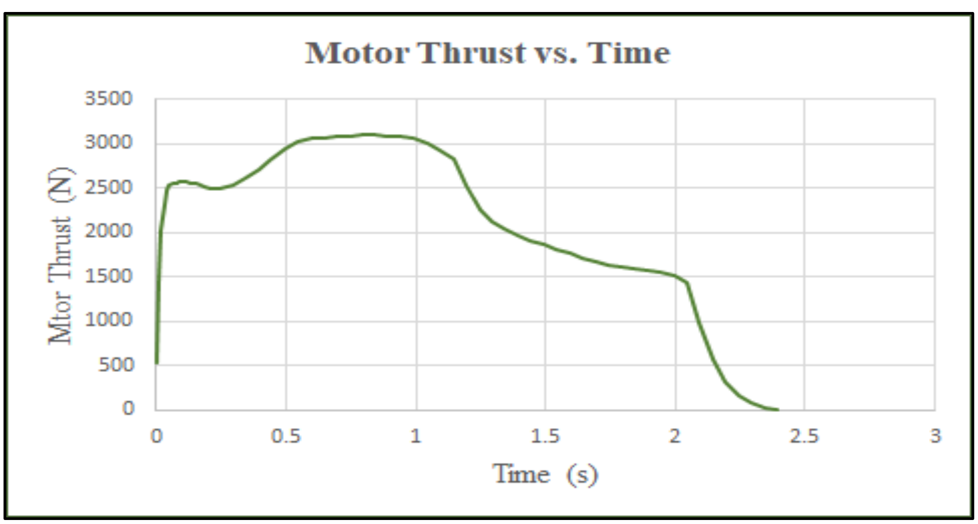

Figure 5.2.2-1: Motor Thrust vs. Time

From our Motor Thrust vs. Time plot we were then able to create our Thrust to Weight ratio vs. Time plot as shown below in **Figure 5.2.2-2.** From the plot, we were able to find a max Thrust/Weight ratio of 15.19.

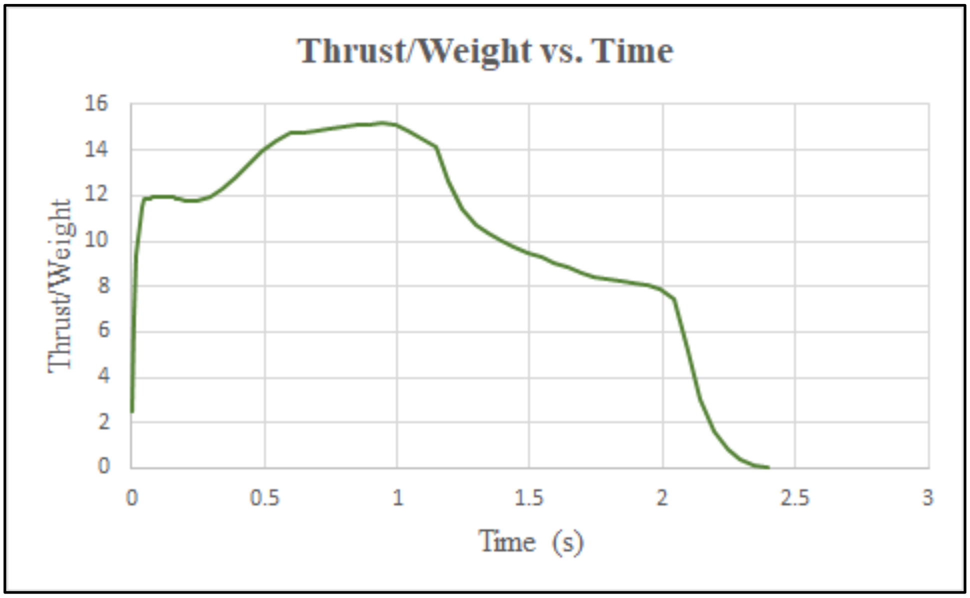

Figure 5.2.2-2: Thrust/Weight vs. Time

Shown below in **Figure 5.2.2-3**, we have the Motor Thrust vs. Time curve provided by the manufacturer which is identical to our developed Motor Thrust vs. Time curve showing the accuracy of our developed Thrust vs. Time curve.

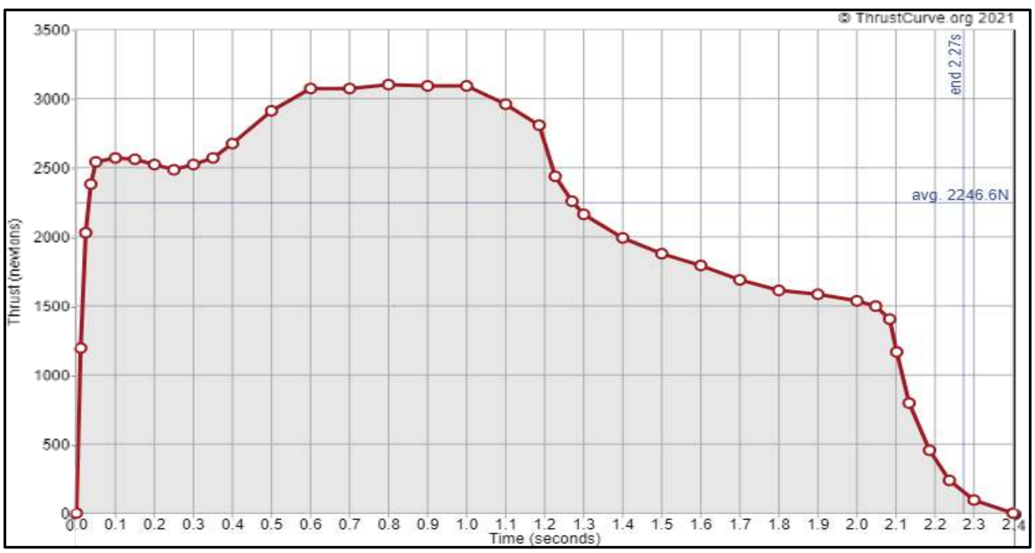

Figure 5.2.2-3: Motor Thrust vs. Time from Manufacturer

5.2.3 Launch Vehicle Expected Airframe Loads

Using a gross simplification of evenly distributed load on the rocket, airframe loads such as axial load, transverse shear, moment, peak stress, peak running load, equivalent axial load, and margin of safety can be calculated for the rocket. To begin, it must be known what thrust, as well as the height of each section of the rocket, will be. Using these values as well as the total height of the rocket, the following equation will be used to calculate axial loading on each section of the rocket:

$$P = (\frac{h}{H}) * T$$

Where:
P = axial load
h = height of section from bottom of rocket
H = total height of rocket
T = thrust of motor

We will also use the same variables along with the value for wind shear to calculate transverse shear using the following equation:

$$V = (H - h) * w$$

Where:
w = wind shear

The moment along any point of the rocket can also be calculated using the following equation:

$$M = \frac{(H - h)^2}{2} * w$$

Now that the force and moment have been obtained, the peak stress and running load, and the equivalent axial loads will be calculated. Peak stress will be calculated using the following equation:

$$f = \frac{P}{A} + \frac{Mc}{I}$$

However, since we know that:

$$c = R$$
$$A = 2\pi R t$$

$$I = \pi R^3 t$$

The equation becomes:

$$f = \frac{P}{2\pi R t} + \frac{M}{\pi R^2 t}$$

Where:
f = peak stress
R = radius of rocket
t = thickness of airframe

The same values will be used to calculate Peak Running Load using the following equation:

$$N = tf = \frac{P}{2\pi R} + \frac{M}{\pi R^2}$$

Similarly, we will use the following equation to calculate equivalent axial loading:

$$P = Af = P + \frac{2M}{R}$$

After attaining the peak stress due to axial load and moment, a simple margin of safety equation can be used to test for failure:

$$MS = \frac{Ftu}{f} - 1$$

Where:
Ftu = stress ultimate for the airframe
f = peak stress

This will help understand the strength of the aircraft and whether it will survive or fail.

After analyzing each section, the expected values are organized along with the values of the launch vehicle used for the calculations in **Table 5.2.3-1** thru **Table 5.2.3-3**:

Table 5.2.3-1: Airframe Section Heights

Section	Height of Item (in.)	Height from Base (in.)
Cone	34.5	112.0
Payload Bay	19	77.5
Avionics/Drogue	19	58.5
Motor/Airbrake Bay	39	39.5
Motor Overhang	0	0

Table 5.2.3-2: Rocket Constants

Ultimate Stress (psi)	Thrust of Motor (lbf)	Wind Shear (lbf)	Density (lb/in^3)	Total Height (in)
224800	696.91	69.61	4.256E-05	112

Table 5.2.3-3: Airframe Loads

Section	Axial Loading (lbf)	Transverse Shear (lbf)	Moment (lbf-in)	Peak Stress (psi)	Peak Running Loads (lbf/in)	Equivalent Axial Load (lbf)	Margin of Safety
Cone	661	69.69	1,254	336.91	28.64	1,079.6	666.2
Payload Bay	458	69.69	1,657	315.17	26.79	1,009.9	712.3
Avionics/Drogue	346	69.69	2,306	347.68	29.55	1,114.1	645.6
Motor/Airbrake Bay	233	69.69	2,962	380.89	32.38	1,220.5	589.2
Motor Overhang	3	69.69	4,315	449.74	38.23	1,441.1	498.8

This proves that the strength of the airframe holds strongly under launch conditions.

5.2.4 Air Brake Expected Loads

A simple analysis allowed for the calculation of expected loads and moments acting on the air brake system (ABS). The transverse loads, moments, and deflections at critical points on the ABS were obtained. Motor selection has dwindled down to three motors and analysis of the ABS has been analyzed for each motor. The following stress analysis will be for the AeroTech L2200G motor that was selected as the leading motor.

Four materials are being considered as possible options for the final ABS design. Material selection was based on available materials to the team and a need to keep the ABS durable. Thicknesses for each material are based on the maximum thickness offered by the manufacturer the air brakes will be outsourced to. The properties for each of the four materials are in **Table 5.2.4-1**.

Table 5.2.4-1: Material Properties for Potential ABS Material

Material	Thickness (in)	Modulus of Elasticity, E (ksi)	Allowable Shear Stress (ksi)
PLA	0.50	304	4.8
Al 5052	0.50	10,200	20
Al 6061	0.375	9,900	27
Al 7075	0.25	10,300	43

The ABS is idealized as a simple cantilever beam (fixed on one end and free on the other end) with a distributed load acting across it. The distributed load was assumed to be 10% of the maximum thrust provided by the AeroTech L2200G motor. Thus, the distributed load was assumed to be 6.97 lbf/in. Using Finite Element Analysis, the reaction forces at the fixed end and of the ABS were calculated. The deflections and rotations at the free end of the ABS were calculated as well. The required reaction forces and moments at the fixed end were also calculated. Reaction forces and moments at the free end for each material are in **Table 5.2.4-2.** Deflections and rotations at the free end for each material are in **Table 5.2.4-3.**

Table 5.2.4-2: Air Brake Loads

Materials	Force (lbf)	Moment (in-lbf)	Shear Stress (psi)	Margin of Safety
PLA	70.0	35.0	46.5	102
Al 5052	70.0	35.0	46.5	429
Al 6061	70.0	35.0	62.0	434
Al 7075	70.0	35.0	93.0	461

Table 5.2.4-3: Deflection and Rotation at the free end of the beam

Materials	Deflection (in)	Rotation (rad)
PLA	-0.000821	-0.00109
Al 5052	-2.73E-05	-3.65E-05
Al 6061	-6.68E-05	-8.91E-05
Al 7075	-0.000217	-0.000289

Based on the margin of safety, PLA would withstand the forces experienced in-flight, however, it offers less structural capability than the other materials. It can be concluded that PLA experiences the most extreme displacements at its free end. These displacements would negatively impact the performance of the rocket, leading to a lower-than-expected apogee. Although Al 7075 does have a large, positive margin of safety, its noticeable deflection would inhibit rocket performance. Alongside durability, down selection of the materials will be based on which is the least expensive and lightest. The pricing for the materials is listed in **Table 5.2.4-3**. The weights for the materials are listed in **Table 5.2.4-4**.

Table 5.2.4-3: Material Pricing

Materials	Price ($)
PLA	34.59
Al 5052	74.78
Al 6061	45.24
Al 7075	34.28

Table 5.2.4-4: Material Weights

Materials	Weight (lbm)
PLA	0.0677
Al 5052	0.145
Al 6061	0.146
Al 7075	0.152

Table 5.2.4-5 reiterates the criteria the materials were considered under. The criteria are durability, cost, availability, and weight. Each criterion has its weighted values based on what the team deems most important to the design of the launch vehicle. The most important criteria are durability and weight because of the impact airbrake deflections and weight will have on rocket performance. If deflections experienced are significant the overall rocket will fall short of the expected apogee. The team anticipates the launch vehicle to become heavier as the design process continues and so the weight of the air brakes must be kept to a minimum. The least important criteria are the cost and availability of the materials because the materials are relatively priced similarly and readily available. The results of the conducted trade study prove the Al 6061 to be the current leading candidate for the design.

Table 5.2.4-5: Material Trade Matrix

Utility Value (1-10)		Option 1		Option 2		Option 3		Option 4	
		PLA		Al 5052		Al 6061		Al 7075	
Criteria	**Weight**	**Utility Value**	**Weighted Value**	**Utility Value**	**Weighted Value**	**Utility Value**	**Weighted Value**	**Utility Value**	**Weighted Value**
Durability	5	7	35	9	45	9	45	5	25
Cost	2	9	18	3	6	7	14	8	16
Availability	2	10	20	10	20	10	20	10	20
Weight	4	9	36	7	28	7	28	6	24
Weighted Total		**109**		**99**		**107**		**85**	

5.2.5 Launch Vehicle Expected Loads for Bulkhead

The launch vehicle consists of 5 bulkheads. The material for the payload bulkhead will be fiberglass and the material for both the air brakes and avionics bay bulkheads will be plywood. The payload bulkhead properties are shown below in **Table 5.2.5-1**. This bulkhead will consist of a stainless steel I-bolt, nut, and washer.

Table 5.2.5-1: Payload Bulkhead Properties

Parameter	Value	Units
Material	Fiberglass	-
Diameter	6	in
Thickness	0.125	in
Epoxied Surface Area	2	in^2
Tensile Strength (F_{tu})	9.00	ksi
Yield Strength (F_{ty})	30.00	ksi
Bending Allowable (F_b)	16.00	ksi
Shear Strength (F_{su})	5.193	ksi
Epoxy Shear Modulus	4.80	ksi

This bulkhead will also have epoxy to secure it. This bulkhead will experience a normal force of 200 lbf, which is estimated by taking four times the loaded weight of the launch vehicle. It will also experience a shearing force of 6.97 lbf, which is estimated by taking ten percent of max thrust. Stress analysis for the bulkheads' I-bolt is shown below in **Table 5.2.5-2**. This analysis was carried out to ensure a positive margin of safety.

Table 5.2.5-2: Payload Bulkhead I-Bolt Stress Analysis

Parameter	Value	Units
Shear Stress	84.88	psi
Bending Stress	1.18	psi
Bearing Stress	223	psi
Shear Tear out Stress	9.30	psi

MS_{epoxy}	55.55	-
$MS_{bending}$	13,571	-
$MS_{bearing}$	725.4	-
$MS_{tearout}$	557.9	-

The avionics bay bulkheads will experience the same applied forces that the payload bulkhead experiences. Avionics bulkhead properties are shown below in **Table 5.2.5-3**. These bulkheads will also have a stainless-steel bolt, nut, and washer.

Table 5.2.5-3: Avionics Bay Bulkheads Properties

Parameter	Value	Units
Material	Birch Plywood	-
Diameter	6	in
Thickness	0.50	in
Tensile Strength (F_{tu})	5.03	ksi
Yield Strength (F_{ty})	2.00	ksi
Bending Allowable (F_b)	1.32	ksi
Shear Strength (F_{su})	89.92	ksi

Stress analysis for the avionics bay bulkheads is shown below in **Table 5.2.5-4.** This analysis was carried out to ensure a positive margin of safety.

Table 5.2.5-4: Avionics Bay Bulkheads I-Bolt Stress Analysis

Parameter	Value	Units
Shear Stress	-	psi
Bending Stress	4.72	psi
Bearing Stress	55.75	psi
Shear Tearout Stress	2.32	psi

$MS_{bending}$	278.9	-
$MS_{bearing}$	2,905	-
$MS_{tearout}$	38,709	-

Stress analysis was also conducted for the fasteners going into the avionics bay bulkheads. The critical fasteners are shown in **Table 5.2.5-5**.

Table 5.2.5-5: Avionics Bay Bulkheads Fastener Stress Analysis

No.	ϴ (degrees)	MS_{shear}	$MS_{shearTO}$	MS_{bear}
2	90	7.33	4.04	12.45
6	270	7.33	4.04	12.45

The air brakes bulkheads will experience an applied force of 35 lbf. The air brake bulkheads properties are the same as the avionics bay bulkheads. Shown below in **Table 5.2.5-6** is the stress analysis of the critical fasteners for these bulkheads to ensure a positive margin of safety.

Table 5.2.5-6: Air Brakes Bulkheads Fastener Stress Analysis

No.	ϴ (degrees)	MS_{shear}	$MS_{shearTO}$	MS_{bear}
1	45	104.7	94.89	169.5
2	90	134.7	122.1	218.0
8	360	134.7	122.1	218.0

5.2.6 Motor Mount Expected Loads

The main expected load for the motor mount tube is the thrusting force created by the motor as it ascends. This thrust will create a shearing force among the motor tube and the centering rings that are epoxied together to hold the motor stationary. The Aerotech L2200G motor is expected to have a peak thrust of 670 lbf. The centering rings are 0.12 in thick and have an inner diameter of 3.135 inches. From the info the calculations are done as followed:

The contact surface area among the centering rings and motor tube,

$$A_s = 2n\pi rt \ = \ 2n\pi(\frac{d}{2})t$$

Where:
n = number of centering rings
d = inner diameter of centering rings
t = thickness of a centering ring

$$A_s = 2n\pi(\frac{d}{2})t = 2(2)\pi(\frac{3.135\ in}{2})(0.12\ in) = 2.364\ in^2$$

The peak thrust is converted,

$$F = 3{,}100\ N = 696.91\ lb_f$$

The resulting shear stress,

$$\tau = \frac{F}{A_s} = \frac{(696.91\ lb_f)}{(2.364\ in^2)} = 294.8\ psi$$

The resulting shear stress is then compared to the lowest allowable shear strength of 580 psi for the epoxy at a temp of 550°F from the J-B Weld properties shown in **Figure 5.2.6-1**.

TECHNICAL DATA SHEET

J-B WELD

TEST	ASTM	RESULTS
Adhesion Strength	D297	1800 psi/126.6 kg/cm^2
Flexural Strength	D790	7320 psi/514.7 kg/cm^2
Tensile Lap Shear	D1002	1040 psi/73.1 kg/cm^2 (Room Temp 25°C Steel) 1840 psi/129.4 kg/cm^2 (3 hrs 400°F/204°C Steel) 671 psi/42.2 kg/cm^2 (3 hrs 550°F/288°C Steel) 1367 psi/96.1 kg/cm^2 (3 hrs 400°F/204°C Alum) 580 psi/40.8 kg./ cm^2 (3 hrs 550°F/288°C Alum)

Figure 5.2.6-1: J-B Weld Strength Properties

The margin of safety is used to evaluate failure in shear,

$$MS = \frac{\tau_{allowable}}{\tau} - 1 = \frac{(580\ psi)}{(294.8\ psi)} - 1 = 0.9672$$

The calculated results are summarized in **Table 5.2.6-1.** The results show that the motor tube would not fail under shear during flight with the margin of safety of 0.9672. This positive margin of safety ensures the team the motor will stay stationary within the rocket.

Table 5.2.6-1: Motor Mount Shear Analysis Results

Motor Mount Sear Analysis Results		
Expected Shear	294.83	psi
Shear Allowable @550°F	580	psi
MS @ 550°F	**0.9672**	**psi**

5.2.7 Fin Flutter Analysis

To conduct fin flutter analysis, we developed an excel to calculate Flutter Mach number of our prospective fins and their margins of safety. To create the excel we referenced the *NACA Technical Note 4197: Summary Of Flutter Experiences As A Guide To The Preliminary Design Of Lifting Surfaces On Missiles* by Dennis J. Martin, Langley Aeronautical Laboratory. As shown below in **Table 5.2.7-1**, we developed margins of safety for each of the fins we considered in our rocket design. For this analysis, the altitude MSL and shear modulus are 2,000 ft and 300 ksi, respectively. For the Flight Speeds, we assumed we were going to use the Aerotech L2200G Motor, as it is our leading candidate choice for our rocket. Upon our first analysis of the fins, we used an original thickness of 0.093 inch which led to all of them failing due to their lower Flutter Mach number. We decided to double the thickness of our fins, which led to positive margins of safety. As shown below, our leading fin candidates are fin models C-09, C-04, and C-05 as those provide us the highest margins of safety against fin flutter. Based on the flutter analysis, fin C-09 provided the least over stable stability of 2.0, whereas all our other fins were giving stability margins between 2.2 - 2.7. High stability margins would lead the rocket to fly directly into the wind, which would result in a lower apogee.

Table 5.2.7-1: Fin Flutter Analysis Spreadsheet

Fin	Root Chord (in)	Tip Chord (in)	Thickness (in)	Span (in)	Sweep Length (in)	Flight Speed, M	Flutter Mach number, M_f	Margin of Safety, MS
C-01	6	3	0.186	6	3	0.6380	1.368	1.143
C-02	6	2.6375	0.186	6	1.6875	0.6372	1.482	1.325
C-04	10	0	0.186	6	10	0.6380	3.531	4.534
C-05	6	2.25	0.186	4.5	2.625	0.6363	2.372	2.727
C-06	9	2.5	0.186	6	6.5	0.6345	1.772	1.793
C-08	6	3.125	0.186	6	4.5	0.6345	1.332	1.100
C-09	**10**	**2**	**0.186**	**4.265**	**7.125**	**0.6140**	**3.215**	**4.236**

5.2.8 Fin Drag Analysis

For our Fin Drag Analysis we also used excel with Root Chord, Tip Chord, Taper Ratio, Mean Aerodynamic Chord (MAC), Thickness, and Thickness to MAC ratio as inputs, which we used to calculate Panel Area and Drag Force. For our calculations the team used the max velocity created by our primary motor, Aerotech L2200G. As shown below in **Table 5.2.8-1,** we have the Drag Analysis of Fin C-09, which is our leading design choice. For all the fins, we compared the drag forces. Our chosen fin C-09 has a drag force of 7.30 lbf. Other fins we were considering using for our rocket were fin C-04 which has a drag of 8.95 lbf. and fin C-05 with a drag of 8.44 lbf. Apart from the lower drag force generated by fin C-09, it is also the fin that least over stabilizes our rocket which would allow us to reach a higher apogee.

Table 5.2.8-1: Fin Drag Analysis

Fin	Panel Area (in^2)	Thickness to MAC	C_{DF}	Drag (lb_f)
C-01	27.00	0.040	0.020	11.59
C-02	25.91	0.041	0.021	11.45

C-04	30.00	0.028	0.014	8.95
C-05	18.56	0.042	0.021	8.44
C-06	34.50	0.029	0.015	10.80
C-08	27.38	0.039	0.020	11.63
C-09	**25.29**	**0.027**	**0.013**	**7.30**

5.3 Launch Vehicle C_P and C_G Location Vs. Time

By using the model shown in **Figure 3.2.5-1**, center of pressure (C_P) and center of gravity (C_G) locations were able to be determined. Shown in **Figure 5.3-1** is the C_P and C_G location with respect to time. The location of these is vital to determining if the launch vehicle will be stable. For it to be stable the C_P location must be behind the cg location. The location is from the tip of the nose cone. The C_G location remains in front of the C_P location during the entire flight demonstrated in **Figure 5.3-1**.

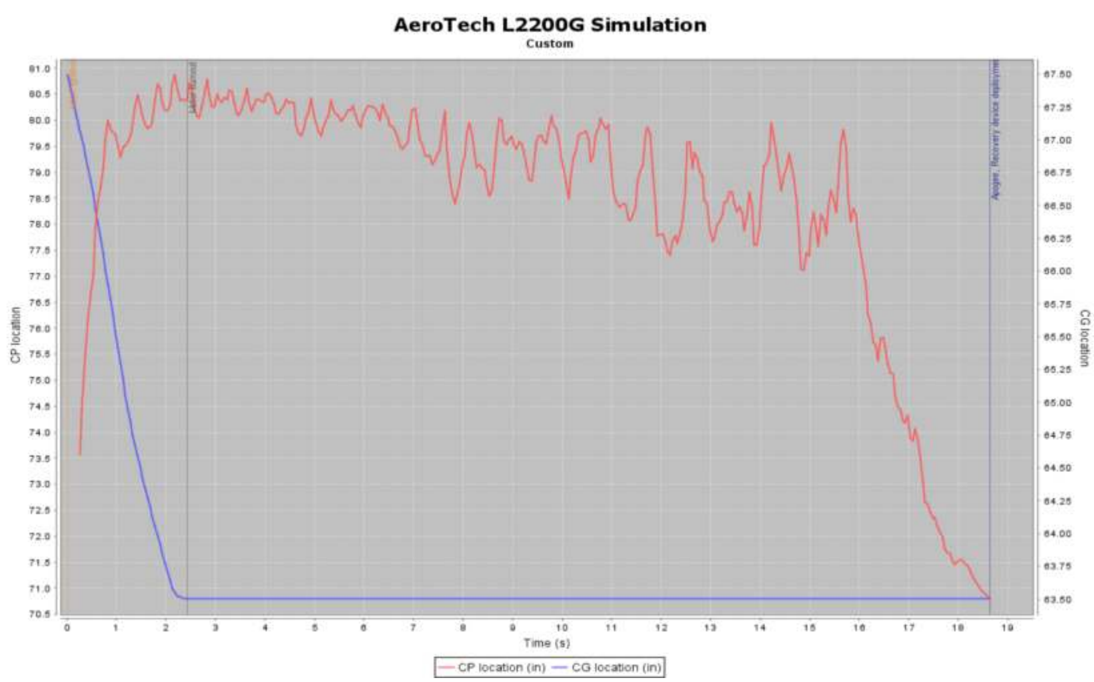

Figure 5.3-1: C_P and C_G Location Vs. Time

5.4 Launch Vehicle Kinetic Energy at Landing

The kinetic energy at landing for each section of the rocket was calculated using the equation $K = \frac{1}{2}mv^2$ with K as the kinetic energy, m as the mass of the section, and v as the ground hit velocity that is assumed to be equal for each section. **Figure 5.4-2** shows a zoomed-in view of the graph from **Figure 5.2.1-1**, around the time where altitude reaches zero, or at the time of the rocket's landing. the vertical velocity when the altitude approaches zero from the OpenRocket simulation is 14.5 ft/sec or 4.42 m/sec.

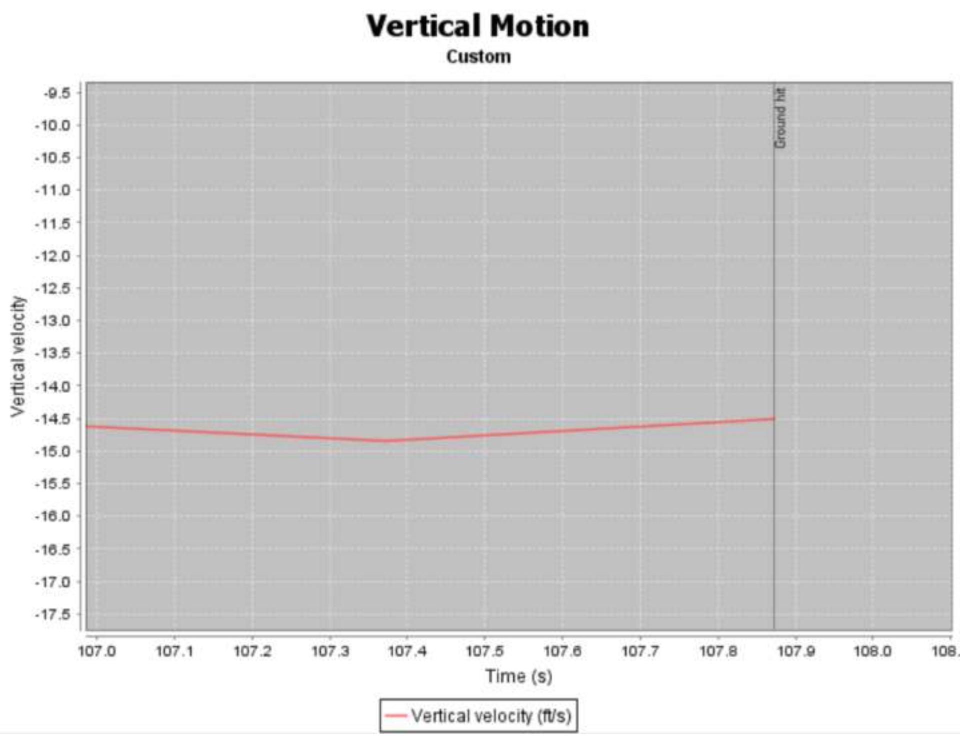

Figure 5.4-2: Vertical Velocity Near Landing

For the kinetic energy at the nose cone and payload section, the total mass is:

$$m_{cone} + m_{payload} - m_{parachute} = m_{nose,payload}$$

Where,

m_{cone}= total cone mass

$m_{payload}$ = total payload mass

$m_{parachute}$= main parachute mass

$m_{nose,payload}$= nose cone and payload section total mass

$$m_{nose,payload} = 2.5401 \text{ kg} + 5.67 \text{ kg} - 0.9072 \text{ kg} = 7.3029 \text{ kg}$$

Using this value for the mass of the nose cone and payload section, the kinetic energy is:

$$K_n = \frac{1}{2}(7.3029kg)(4.4196\frac{m}{s})^2$$
$$K_n = 71.32\ N - m\ \ or\ \ 52.61\ ft - lbs$$

For the kinetic energy at the avionics bay section, the total mass is:

$$m_{avionics} - m_{drogue} = m_{av.bay}$$

Where,
$m_{avionics}$= total avionics mass
m_{drogue}= drogue parachute mass
$m_{av.bay}$= avionics bay section toal mass

$$m_{av.bay} = 3.4162\text{ kg} - 0.6804\text{ kg} = 2.7358\text{ kg}$$

Using this value for the mass of the nose cone and payload, the kinetic energy at this section is:

$$K_a = \frac{1}{2}(2.7358kg)(4.4196\frac{m}{s})^2$$
$$K_a = 26.72\ N - m\ \ or\ \ 19.72\ ft - lbs$$

For the kinetic energy at the motor bay, the total mass is:

$$m_{motor\ bay\ total} + m_{burnout} = m_{motor\ bay}$$

Where,
$m_{motor\ bay}$= motor bay total mass
$m_{burnouts}$= motor burnout mass
$m_{motor\ bay}$= motor bay mass

$$m_{motor\ bay}\text{= 5.72229 kg + 2.265 kg = 7.98729 kg}$$

Using this value for the mass of the total motor bay, the kinetic energy at this section is:

$$K_m = \frac{1}{2}(7.98729kg)(4.4196\frac{m}{s})^2$$
$$K_m = 78.01\ N - m\ \ or\ \ 57.54\ ft - lbs$$

Table 5.4-1 summarizes the kinetic energy at each section of the rocket in N-m and ft-lb. The kinetic energy at all three sections does not reach the maximum allowable kinetic energy, which is 75 ft-lb, or 101.686 N-m.

Table 5.4-1: Kinetic Energy at Landing

Section	Kinetic energy (N-m)	Kinetic Energy (ft-lb)
Nose Cone and Payload	71.3233 N-m	52.6053 ft-lb
Avionics Bay	26.7190 N-m	19.7069 ft-lb
Motor Bay	78.0073 N-m	57.535 ft-lb

5.5 Launch Vehicle Descent Time

The launch vehicle descent time was determined using an OpenRocket simulation. This is the elapsed time from apogee to the point at which the launch vehicle reaches the ground. At approximately 18.5 seconds, the launch vehicle reaches apogee, which triggers the deployment of the drogue chute. It is then followed by the main chute deployment at approximately 78.2 seconds, further reducing descent velocity. Lastly, it will reach the ground at approximately 107 seconds. Based on these flight events, the calculated descent time is 88.5 seconds. This is also reflected in **Figure 5.5-1** below.

The simulated altitude was modeled for wind speeds ranging from 5 to 20 mph. This variation in wind speed produced negligible differences in altitude, showing that the horizontal force of the wind does not affect the vertical descent velocity in the OpenRocket model.

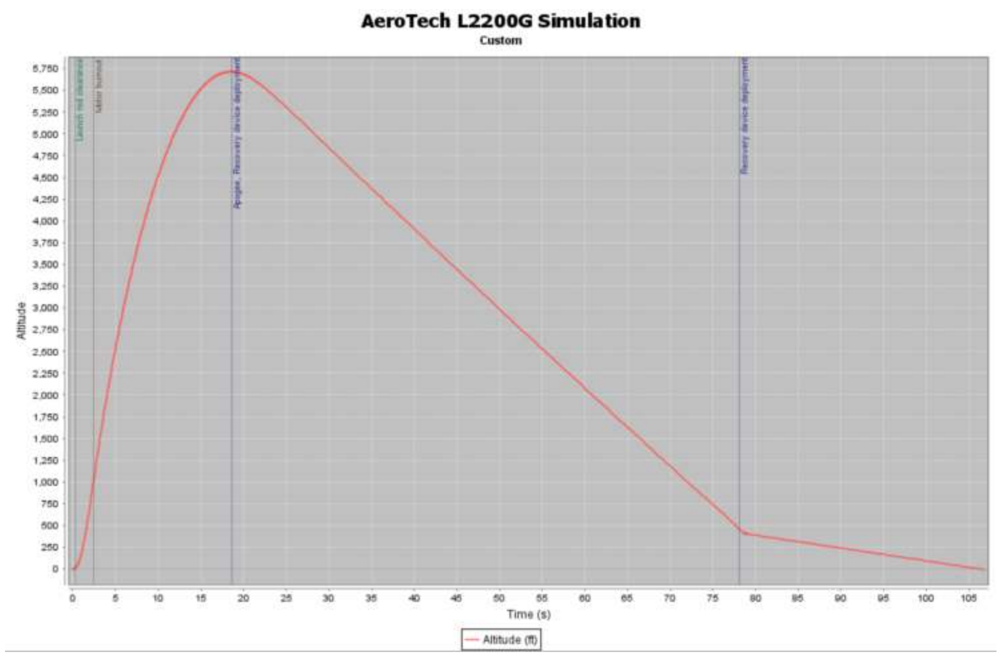

Figure 5.5-1: Altitude vs. Time

5.6 Launch Vehicle Expected Drift

As mentioned in the previous section, OpenRocket was utilized to simulate lateral distances for different wind speeds. Two different models were generated. The first model had a launch condition of launching in the direction of the wind, or downwind. The second model was launched against the wind, or upwind. The downwind model in **Figure 5-6.1** shows that the lateral distance increases linearly. As wind speed increases, the slope of the curve also increases.

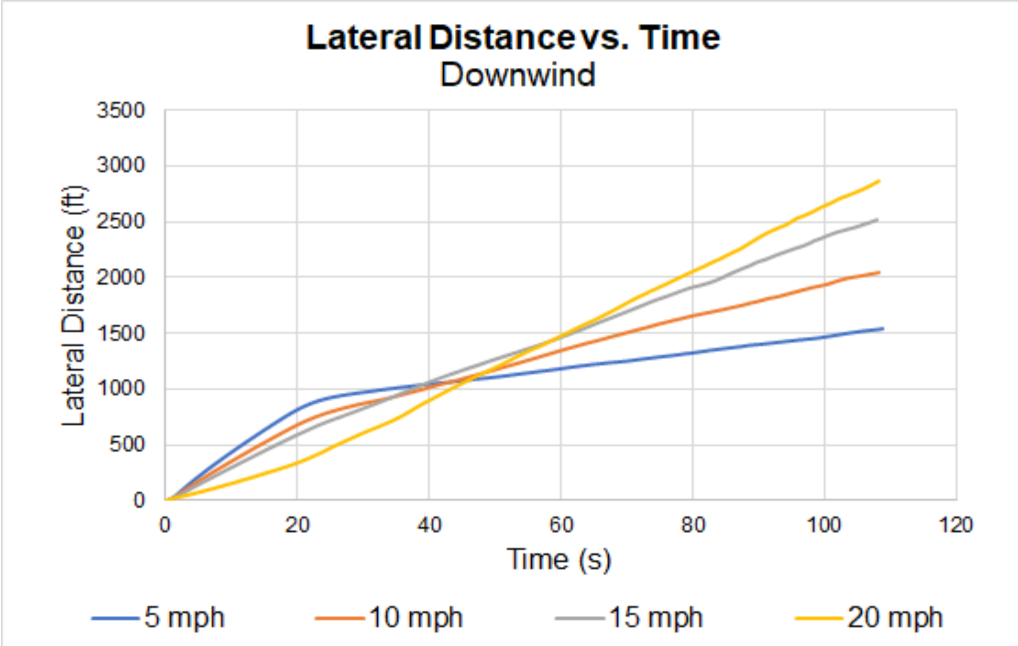

Figure 5.6-1: Lateral Distance vs. Time for Downwind Model

The upwind model in **Figure 5.6-2** begins with a linear increase in lateral distance, followed by a linear decrease. It reaches a point where it crosses the launch site, and then continues to drift past it. This is the result of launching directly toward the wind, which causes the launch vehicle to drift back toward the launch site.

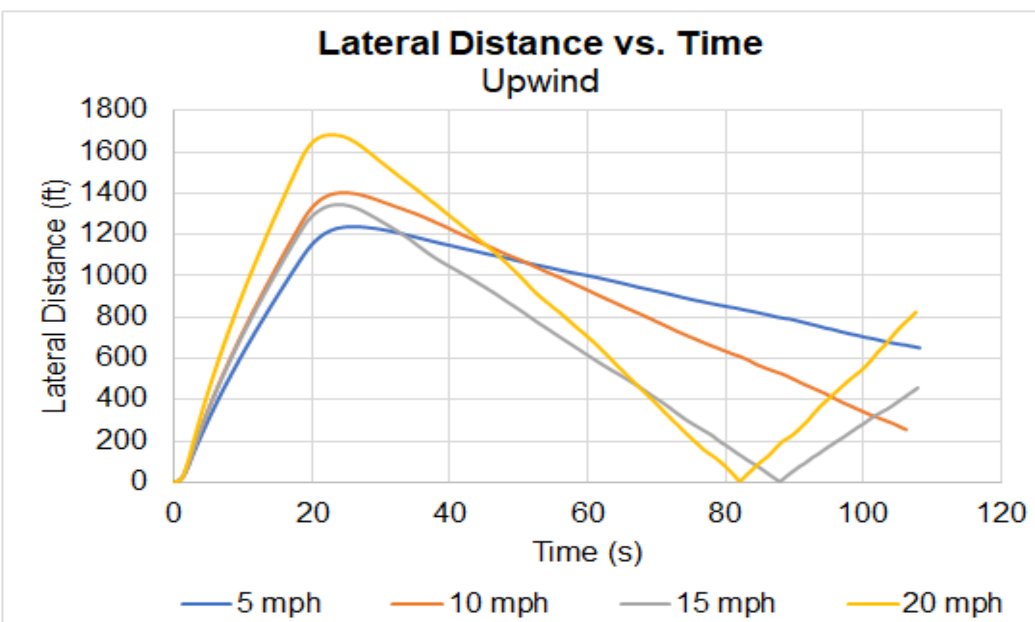

Figure 5.6-2: Lateral Distance vs. Time for Upwind Model

Comparing both models, the smallest lateral distance was approximately 253 ft, which resulted from the upwind condition with 10 mph winds. Shown in **Figure 5.6-3**, the worst-case scenario yielded a lateral distance of approximately 2,870 ft. This was for the downwind launch condition with 20 mph winds. This worst-case scenario includes the assumption of perfectly parallel winds relative to the launch direction, as well as a turbulence intensity of 20%. This result, of course, requires very exact conditions, which is highly unlikely to occur.

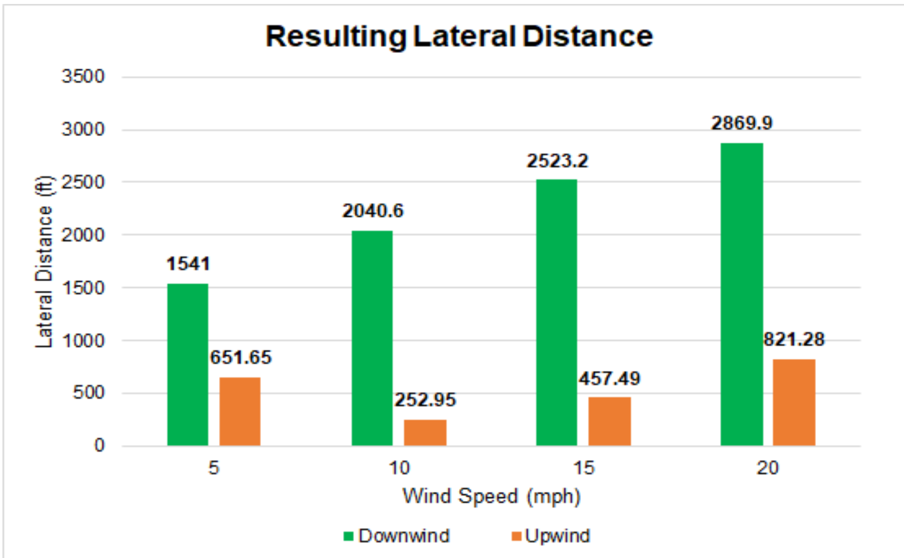

Figure 5.6-3: Resulting Lateral Distance

5.7 Alternate Calculation Method

In determining our locations for Center of Pressure (C_P) and Center of Gravity (C_G), we have defined the following coordinate system in **Figure 5.7-1**. For our analysis, the origin has been defined at the tip of the nose cone with the positive Y direction going toward the aft end of the launch vehicle.

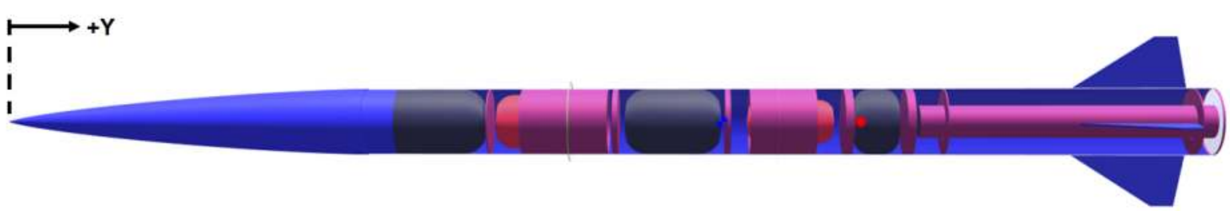

Figure 5.7-1: Launch Vehicle Coordinate System

5.7.1 Alternate Calculation Method for C_p and C_g

The center of pressure (C_p) location is critical in determining if the rocket will be stable. For the rocket to be stable, the C_p must be behind the center of gravity. The alternative method to find the C_p location from the OpenRocket simulation was through hand calculations. The analysis conducted had to be separated by regions of the launch vehicle, which consisted of the nose and fins. The hand calculations are executed as follows:

The launch vehicle will have an Ogive nose cone, giving its dimensionless coefficient that accounts for the shape of the nose to be equal to 2.

$$(C_{N\alpha})_n = 2$$

The center of pressure location for an ogive nose cone is,

$$\underline{x}_n = 0.466 \times l_{cone} = 0.466 \times 34.5\ in = 16.08\ in$$

Next was to find the dimensionless coefficient that accounts for the shape of the fins.

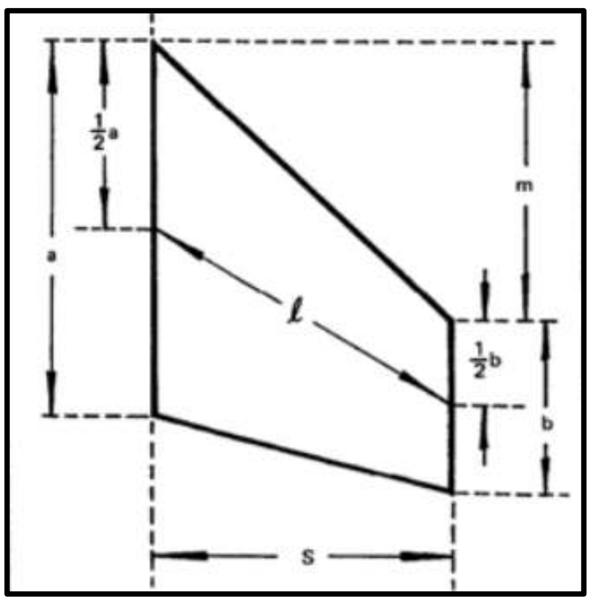

Figure 5.7.1-1: Fin Shape and Dimensions

The n in this next equation accounts for the number of fins for the launch vehicle and the d is the outer diameter of the launch vehicle.

$$(C_{N\alpha})_f = \frac{4 \times n \times \left(\frac{s}{d}\right)^2}{1 + \sqrt{1 + \left(\frac{2 \times l}{a + b}\right)^2}} = \frac{4 \times 4 \times \left(\frac{4.625}{6.17}\right)^2}{1 + \sqrt{1 + \left(\frac{2 \times 5.875}{10 + 2}\right)^2}} = 3.747$$

The center of pressure location for the fins is,

$$\underline{x}_f = x_f + \frac{m \times (a + 2b)}{3 \times (a + b)} + \left[\frac{1}{6} \times \left(a + b - \frac{a \times b}{a + b}\right)\right]$$
$$= 102 + \frac{7.125 \times (10 + (2 \times 2))}{3 \times (10 + 2)} + \left[\frac{1}{6} \times \left(10 + 2 - \frac{10 \times 2}{10 + 2}\right)\right] = 103.5\ in$$

A fin interference factor for 4 fins is needed to find the coefficient of the shape of the tail in the presence of the body. R is this next equation is the radius of the launch vehicle.

$$K_{fb} = 1 + \frac{R}{s + R} = 1 + \frac{3.085}{4.625} = 1.4$$

Giving the coefficient of the shape of the tail in the presence of the body to be:

$$(C_{N\alpha})_{fb} = 5.246$$

The center of pressure of the entire rocket is:

$$\underline{x} = \frac{(C_{N\alpha})_n \underline{x}_n + (C_{N\alpha})_{fb} \underline{x}_f}{(C_{N\alpha})_n + (C_{N\alpha})_{fb}} = 79.36\ in$$

Now comparing the hand calculation center of pressure with the OpenRocket simulated center of pressure at the launch pad.

$$\%\ difference\ = \frac{C_{P,_{OR}} - C_{P,_{handcalc}}}{C_{P,_{avg}}} \times 100 = \frac{(80.123\ in)\ -\ (79.36\ in)}{(79.74\ in)} \times 100$$
$$= 0.9568\%\ diff$$

For the calculation of the center of gravity (C_g), the team first determined the mass of each component within the launch vehicle. Then, the center of gravity location of each individual mass relative to the tip of the launch vehicle was determined. The mass and location of each component are then multiplied together to find the mass moment. The total of the mass moments is then divided by the total component masses to find the estimated C_g of the launch vehicle. The equations are shown below.

$$M_m = m * y$$

Where,
M_m = the mass moment
m = mass of the section
y= location of the center of section relative to the tip

Then finding the C_g,

$$C_g = \frac{\Sigma M_m}{\Sigma m}$$

The results of the calculations are shown in **Table 5.7.1-1** below,

Table 5.7.1-1: Alternate C_g Calculation

Section	Mass (lb)	Y Location (in)	Mass * Y (lb-in)
Nose Cone w/ballast	5.60	15.09	84.53
Payload Tube	2.38	44.00	104.72
Payload Integration	6.61	40.70	269.03
Payload Bulkhead	0.50	46.05	23.03
Main Chute	2.00	51.60	103.20
Payload Tube Coupler	1.00	53.05	53.05
AV Tube	2.34	63.00	147.42
Main Bulkhead	0.50	57.75	28.88
AV Bay	1.75	63.00	110.25
Drogue Bulkhead	0.50	68.00	34.00
Bottom Tube Coupler	0.94	73.00	68.91
Drogue Chute	1.50	73.73	110.59

Motor Body Tube	4.88	92.00	448.96
Upper Brake Bulkhead	0.63	78.85	49.28
Lower Brake Bulkhead	0.63	84.35	52.72
Top Centering Ring	0.19	87.55	16.20
Bottom Centering Ring	0.19	109.65	20.29
Inner Tube	1.20	98.38	118.05
Fins	0.70	105.05	73.54
Airbrake System	4.00	81.50	326.00
Totals	**38.02**	**58.98**	**2,242.62**

Shown in **Table 5.7.1-2** is the percent difference between the calculated center of gravity and simulated gravity. Also shown below is the equation used to obtain the value.

$$\% \, difference = \frac{C_{g,OR} - C_{g,handcalc}}{C_{g,avg}} \times 100$$

Table 5.7.1-2: C_G % Difference

Item	Calculated	OpenRocket
Center of Gravity	58.98 in	67.50 in
% Difference	**12.62%**	

5.7.2 Alternate Calculation Method for Apogee

The alternative method to find the resulting apogee from the OpenRocket simulation was through a hand calculation. The current selected motor is the AeroTech L2200G which has a total impulse of 5,104 Newton-seconds and a burn time of 2.30 seconds. The projected altitude relied heavily on two key factors: the distance to burnout and the coast distance to apogee.

The first step was to find the average thrust. The total impulse and burn time were needed to calculate this, which were provided by the AeroTech L2200G specifications. The next step was to verify the thrust to weight ratio meets the requirement of 5. Taking the thrust and dividing it by the rocket's weight, yielded the thrust to weight ratio of 9.84 at the accent portion. This was followed by the calculation of the max drag force using the max drag coefficient, C_a. This maximum drag force was subtracted from the thrust to determine the net thrust. The average velocity was then calculated using the equation below. This was needed to find both the distance to burnout and the coast distance to apogee. Lastly, those distances were added to find the projected apogee.

The model previously shown in **Figure 5.1-1** was used for flight simulation in OpenRocket, resulting in a projected altitude of about 5,735 ft. The projected altitude and other flight characteristics from the simulation are shown below in **Figure 5.7.2-1**.

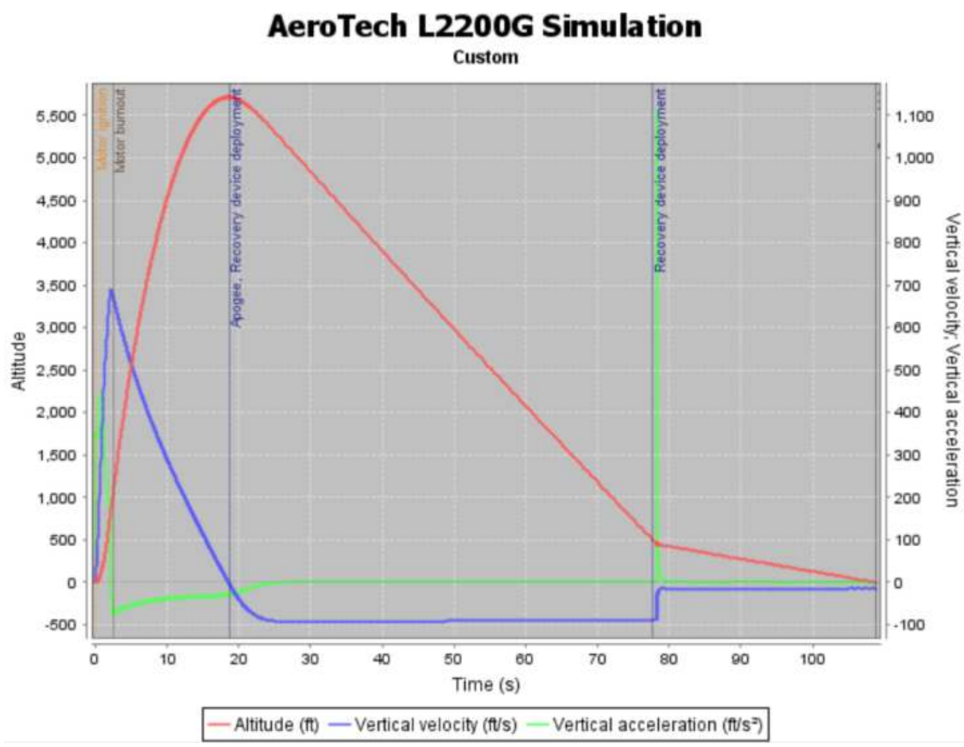

Figure 5.7.2-1: Simulated Flight Characteristics

The hand calculations are executed as followed:

The average thrust is shown as,

$$T_{avg} = \frac{I_{total}}{t_{burn}} = \frac{5{,}104\ N - s}{2.30\ sec} = 2{,}219.13\ N$$

The thrust to weight ratio found as,

$$\frac{T_{avg}}{W} = \frac{(2219.13\ N)}{(22.056\ kg)(9.8\ 1\ m/s^2)} = 10.26$$

Then finding avg velocity using the ratio,

$$v_{avg} = (\frac{T_{avg}}{W} - 1) - g - t_{burn} = (\ (10.26) - 1)(9.81\frac{m}{s^2})(2.30\ sec) = 208.85\ \frac{m}{s}$$

The max drag coefficient is $C_{d,max} = 0.54133$. The launch altitude is 2100 ft which results to an air density of$1.185\ kg/m^3$. The cross-sectional area of the 6-in diameter rocket body is $A = 0.019289\ m^2$. Now solving for solving for the max drag force,

$$D_{max} = \frac{1}{2}\rho v_{avg}^2 A C_{d,max} = \frac{1}{2}(1.185\frac{kg}{m^3})(208.85\ \frac{m}{s})^2(0.019289\ m^2)(0.54133) = 269.85\ N$$

Since this is the max drag force, it would be an overestimate to utilize it as a constant force during the burn time, so the team would estimate a third of the drag force to be an average constant drag force.

$$D_{avg} = \frac{1}{3}D_{max} = \frac{1}{3}(269.85\ N) = 89.95\ N$$

Now subtracting the average drag from the average thrust to get the net thrust,

$$T_{net} = T_{avg} - D_{avg} = (2{,}219.13\ N) - (89.95\ N) = 2{,}129.18\ N$$

Now adjusting the thrust to weight ratio,

$$\frac{T_{net}}{W} = \frac{(2{,}129.18\ N)}{(22.056\ kg)(9.8\ 1\ m/s^2)} = 9.8405$$

Now adjusting the average velocity after incorporating drag,

$$v_{adj} = (\frac{T_{\text{net}}}{W} - 1) - g - t_{burn} = (\ (9.8405) - 1)(9.81\frac{m}{s^2})(2.30\ sec) = 199.47\ \frac{m}{s}$$

Now solving for the distance covered during burnout,

$$s_{burnout} = \frac{1}{2}v_{adj}\ t_{burn} = \frac{1}{2}(199.47\ \frac{m}{s})(2.30\ sec) = 229.39\ m$$

Now solving for the terminal velocity after the burnout stage of the ascent to apogee,

$$v_t = \sqrt{\frac{2mg}{C_d \rho A}} = \sqrt{\frac{2(22.056\ kg)(9.81\ m/s^2)}{(0.54133)(1.185\ kg/m^3)(0.019289\ m^2)}} = 187.011\ \frac{m}{s}$$

Solving for the coasting distance after motor burnout to apogee,

$$s_{coast} = \frac{v_t^2}{2g} - ln\left(\frac{v_{adj}^2 + v_t^2}{v_t^2}\right) = \frac{(187.011\ m/s)^2}{2(9.81\ m/s^2)} - ln(\frac{(199.47\ m/s)^2 + (187.011\ m/s)^2}{(187.011\ m/s)^2})$$
$$= 1{,}354.22\ m$$

Apogee altitude resulting,

$$s_{alt} = s_{burnout} + s_{coast} = (229.39\ m) + (1354.22\ m) = 1{,}583.6\ m = 5{,}196\ ft$$

Now comparing the hand calculation apogee with the OpenRocket simulated apogee of 5,735 ft.

$$\%\ difference\ = \frac{s_{OR} - s_{alt}}{s_{avg}} \times 100 = \frac{(5{,}735\ ft)\ -\ (5{,}196\ ft)}{(5{,}465\ ft)} \times 100\ = 9.88\%\ diff$$

5.7.3 Alternative Calculation Method Differences

The alternative apogee hand calculations had gone under several assumptions to achieve an estimated apogee. The main assumption is considering the average thrust as a constant force. The team understands the thrust of the launch vehicle will be changing over time, but to make the computation easier the team used the average thrust (T_{avg}) as a constant force. Another main assumption used in the computation is the estimated average drag force (D_{avg}) being one-third of the max drag force (D_{max}). This was done to not estimate the effects of the drag force acting on the launch vehicle if the team had used the max drag force throughout the calculations. Lastly, the air density was assumed to be air density at 200 ft above sea level, which is the altitude of the nearest local launch site. This air density was considered a constant value during the calculations. These assumptions resulted in a percent difference of 9.88%, which indicates the sources of errors. These errors are most likely coming from the generalized assumptions as discussed earlier.

The alternative center of pressure (C_p) hand calculations were done by equations drawn from a technical report *Calculating the Center of Pressure of a Model Rocket,* written by James Barrowman. The equations stated in text were theoretically derived by the author for a research and development project which were published, so it was deemed as a reliable source. The calculations resulted in a percent difference of 0.986%, which further indicates the reliability of the technical report.

The alternative center of gravity (C_g) hand calculations were done using an assumption of all the components having uniform density. It's also assumed to be along the central line coming from the tip to base of the launch vehicle. The percent error of the calculation resulted in 12.62%, which is a bit high. A source for error could be from the assumption that the components have uniform density. This leads to the center of gravity to be at the geometric center of each section, which is not always true.

5.8 Alternative Simulation

For the chosen means of alternate simulations, Rocksim data was used to compare with the OpenRocket data. The same mass, motor, and surface finish properties were used in addition with the same locations of all structural components and subsystems with respect to the OpenRocket model to maintain as much similarity as possible. **Figure 5.8-1** shows the launch vehicle model that has been created in Rocksim.

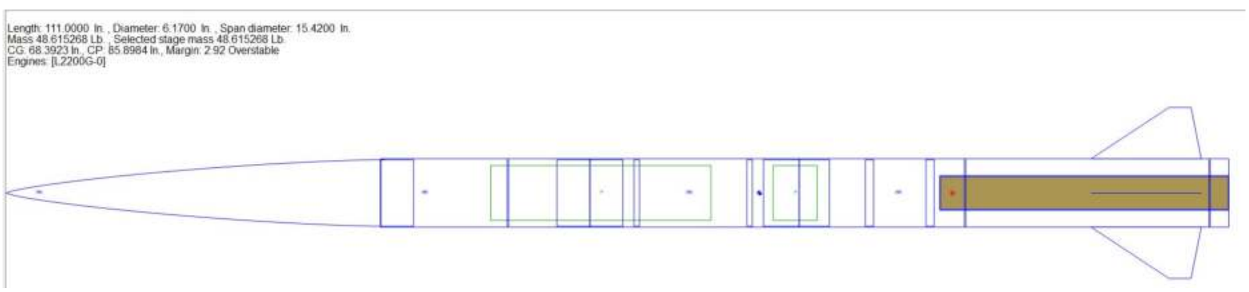

Figure 5.8-1: Rocksim Launch Vehicle

From this data, maximum velocity, acceleration, and apogee are shown in **Table 5.8-1,** which were used in comparison to the OpenRocket model.

Table 5.8-1: Rocksim vs. OpenRocket Results

Software	**Wet Mass** (lbm)	**Apogee (ft)**	**Max Velocity (ft/s)**	**Max Acceleration** (ft/s^2)	**Launch Stability**
OpenRocket	48.5	5,735	690	444	2.04
Rocksim	48.6	5,532	685	444	2.92

Rocksim % Difference	0.2 %	-3.54 %	-0.72 %	0 %	43.14%

From this data, the apogee, max velocity, and acceleration appear to be consistent between the two software programs. This gives growing confidence in flight predictions going forward considering that the predicted results are similar. It is still expected that the launch vehicle will gain mass due to manufacturing and further design details; however, it is very likely to achieve the target apogee of 5,100 ft with expected mass growth and the use of the air brake system.

The main difference in the simulation is the stability at launch with a 43.14% higher stability using Rocksim. Although both models show that the stability requirement of 2.0 is met, the high stability margin brings concern given that an over stable rocket could weathercock. Going into CDR, further analysis into the C_P and C_G locations will be done in both Rocksim and OpenRocket in conjunction with hand analysis to find more accurate stability approximations.

6.0 Payload Criteria

6.1 Payload Objective

6.1.1 Purpose Statement

The purpose of the 2021-2022 payload experiment is to design a payload capable of autonomously determining the location of the launch vehicle on a gridded, aerial image of the launch site without the use of a GPS. The gridded launch field image shall be of high quality and not extend beyond 5,000 ft by 5,000 ft.

6.1.2 Success Criteria

In addition to the statement above, additional criteria were set to better define what would be considered a successful payload mission. The success criteria are stated below:

1. The Payload shall be capable of remaining in the launch-ready configuration on the pad for a minimum of 2 hours.
2. The Payload shall be able to determine the location of the rocket within 165ft of its actual position.
3. The Payload shall be capable of transmitting location information back to the ground station after being ejected from the rocket.
4. The Ground Station shall be capable of receiving data that is transmitted from the payload.

6.2 System Level Design Alternatives

The following section examines the alternative system-level designs that were considered for the payload system. The group finalized the decision to avoid a ground rover payload design after viewing the terrain of the launch site shown in the PDR Q&A session. Alternative system-level designs included an Unmanned Aerial System (UAS) and a Capsule Style payload. These two candidate architectures are evaluated upon their characteristics, advantages, and disadvantages.

The first design that was considered was the Unmanned Aerial System (UAS), shown in **Figure 6.2-1** below. It is a quadrotor, multilayered UAS with an HX frame style, utilizing an IMU to track the Payload's trajectory from the launch pad and provide position data during a drone flight. This configuration has a propeller diameter of 3 in. The two layers are separated by standoffs, providing enough space for onboard electronics mounting. On the lower layer of the candidate architecture, the receiver, flight controller, electronic speed controller (ESC), an Arduino nano, and the four motors are placed. The battery and power distribution board that power the Payload system is positioned on the second layer. On the underside of the second layer, an inertial measurement unit (IMU) is mounted.

Pros:

- Allows movement in all three dimensions
- Allows possibility of launch vehicle identification through aerial imaging
- Can be custom built to conform to requirements
- Provides the possibility of flying back to the launchpad, allowing re-capture of data

Cons:

- Stability issues in windy conditions
- Limited electronics space
- Clearance for propellers necessary in every design
- Requires specific orientation for deployment

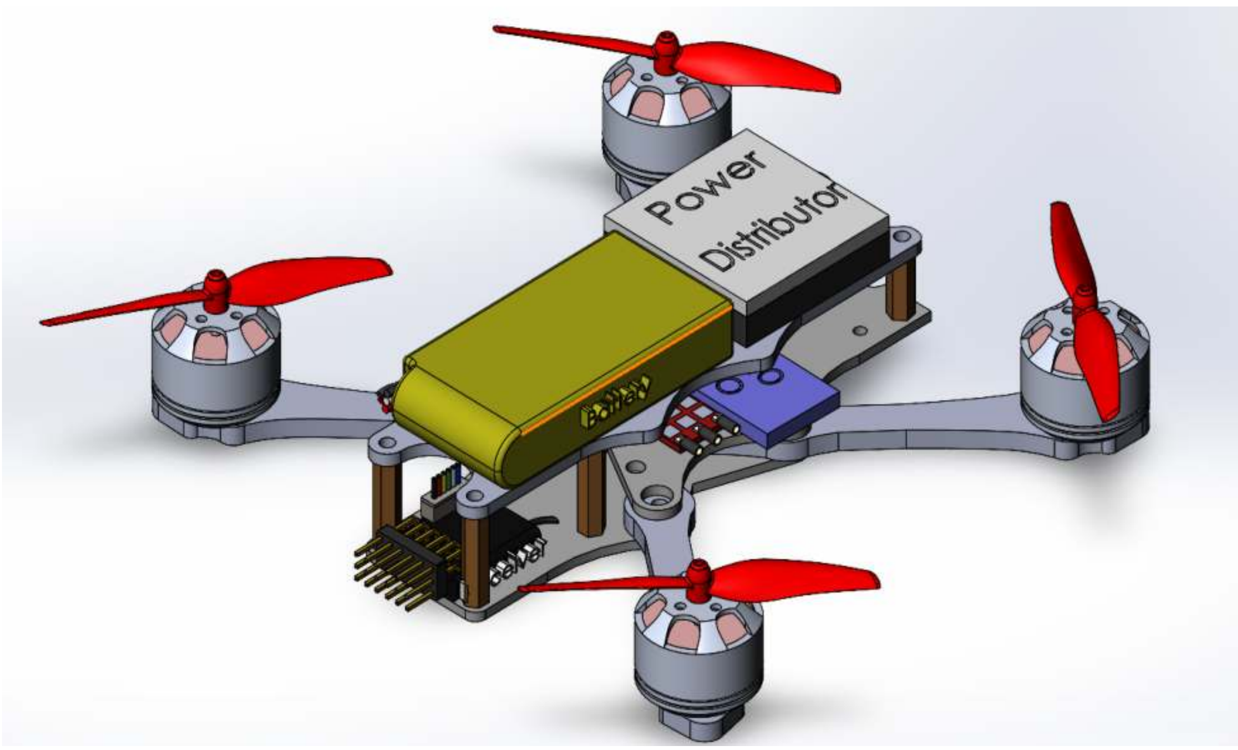

Figure 6.2-1: UAS Payload Isometric

The Capsule Style payload is a system of encapsulated electronics within the rocket, requiring no movement once deployed. This system is much easier to design and manufacture than the UAS, having no moving components and not requiring any special storage methods to fit within the rocket or special deployment methods to orient it correctly. The design is relatively basic, as it is essentially an enclosed electronics stack that will be deployed from the rocket. The electronics included to complete the mission are a microcontroller, an inertial measurement unit (IMU), two barometers, a wireless communication module, a battery, and a GPS module. In **Figure 6.2-2** below, a preliminary image of the Capsule Style payload is shown. It is a cylinder with multiple layers on the interior that provide adequate protection and mounting space for the electronics.

Pros:

- Simple to design and manufacture
- Fewer points of failure during mission execution
- Adequate room for electronics
- Does not require any special orientation for deployment

Cons:

- No way to reproduce data to compare with mid-flight data
- A larger body means that it will be heavier than the UAS design

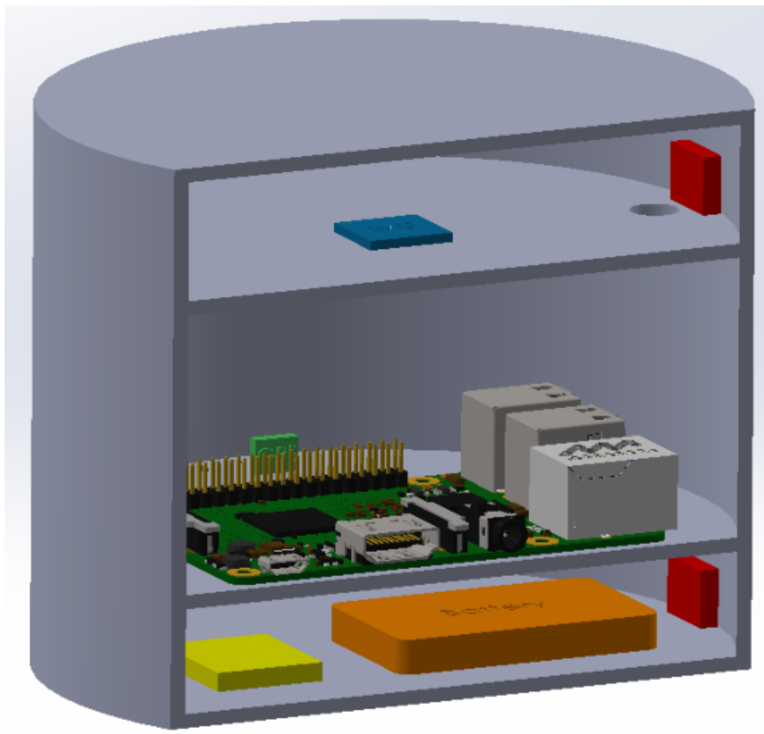

Figure 6.2-2: Capsule Payload Cutaway View

6.2.1 Candidate Architecture Alternatives

Table 6.2.1-1: Candidate Architecture Trade Matrix

Utility Value (1-10)		Option 1		Option 2	
		UAS		Capsule	
Criteria	**Weight**	**Utility Value**	**Weighted Value**	**Utility Value**	**Weighted Value**
On-Board Mounting Space	**2**	5	10	10	20

Deployment	**3**	6	18	6	18
Manufacturability	**5**	6	30	8	40
Reliability	**4**	8	32	6	24
Cost	**1**	5	5	9	9
Weighted Total		95		111	

After looking at the pros and cons for each of the design alternatives, the team went more in-depth into the two designs, quantifying the important characteristics for each of the alternatives in **Table 6.2.1-1** above. Each criterion is weighted from 1-5 going from least important to most important. The candidate architectures are then given a utility value from 1-10, 1 being the lowest utility and 10 being the highest utility. Multiplying the utility factor by the weight of the criterion produces the weighted values, which are then summed to provide the weighted total.

A post-Proposal design change reduced the diameter of the rocket, which necessitated a redesign of the payload. The UAS would be designed to have either spring-loaded flip-out arms or have its wheelbase reduced enough so that the payload fits. Flip-out arms increase the complexity of our payload and add an additional failure point to our mission; reducing the wheelbase of the payload makes it difficult to fit all the necessary electronics onboard. Because of the difficulties that these changes impose, the team determined that a stationary payload in the shape of a capsule would be most desirable. Thus, we deemed that this payload candidate architecture is the Capsule Style payload. This payload system is not mobile once deployed from the rocket and tracks the trajectory of the rocket during flight utilizing an IMU, corrected with pressure sensors, emulating a basic inertial navigation system. Manufacturability and reliability are the two most important criteria when grading candidate architectures. According to **Table 6.2.1-1**, the Capsule Style payload has the highest weighted total value because it has greater manufacturability, on-board mounting space, and cost ratings. The Capsule Style has better manufacturability because it is a simple 3D printed shape, with a few layers to separate the electronics and provide mounting room for them. The additional layers provide much more space for electronics than the UAS design because there is no need to account for propeller clearance and the center of mass location is negligible to the Capsule Style's performance. The Capsule Style is cheaper than the UAS design because it does not require a flight controller, motors, and a power distribution board.

6.3 Leading Candidate Design

From **Table 6.3.1-1** and the discussion in the previous section, the leading payload candidate architecture is a Capsule Style payload capsule containing an IMU and barometric pressure sensors that will act as a simple inertial navigation system. The following section will detail the chosen shape, material, and leading electronics components chosen for the Capsule Style payload.

6.3.1 Payload Capsule and Material Selection

The Capsule Style payload is designed to contain all necessary electronics while being easy to hold within the payload bay and easy to manufacture. The three capsule geometry options are a cuboid, a cylinder, and an ovoid, shown in **Table 6.4-1** below.

Table 6.3.1-1: Payload Shape Pros & Cons

Cuboid	Cylinder	Ovoid
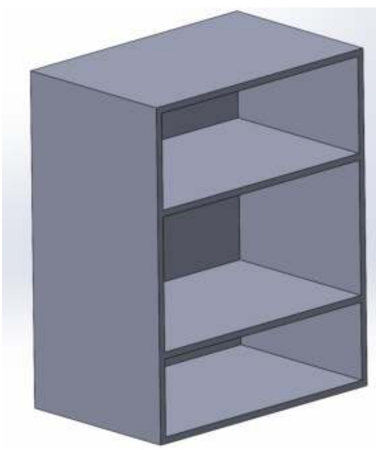	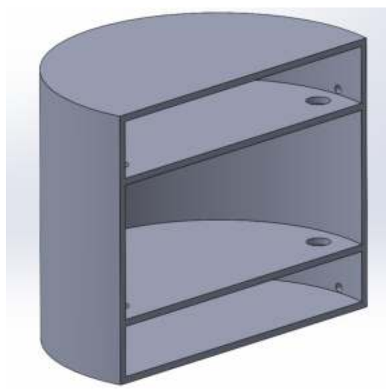	
Pros: ● Plenty of electronics mounting space	Pros: ● Plenty of electronics mounting space ● Easy to interface with payload integration	Pros: ● Easier fitment within the launch vehicle ● Provides more space to payload integration for deployment
Cons: ● The geometry makes launch vehicle fitment difficult	Cons: ● Less space for payload integration deployment	Cons: ● Comparably less mounting space ● More complex shape

Based upon the pros and cons listed above, the team decided to choose a cylindrical shape for the payload capsule. A cylindrical capsule provides slightly more area to mount electronics than the cuboid shape and significantly more room than the ovoid shape. Additionally, it is easier to put a cylindrical capsule into a cylindrical launch vehicle than it would be to interface a cuboid capsule with the cylindrical launch vehicle.

Polylactic Acid (PLA) is a well-known filament because of its high strength, hardness, and thermal capabilities. This material is also lightweight, easy to print, is not as prone to warping during print, and has a low shrinkage rate. However, it is a brittle and weaker material at fracture, has low thermal capabilities, and is highly biodegradable when exposed for an extended period in sunlight.

Polyethylene Terephthalate Glycol (PETG) is often considered the middle ground between PLA and ABS because it has lower strength than PLA while being more ductile than ABS. Some of the advantages that PETG offers are its higher UV and heat resistance, lower brittleness, and higher hardness compared to PLA and ABS. These properties place it as a running candidate for the drone body based upon the 3D filament trade matrix. The downsides are that it is more likely to warp during print, is less user-friendly, is susceptible to moisture, and has lower thermal properties than PLA.

Polypropylene (PP) offers very high toughness and ductility while also having superior chemical and electrical resistance compared to PLA, ABS, and PETG. However, this material does have a high rate of warping during print and issues with poor bed adhesion during print.

Thermoplastic Polyurethane or TPU has high toughness under load and is very ductile, giving it high impact resistance and vibration damping. TPU has a lower chance to warp during printing, a lower chance of shrinking after printing, and is also chemically resistant. On the other hand, it is prone to brittleness in moist environments and has a higher chance to string during printing. This causes clogging issues as material builds up on the bed nozzle, creating irregularities in certain areas during printing. All the materials discussed above are rated based upon thermal applications, cost, ductility, toughness, stiffness, and ease of printing in **Table 6.3.1-2** below.

Table 6.3.1-2: Payload Frame Material Trade Matrix

Utility Value (1-10)		Option 1		Option 2		Option 3		Option 4	
		PLA		PETG		Polypropylene (PP)		TPU (Thermoplastic Polyurethane)	
Criteria	Weight Factor	Utility Value	Weighted Value	Utility Value	Weighted Value	Utility Value	Weighted Value	Utility Value	Weighted Value

Thermal Capabilities	**1**	2	2	8	8	4	4	6	6
Cost	**2**	10	20	10	20	10	20	10	20
Ductility	**4**	4	16	6	24	10	40	10	40
Toughness	**5**	8	40	4	20	10	50	8	40
Stiffness	**4**	6	24	4	16	8	32	8	32
Ease of Printing	**3**	10	30	6	18	6	18	6	18
Weighted Total		**132**		**106**		**164**		**156**	

Based upon the above evaluation, the team will be printing the payload capsule with Polypropylene. Polypropylene has high heat and UV resistance, which is essential for long outside exposure, as all candidates face the issue of polymer's natural biodegradability in sunlight. While not a launch day concern, Polypropylene can tolerate temperatures as low as 32° Fahrenheit without fracture or noticeable degradation of the structure and temperatures as high as 180° Fahrenheit without warping. Additionally, its high toughness and ductility ensures that the structure and electronics will not be at risk under launch conditions.

6.3.2 Microcontroller Selection

The payload will include multiple sensors that are critical for the mission objective. Along with being able to interpret the data, onboard data processing is necessary to transmit the position to the ground station. The microcontroller will have to interface with barometers, radio modules, GPS modules, gyroscopes, accelerometers, and magnetometers.

The leading selections for microcontroller systems are an Arduino Uno Rev3, a Raspberry Pi 0W, and a Raspberry Pi 4B. To select the system that would best meet the needs of the payload system, **Table 6.3.2-1** below was developed for comparison.

Table 6.3.2-1: Comparison of Microcontrollers

Microcontroller Candidates			
Criteria	**Arduino Uno**	**Raspberry Pi 0W**	**Raspberry Pi 4 Model B**
Image			
Info	The Arduino Uno is an Open-Source Microcontroller with extensive libraries, built around the Internet of Things. (IoT)	The Raspberry Pi (Rpi) 0W is a single board computer, with built-in Wi-Fi and Bluetooth. It has the capabilities of a microcontroller being able to use several different common sensor communication protocols, while still having the power to compile data streams.	The Raspberry Pi 4 Model B is a single board computer like that of a 0W. Instead, it comes with an added benefit of a quad-core processor, higher CPU Clock rates, additional ram, and finally additional User Interfacing Ports
Advantages	● Extensive Developer Libraries ● Very Low Power Draw	● Small and Slim Form Factor ● Significantly Lower Cost ● Lightweight	● Significantly Higher CPU Clock Rate ● Significantly Higher Ram Amount ● Extensive UI Ports
Disadvantages	● Large Size ● Very Limited Storage Capacity ● Weakest Computationally ● Least Amount of IO Pins	● No Built-In Integrated Development Environment (IDE) ● Processing Power Limited by Single Core & Clock Rate	● No Built-In Integrated Development Environment (IDE) ● Heaviest ● Most Expensive

The first considered microcontroller is the Arduino Uno. At $23, it is at a competitive price regarding the other selections. Arduino's open-source community Developer libraries will significantly decrease the amount of time spent developing our code. Additionally, the minuscule power draw of the Uno is an advantage when considering the battery requirements. Though the Arduino can receive data from multiple sensors, it is limited in processing multiple data streams. This is due to its limited CPU clock speed and RAM, and its lack of onboard storage severely limits the potential for storing critical flight data to be used in future analysis.

The second microcontroller option is the Raspberry Pi 0W (RPi 0W). The RPi 0W offers significant weight savings when compared to the other options. Measuring at only 8 grams, it balances processing power with weight. It has a small form factor that allows it to easily fit within the 5-in diameter PLI system. Where the Pi 0W falls short is the amount of processing power available. Although it clocks faster, has more RAM, and has more onboard storage than the Arduino, the number of sensors required for the mission is likely too much for the single core. Finally, the cost of the Pi 0W is significantly lower when compared to the alternatives, at only $5.

The third microcontroller option is the Raspberry Pi 4 Model B (RPi 4B). The RPi 4B is like the RPi 0W, as they both host 26 General Purpose Input & Output (GPIO) Pins. They share the same communication protocols used in sensor data retrieval: UART, I2C, SPI, and USB. Both the RPi 0W and RPi 4B are lacking in terms of software development as the libraries are not as extensive as those available to the Arduino Uno. Additionally, the microcontrollers require an external Analog to Digital Converters (ADC) because they do not have ADC pins on the board.

Where the RPi 4B has a CPU Frequency, number of cores, and RAM than the RPi 0W. The clock rate of the RPi 4B is 40% faster and has 4 times the number of cores and the amount of RAM when compared to the RPi 0W. These become significant when compiling the data streams received from the peripherals of the system. With the advantage of more cores, multithreading becomes a viable option. This increase in computational potential allows for more reliability in processing, as there will be leftover processing bandwidth.

Table 6.3.2-2: Selection Technical Data Comparison

Microcontroller/SBC			
Category	**Arduino Uno**	**Raspberry Pi 0W**	**Raspberry Pi 4B**
Price (USD)	23	10	45
Mass (grams)	25	8	46
CPU Frequency (GHz)	0.016	0.9	1.5
# Of Cores	1	1	4
RAM (Mb)	0.002	512	2048
Onboard Storage	32 Kb	Up to 32 Gb	Up to 32 Gb
# of IO Pins	12	26	26

Table 6.3.2-2 above compares the technical data of each system. Based upon its superior computational capabilities, the Raspberry Pi 4 Model B is the leading candidate.

6.3.3 Leading Primary Sensor Selection

To address the challenges proposed by this year's mission we considered multiple peripheral sensors that would enable us to identify the launch vehicle's grid position on an aerial image of the launch site without the use of a global positioning system. The leading peripherals we considered to be most viable for our mission included two Inertial Measurement Unit (IMU) / Attitude and Heading Reference System (AHRS), the 3-Space Embedded LX Evaluation Kit and Xsens MTi-1-0l-T, as well as a tracking camera, the Intel RealSense T265. To determine which peripheral would be best suited for our mission objectives, we compared the three options and identified the advantages and disadvantages of each.

Table 6.3.3-1: Primary Peripheral Comparison

Primary IMU Candidates		
 **Intel® RealSense™ Tracking Camera T265**	 **3-Space™ Embedded LX Evaluation Kit**	 **Xsens MTi-1-0I-T**
• Dimensions: **4.25in x 0.96in x 0.5in** • Weight: **2.1 oz** • Acceleration Range: **±4g** • Supply Voltage: **+4.5v ~ +5.25v** • Power Consumption: **300mA @ 5v**	• Dimensions: **0.62in x 0.59in x 0.06in** • Weight: **0.032 oz** • Acceleration Range: **±8g** • Supply Voltage: **+3.3v ~ +6.0v** • Power Consumption: **22mA @ 3.3v**	• Dimensions: **0.48 in x 0.48 in x 0.1 in** • Weight: **0.021 oz** • Acceleration Range: **±16g** • Supply Voltage: **+2.16v ~ +3.6v** • Power Consumption: **33mA @ 3v**

The Intel RealSense Tracking Camera T265, pictured in the table above, utilizes dual wide-angle cameras (OV9282), an IMU module (BMI055), and a processing ASIC (Intel Movidius Myriad 2 MA215x VPU) with a USB 3.0 interface to host processor SoC. The fisheye image sensors provide

IR Cut Filters to prevent IR light from reaching the imagers, making it ideal for outdoor usage. Additionally, the camera utilizes simultaneous localization and mapping (SLAM) to keep track of its own location within its environment without the use of GPS. The SLAM algorithms run directly on the VPU, allowing for low latency and efficient power consumption. All these features, in addition to its low power draw (1.5W), minimal weight (2.1oz), and precision tracking, are advantages of utilizing this sensor in our mission. However, one of the major disadvantages of this peripheral is that its onboard IMU accelerometer has a range of only ±4g.

The 3-Space Embedded LX Evaluation Kit, pictured in the table above, includes a DFN AHRS and an IMU which uses a triaxial gyroscope, accelerometer with a range of ±8g, and compass sensors. Additionally, it includes advanced processing and on-board quaternion-based orientation filtering algorithms to determine orientation relative to an absolute reference in real-time. All these features, in addition to its compact size (0.032oz), low cost, extremely low power consumption (0.02W), high reliability, and precision are advantages of utilizing this sensor kit in our mission.

The Xsens MTi-1-0l-T sensor, pictured in the table above, is one of the smallest industrial-grade self-contained IMU's available, weighing only 0.021 ounces. It has an onboard accelerometer with a range of ±16g, triaxial gyroscope, and magnetometer. The Xsens AttitudeEngine, a strap-down inertial navigation system algorithm, performs high-speed dead-reckoning calculations. This sensor would enable us to accurately track our payload's acceleration and possibly perform dead-reckoning calculations to track our payload's position dynamically while maintaining a low power draw (0.3W). However, one of the major disadvantages of this sensor is its lack of documentation and existing use case examples.

Table 6.3.3-2: Primary IMU Trade Matrix

Utility Value (1-10)		Option 1		Option 2		Option 3	
		Intel® RealSense™ Tracking Camera T265		3-Space™ Embedded LX Evaluation Kit		Xsens MTi-1-0I-T	
Criteria	**Weight Factor**	**UV**	**WV**	**UV**	**WV**	**UV**	**WV**
Dimensions	**4**	4	16	7	28	8	32
Ease of Use	**4**	8	32	5	20	2	8
Weight	**3**	6	18	7	21	8	24
Acceleration Range	**3**	2	6	9	27	10	30

Supply Voltage	**2**	5	10	7	14	6	12
Power Consumption	**2**	3	6	8	16	7	14
Price	**1**	4	4	9	9	6	6
Weighted Total		**92**		**135**		**126**	

When comparing the different alternatives for peripheral sensors, we determined that the sensor's dimensions and ease of use were two of the most important factors, given that we have limited space within the payload and the easier it is to retrieve data, develop code, and use the sensor, the easier the completion of our mission will be. Additionally, the sensor's weight and acceleration range are also important considerations. A lightweight sensor is preferable, as we strive to maintain a lightweight payload and minimize unnecessary weight. Throughout our flight, we plan on reaching over ± 4gs of acceleration and therefore must have a sensor capable of operating reliably within that range. The supply voltage necessary and the amount of power to be consumed are criteria to be considered for the sensor. The payload will be limited to our onboard power supply and must be capable of running for a minimum of 2 hours. Finally, the sensors' price was another factor to consider in our selection, as we strive to use the most cost-efficient components to successfully carry out our mission.

As shown in **Table 6.3.3-2**, we compared the three candidate peripheral sensors, using the previously stated criterion. Our first option, the Intel RealSense Tracking Camera T265, while it was determined to be easy to use and has a lot of documentation, it lacked in other categories. Despite having small dimensions, low supply voltage, low power consumption, and lightweight, it was still lacking when compared to the other options. Ultimately, Option 1's acceleration range of ± 4g eliminated this sensor as we expect to reach at least ± 4.5g. Our second option, the 3-Space Embedded LX Evaluation Kit had high values in almost every criterion. The sensor's small size, low power consumption, acceptable acceleration range, and competitive price make it stand out against our other options. The third sensor we considered, the Xsens MTi-1-0I-T, is very similar to Option 2 in terms of size and functionality. However, we determined that it lacked ample documentation and previously existing examples of use, especially compared to our other sensor options. For these reasons, we have determined Option 2, the 3-Space Embedded LX Evaluation Kit to be the most promising and have selected this sensor to utilize to complete our payload's mission.

6.3.4 Leading Barometer Selection

The requirements for this mission denied the use of GPS, therefore the utilization of a barometric pressure sensor to estimate altitude and velocity is the next best thing. Barometric pressure sensors will be used to measure the atmospheric pressure to determine the vertical position and provide a velocity magnitude. The selected pressure sensor is the MPL3115A2-I2C, which has an operating range of 2.9psi to 15.95psi. The target altitude is estimated to be 5,100ft, which means the conditions that the pressure sensor will experience ambient pressures of 12.18psi to 14.69psi, falling within the operating range of the sensor. When in flight, the data will be processed to provide outputs for pressure in Pa and this will be used to find the altitude given a derived formula found in the MPL3115A2-I2C datasheet. Additionally, the integrated altimeter can process this calculation without any extra code, simplifying our altitude determination. Furthermore, the accuracy of this device is decent, with 2.2e-4 psi of error or within one ft of actual altitude.

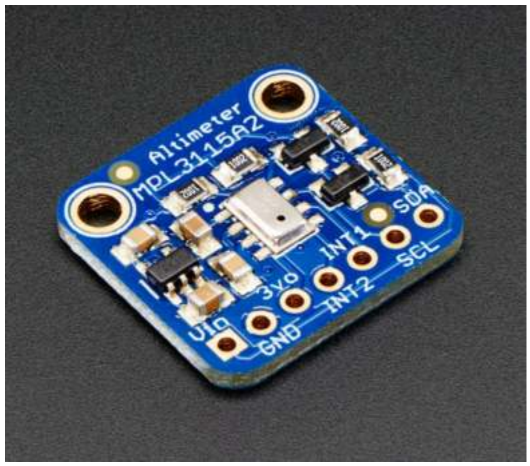

Figure 6.3.4-1: MPL3115A2 Altimeter Module

6.3.5 Wireless Communication Module Selection

To transmit the location data of the rocket back to the ground station, LoRa, XBee, and LTE Hat modules were analyzed in **Table 6.3.5-1**. These modules wirelessly transmit data at long range (2,500 ft radius or more), have low power capabilities, are compatible with communication protocols SPI, I2C, or UART, are user friendly via a chosen microcontroller (raspberry pi), have a high link budget, and operate on an unlicensed ISM band to comply with the Federal Communications Commission (FCC).

LoRa or Long-Range Radio is specifically designed to transmit data packets at low power with the added cost of low bandwidth. In other words, this enables two LoRa devices to transmit and receive data packets over great distances (depending on power supplementation and antenna selection) with the added benefit of reduced power consumption but with the disservice of only transmitting small data packets such as in ASCII or .txt, files essential for streaming our captured data from our chosen sensor.

LoRa works by creating and converting radiofrequency waves into standard bytes or bits. These bits represented in binary can then be converted and saved into hexadecimal format; after which can be reconstructed into an ASCII or .txt file format, which is useful for our application. Another way to transmit this data is using LoRaWAN which connects IoT devices to a network that is ID specific to all other IoT devices or nodes, which can connect wirelessly to said network and transmit data. On this network, a node can also be connected via a gateway that not only has the pre-described ability to transmit said data back and forth through that network but can also send and receive that data to an external network such as the internet.

Using LoRaWAN we can find some useful applications to approximate a given position from a direction or origin of a signal without using GPS. One technique is to approximate a signal's given directional origin using a small, differential time delay technique using several gateways as a second approach to locating our launch vehicle.

Figure 6.3.5-1 features Adafruit's Feather M0 with RFM95 LoRa Radio module that includes a LoRa radio operating at license-free ISM band of 900MHz capable of reaching (on default settings) up to 1.2 miles or 2 km total line of sight signal range. In addition, it features 20 GPIO pins of which 10 are analog inputs and 1 is analog output, a reset button, 4 mounting holes for standoff screws, an SPI and I2C interface protocol, and multiple pre-developed libraries for ease of programming. Some downsides of using LoRa radio are some expected losses that could affect the link budget between the two LoRa modules. This loss is attributed to the physical cable length between the leading sensor, weather, large trees, reflective surfaces, and other surfaces that radio waves can bounce off such as buildings. Looking at the launch field, it appears to be flat farmland with no surrounding trees or buildings in proximity to our expected launch area. Additionally, harsh weather conditions are not to be expected on launch day and thus only leave one operational concern, cable length.

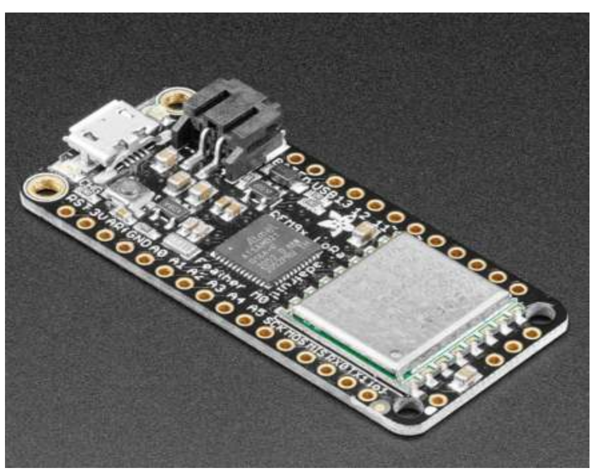

Figure 6.3.5-1: Adafruit Feather M0 with RFM95 LoRa Radio

XBee modules transmit data via wireless communication between two modules via UART or SPI protocol on ISM bands at 900 MHz or 2.4-2.5 GHz and can be set at two different operating modes. Firstly however, XBee modules operate on a 3-tier network system starting at the first tier which is the coordinator. The coordinator is required in every network, and it can never sleep. Stepping down leads to the router which may have multiple signals within a network and can relay signals between each router and endpoints (nodes) but can never sleep. Lastly, end points are connected to routers and can go to sleep but cannot relay signals to routers. This mockup can be seen in **Figure 6.3.5-2**. Essentially, a coordinator can be chosen to act as the master controller to transmit or relay signals to a router and or an endpoint. A router can serve to direct or redirect traffic to another router, endpoint, or the coordinator; and an endpoint serves as a node within the network. These different classes can be chosen with each device to specify their role within the network.

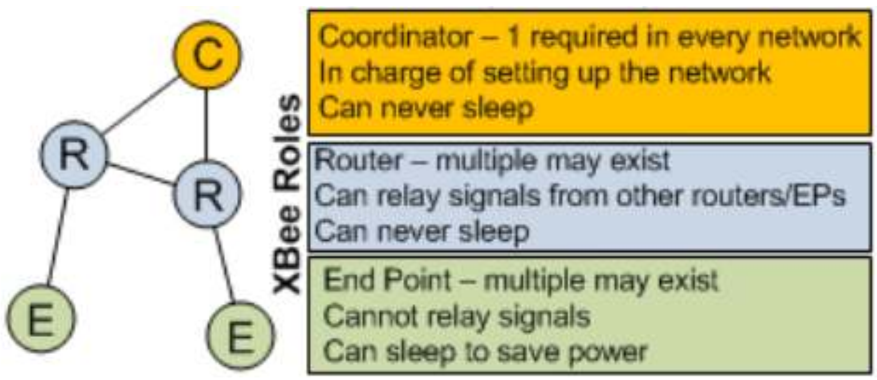

Figure 6.3.5-2: Mockup Diagram of XBee Relationship

To determine how the signals are sent through both XBee modules themselves, two modes determine how each XBee receives and transmits data from between modules. In transparent mode, if data is not generated but sent through the XBee itself, then both XBee modules should be set in the AT protocol. In command mode, if data is sent to the XBee itself such that one module is sensing data and transmitting data while the other is receiving data, the transmitting XBee should be in AT mode while the receiving XBee should be in API mode. XBee modules work in the same radio frequency modulation as LoRa radios but have higher power consumption (depending on the model) which presents a less desirable option in our application.

Figure 6.3.5-3 displays an XBee Pro S2C model which has a maximum outdoor line of sight range of 2 miles (3.2 km) and operates at ISM band at 2.4 GHz. In addition, using SPI protocol, this module can transmit at a rate of 5 Mbps, has both SPI and UART communication protocol (with adapter), has a voltage supply of 2.7 - 3.6 V, a maximum transmit power output of 63mW (+18 dBm), and has 20 GPIO pins.

Some additional downsides of using XBee are some expected losses that could affect the link budget between the two XBee modules. This loss is attributed to the physical cable length between the leading sensor, weather, large trees, reflective surfaces, and surfaces that radio waves can bounce off such as buildings. Looking at the launch field, it appears to be flat farmland with no surrounding trees or buildings in proximity to our expected launch area. Additionally, harsh weather conditions are not to be expected on launch day and thus only leave one operational concern, cable length. Furthermore, there are no noticeable mounting spaces and pin shape for the XBee module to attach to, making an adapter essential for physical mounting.

Figure 6.3.5-3: XBee Pro S2C Zigbee

The Sixfab 3G/4G & LTE Base HAT provides a simple interface bridge between small peripheral component interconnect express(PCIe) cellular modems and the raspberry-pi. This PCIe is crucial because it's the connection between the computer's motherboard and the endpoints. The LTE Base HAT allows the use of any cellular module on mini-PCIe cards to connect to different data networks. A few mini-PCIe's that can be used is the LTE-M that is used for low power consumption applications and if ultra-high-speed is needed then the LTE-Advanced can be used. It all depends on the needs of the user. This device would also give the team high-bandwidth cellular communication between different remote devices.

The LTE Base HAT has a low power consumption that is powered by the 5V pins directly from the RaspberryPi and it is efficient due to the 3Amps it draws which is relatively low. The LTE Base HAT has a pretty good range of about 1.5 miles. In addition, if a module with the ability to connect to 4G is used, it's possible to reach up to 150Mbps downlink and 50Mbps for uplink. These rates are enough for many applications. When compared to the other two communication modules, this device is relatively larger and heavier. It stands at about 2.56 in by 2.24 in and weighs about 1.25 oz. The team is trying to utilize lighter components to reach a higher apogee which is why this component would be less favorable. Furthermore, this device would be simple to interface with the RaspberryPi and our other components, but due to the need of acquiring other components, the mini PCIe module, another communications module is preferred.

Figure 6.3.5-4: Sixfab 3G/4G & LTE Base HAT

Table 6.3.5-1: Wireless Communication Module Trade Matrix

Utility Value (1-10)		Option 1		Option 2		Option 3	
		LoRA		XBee Pro S2C Zigbee		LTE Hat	
Criteria	**Weight Factor**	**UV**	**WV**	**UV**	**WV**	**UV**	**WV**
Power Consumption	**4**	10	40	10	40	6	24
Range	**4**	10	40	8	32	10	40
Packet Size	**2**	3	6	5	10	10	20
Weight	**1**	6	6	4	4	3	3
User Friendly	**3**	6	18	7	21	5	15
Weighted Total		**110**		**107**		**102**	

6.3.6 Battery Selection

For this payload, the key parameter in selecting a battery is its capacity. The selected battery must have enough capacity to power a Raspberry Pi 4B, GPS sensor, embedded IMU, and LoRa module for at least two hours (according to Requirement 2.7). However, with the team's factor of safety of 1.5, the battery will be selected so that it lasts for as long as three hours. To calculate the necessary capacity, the following equation was used:

$$\text{Capacity} = A*t*1000$$

Where A is the amperage drawn and t is the time in hours that the Raspberry Pi will be in operation. With an amperage of 0.650 A and a time of three hours, the battery that we select must have a capacity of 2400 mAh. The voltage of the battery is not an important parameter because a voltage stepper can be used to supply the necessary potential for the Raspberry Pi. Another parameter that must be decided upon is the battery cell count. Increasing the number of cells only increases the amount of voltage the battery can provide, but the capacity does not change. Therefore, a single cell battery would be optimal for this application because the battery needs to be light and have a small footprint within the payload bay. Lastly, the Raspberry Pi 4B requires a voltage input of 5V which means that a voltage regulator will be required for any Li-po battery that is selected because Li-po batteries have voltage options in multiples of 3.7V. Using the information stated, the team decided on the AKZYTUE 3.7V 2400 mAh Li-po battery in conjunction with the HiLetGo XL6009 Voltage Boost Module to power the payload's Raspberry Pi. The battery has an over-current protection circuit board and is 1.97 in x 2.05 in x .31 in while the voltage regulator is 1.69 in x .83 in x .55 in.

Figure 6.3.6-1: AKZYTUE 3.7V 2400 mAh Li-po Battery

Figure 6.3.6-2: HiLetGo XL6009 Voltage Boost Module

6.3.7 GPS Selection

Requirement 4.2.3 states that GPS cannot be used to aid in any part of the payload mission. A GPS is needed however to verify the functionality of our payload system and meet requirement 3.12. The main elements required for the GPS module to be compatible with the raspberry pi are the VCC, RX, TX, and GND pins. This ensures a proper interface between the module and the computer. Additionally, because the team is using a raspberry pi, a driver is not needed but specific software will have to be installed. The GPS module that fits these requirements is the BN-880, which has a small form factor and quick satellite lock, sufficient to verify the location of the launch vehicle. The GPS module is shown below in **Figure 6.3.7-1**

Figure 6.3.7-1: BN-880 GPS Module

6.4 Drawings and Schematics

6.4.1 Palantir Drawings

Below are the key dimensions for the current payload design, all provided measurements are in in.

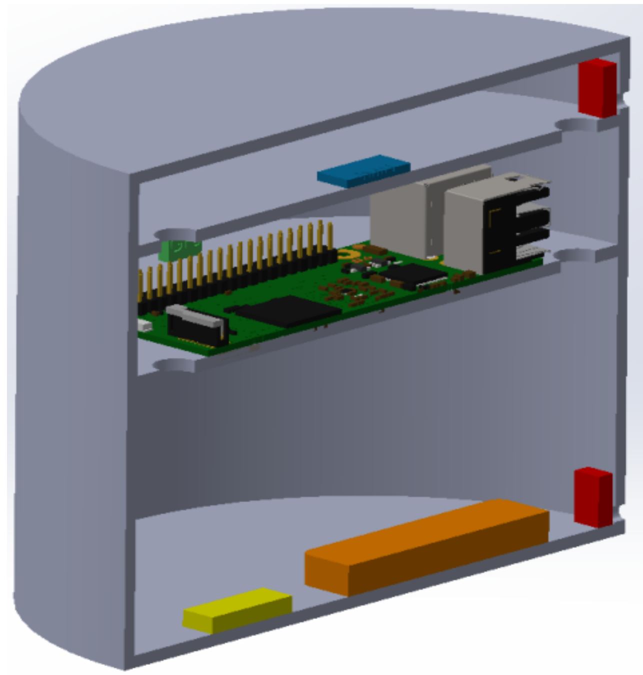

Figure 6.4.1-1: Palantir Assembly Cutaway

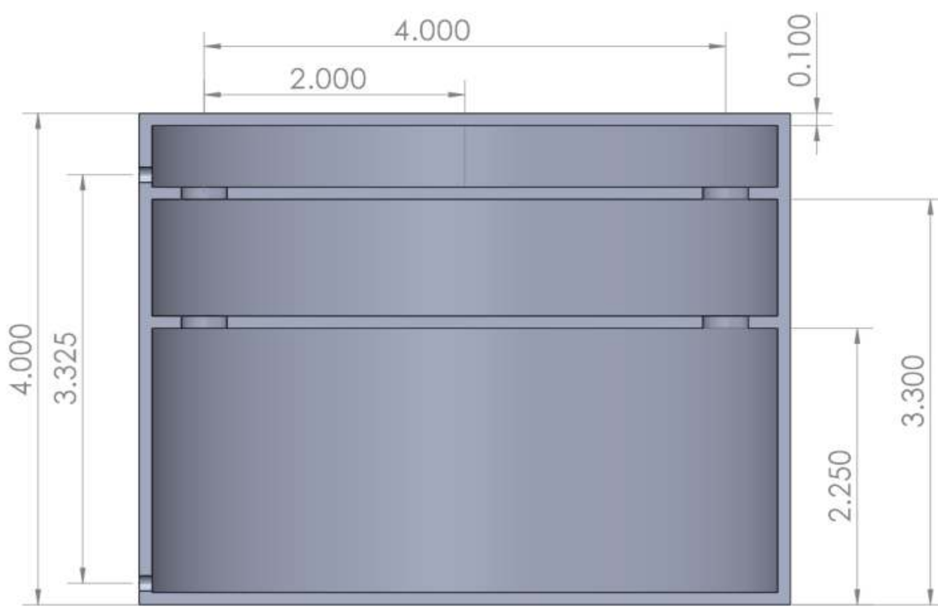

Figure 6.4.1-2: Dimensioned Cutaway Side View of the Palantir Capsule

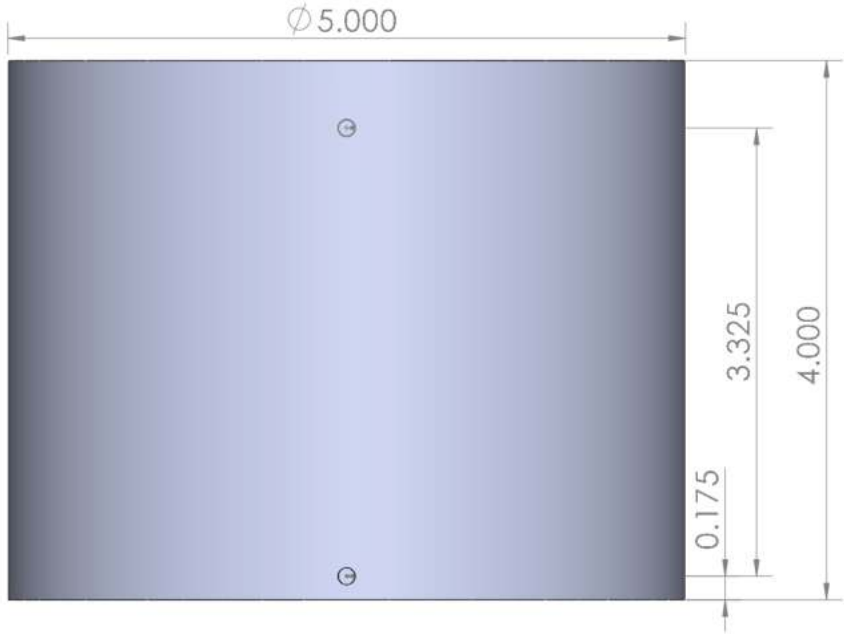

Figure 6.4.1-3: Right Face of the Palantir

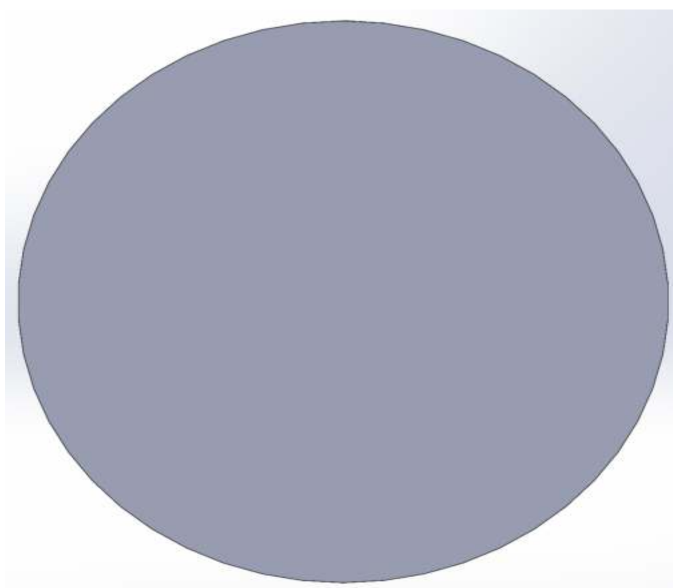

Figure 6.4.1-4: Top Face of the Palantir

6.5 Payload Electrical Schematic

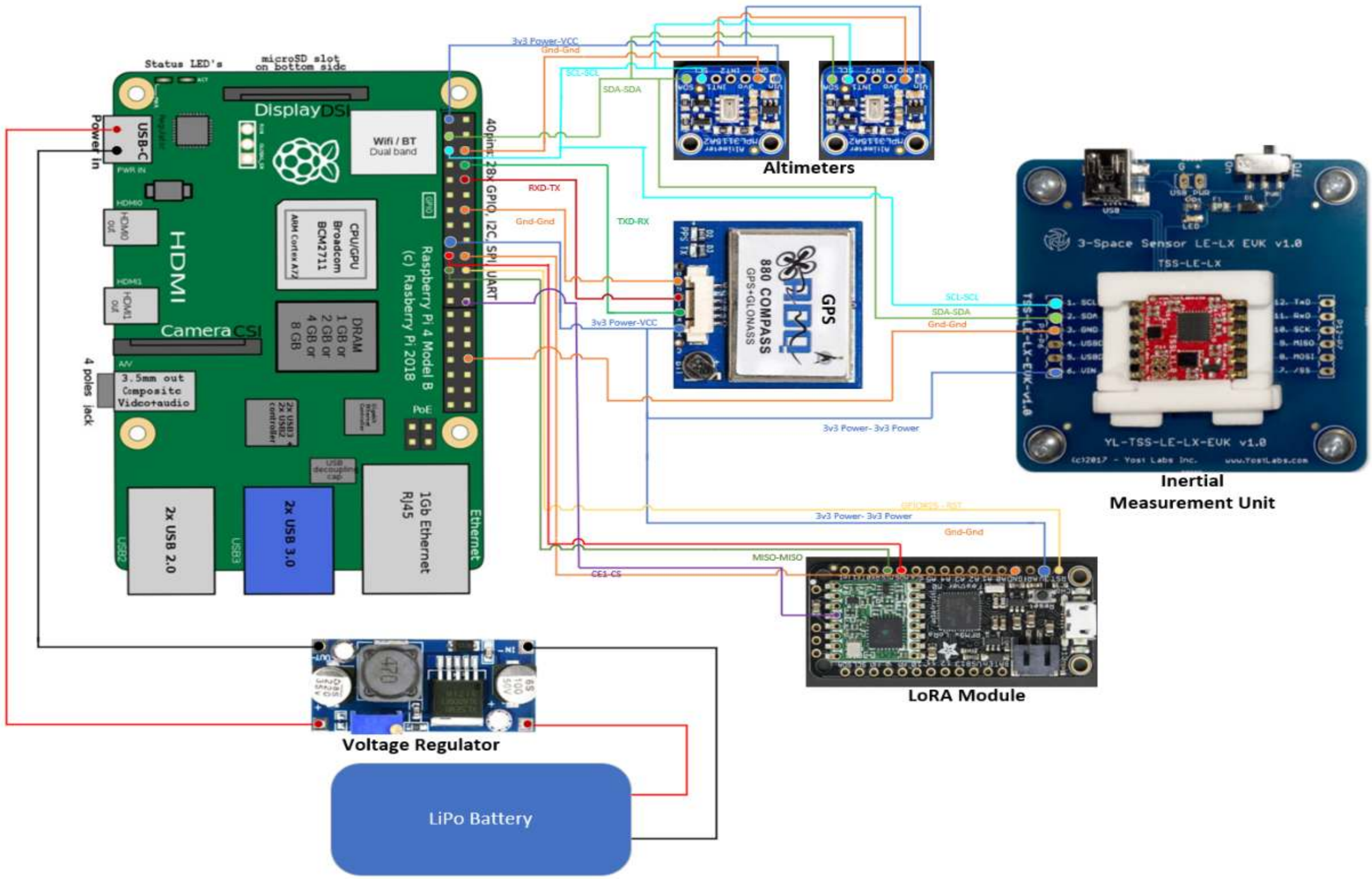

Figure 6.5-1: Palantir Electrical Wiring Diagram

6.6 Payload Integration System Summary

The payload integration (PLI) system can be summarized as a remote ground-extruding housing sitting directly adjacent to the friction fit nose cone. Specifically, inside the rocket sits a cylindrical container designed to hold the payload assembly. This container sits within two bearing rings which, before the deployment begins, sit in a compressed state immediately next to each other. One of these rings is fixed to the launch vehicle body, while the other is fixed to the nose cone. Once the launch vehicle touches down and the separation of components from the rocket is greenlit, a leadscrew stepper motor assembly sitting in the launch vehicle directly behind the payload integration assembly will push the end of the assembly forward, extruding it out of the launch vehicle. Since the nose cone is only held in place via friction fit aside from the lead screw, as the lead screw pushes the assembly out the nose cone will be pushed out as well. As it does so the bearing ring will slide along the cylindrical housing it sits on until it reaches the end of it. At this point, the lead screw stops, and the nose cone is extended away from the body of the launch vehicle by a gap of about 6 in. The payload housing sits between the two rings, thus exposing the payload and more easily allowing it to send requisite signals back to the base station. A general overview of the design can be seen below in **Figure 6.6-1**. It's estimated mass including all necessary components of approximately 5.96 lb.

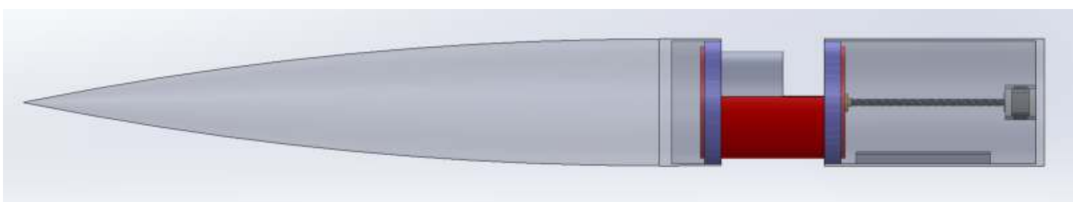

Figure 6.6-1: Payload Integration System Side View

The overall PLI system can be broken up into 3 main subsystems: payload integration into the launch vehicle prior to launch, payload retention during launch, and payload disengagement after launch.

The first major subsystem, payload integration, is how the payload is integrated into the launch vehicle. This is accomplished via the 5-in diameter, 7-in-long payload barrel that sits inside the launch vehicle. While the launch vehicle is still grounded prior to launch, the system can be manually extruded so that the open top of the barrel is exposed, a process described more in-depth in the payload disengagement description. This allows the payload to easily be placed in the barrel and attached to its end where it can be locked into place via fitting tabs and Velcro straps. The barrel itself can be seen below in **Figure 6.6-2**

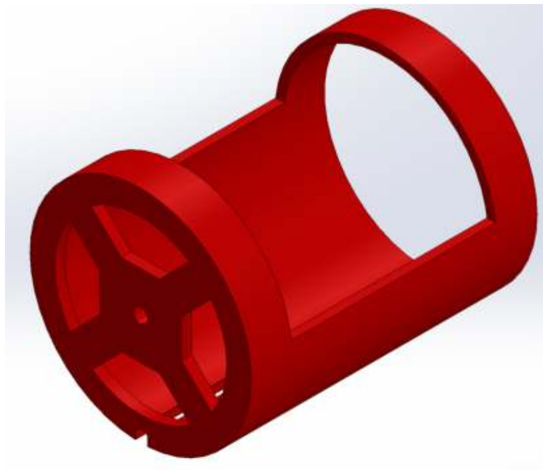

Figure 6.6-2: Payload Barrel Orthogonal View

The Payload barrel itself is secured between two bearing rings attached to the inside of the nose cone and inside of the launch vehicle respectively. The rings have 40 pockets all along their inner diameter so that 5/16 inch bearing balls can be placed throughout. These pockets are large enough to ensure that the bearing balls can freely spin while sitting inside but are dug deeper down than the actual center of the bearing ball sphere so that they can sit in the pockets without falling out. One of these rings is attached to the nose cone and is also fixed in place with the payload barrel so that it is free to rotate about it, but not free to translate horizontally relative to it. The other bearing ring on the launch vehicle side however is free to translate along the body of the barrel. This is so that the barrel, along with the nose cone, can be extruded outwards along the barrel's body. This ring can be seen in the following **Figure 6.6-3**

Figure 6.6-3: Bearing Ring with Bearing Ball Placement Orthogonal View

Once the payload has been placed into the barrel, the lead screw can be manually retracted to bring the nose cone bearing ring, and thus the barrel fixed to it, inside of the launch vehicle in a closed state. The integration of the payload can be summarized as manually extruding out the nose cone to expose the payload bay cavity, inserting and securing the payload, then retracting the lead screw so that the nose cone sits up against the body of the launch vehicle ready for launch. The closed and open positions described can be seen below in **Figure 6.6-4**

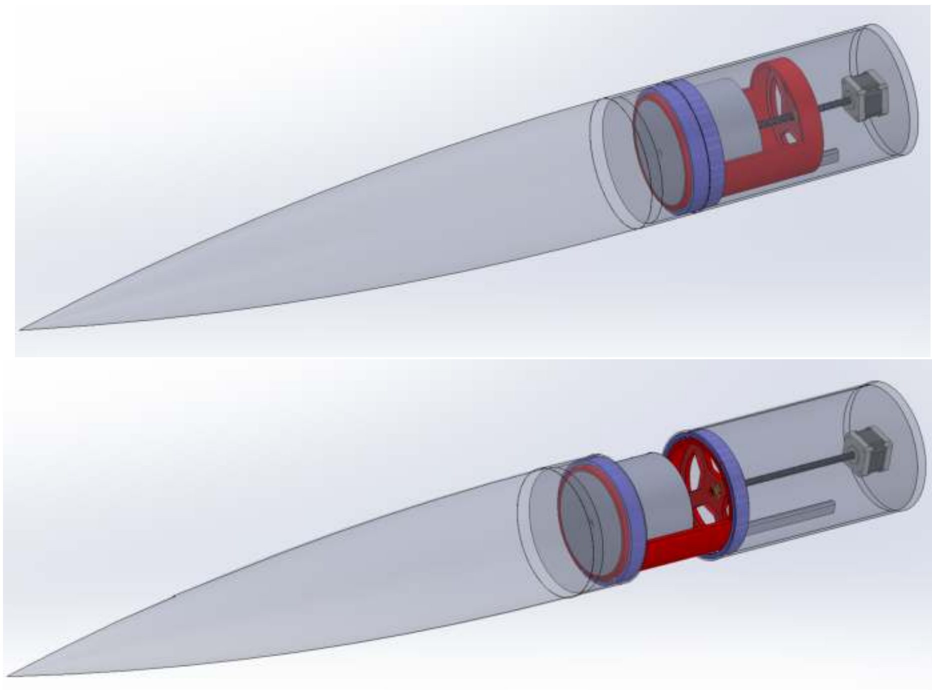

Figure 6.6-4: PLI System in Open Position (Top) and Closed Position (Bottom)

The next key subsystem in PLI is payload retention. This is crucial to ensuring the payload does not come loose or fall out during the launch of the vehicle. Additionally, since the nose cone is now fixed to the PLI system, retention also involves ensuring the nose cone remains attached to the launch vehicle during flight. This is deemed the more critical aspect of retention as if the nose cone is not secured, the payload itself cannot be secured, and flight could potentially be compromised. The nose cone itself is held by two means. First, there is a rail that the payload barrel slides across as it extrudes out. This rail is designed to have a very snug fit with the assembly so that the weight of the nose cone section is not alone sufficient to pull the payload barrel out. Additionally, the lead screw stepper motor is fixed to the payload barrel itself with the traveling nut that will push it out during the disengagement procedure. The entire nose cone assembly is therefore also held by the holding torque of the stepper motor, which was verified to be within a comfortable factor of safety to do so during the selection of components. The rail implementation in the launch vehicle behind the nose cone can be seen below in **Figure 6.6-5**

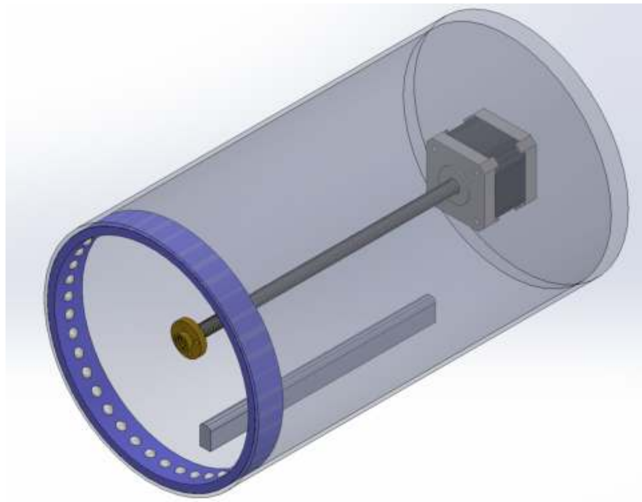

Figure 6.6-5: Rail Implementation in Launch Vehicle, Orthogonal View

The final key subsystem within PLI is the payload disengagement from the launch vehicle. This system is a remotely triggered sequence that sees the payload barrel and nose cone extruded outwards so that the payload is exposed to the open environment and can get more accurate sensor readings as well as free up communication between its on-board computer and the ground station to locate the launch vehicle. This is achieved by having a stepper motor fixed inside the launch vehicle centered about the diameter. Attached to this stepper motor is a lead screw that passes through the PLI system and part of the payload assembly without interfering with any of its electronics or components. Fixed to the back end of the payload barrel is a traveling nut that rests on the lead screw. While the barrel sits within the launch vehicle, the rail slots into the bottom of it so that it is prevented from rotating.

This is important in ensuring the payload can accurately measure the flight path of the rocket without interference. However, it is also crucial to make sure the traveling nut can push the assembly out along the lead screw. For, if it was allowed to freely rotate the assembly would simply spin in place instead of translating linearly. At a certain point during the translation of the barrel, it will come off the rail and lead screw simultaneously and thus become free to start spinning. That is, once the barrel becomes fully exposed, the inner bearing that is the payload barrel is free to rotate. With a weighted distribution placed directly under the barrel, gravity will naturally ensure the bottom of the barrel is always face down, shielding the payload from any oncoming debris or flying rockets should the parachute drag the rocket along the ground.

6.7 Payload Integration Technical Approach Manufacturing

The payload integration system was designed to be additively manufactured to reduce the cost of manufacturing and as a result the total cost of the project. This also allows the team the ability to produce multiple models for testing at quick turnaround times. Due in part to the size constraint of the available machines, the team has plans on designing the integration system such that fasteners and adhesives are used seamlessly with ease of assembly and disassembly which will be discussed in more detail. With the wide range of materials available for additive manufacturing, the team has chosen to use 3D-Fuel Pro PLA (see **Figure 6.7-1**) over others for a few specific reasons.

Figure 6.7-1: Pro PLA Filament

6.7.1 Material Choice

With most forces anticipated in the payload integration system to be impact forces upon touchdown, a high-impact resistant material is needed to produce a model with a high enough factor of safety for mission success. Considering the high heat resistance and impact strength listed on 3D-Fuel's website, as seen in **Figure 6.7.1-1**, Pro PLA filament also offers ease of use with the manufacturing process in comparison to other materials such as ABS and Nylon.

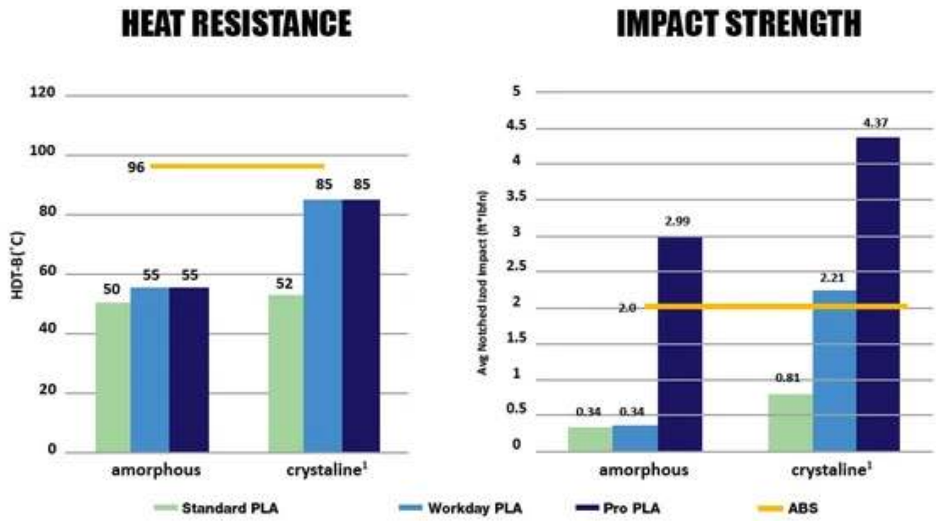

Figure 6.7.1-1: Standard, Workday and Pro PLA Compared to ABS

By the nature of additive manufacturing with the technology available to the team, considerations in the orientation, infill pattern, infill density, and weight of the parts produced must be addressed and decided prior to beginning manufacturing. Examples of infill patterns and infill density can be seen in **Figure 6.7-2**.

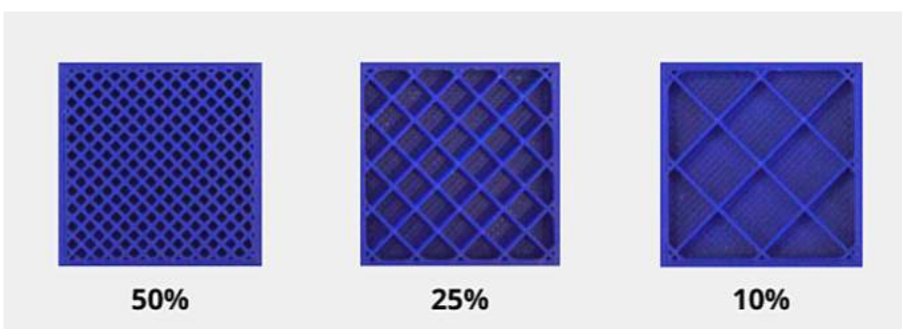

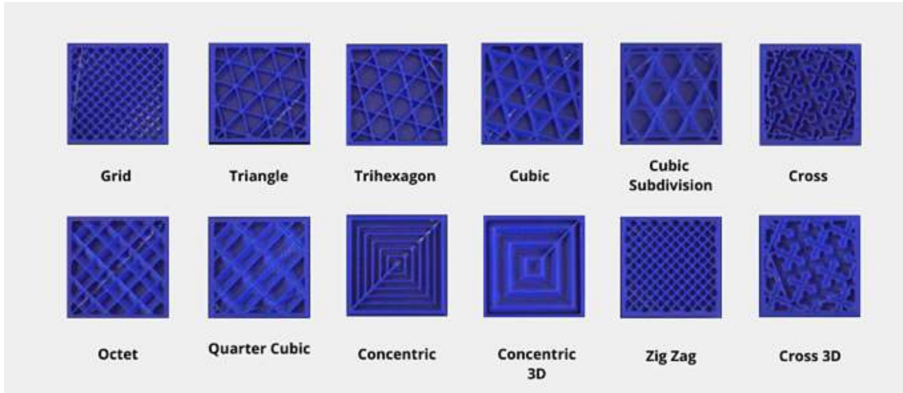

Figure 6.7.1-2: Infill Density (Top) and Infill Patterns (Bottom) Visualized

The following infill and additional settings have been decided with strength and weight as the driving factor. Additionally, total manufacturing time and manufacturing qualities were also considered, listed below in **Table 6.7.1-1**.

Table 6.7.1-1: Print settings to be used for manufacturing

Infill Density	50%
Infill Pattern	Cubic
Layer Height	0.16 mm
Wall Thickness	0.8 mm
Nozzle Temperature	210.0 °C
Bed Temperature	60.0 °C
Bed Adhesion	Brim
Print Speed	60 mm/s

Following the manufacturing of a part, post-processing steps will be taken as follows:

- Annealing - Further strengthens the part by removing internal stresses and making molecules in parts from amorphous to crystalline.
- Body Filler and Sanding - Removing surface imperfections and prepping for paint

- Paint and Clear Coat - The final step to produce a functional and presentable payload integration system.

6.7.3 Assembly and Disassembly

To address unforeseen challenges throughout the manufacturing, assembly, testing, and flight of the payload integration system, ease of assembly and disassembly has been a driving force for the design of the system. This effort has been achieved through a few design choices already seen with the payload bearing rings as an example. Although a part with multiple components, once manufactured it will act and be treated as a single piece that interacts with the rest of the system. This is only one example of more existing ones, such as the placement of pilot holes for threaded inserts and therefore bolts and nuts that will hold the system together.

Having this criterion set at this point in the design process allows for the team to begin to design towards the mission set. By achieving this criterion, any testing and adjustments can be made quickly, and components are able to be swapped out from both the payload and payload integration system which will only benefit the team heavily.

6.8 PLI System Alternatives

At a system level, the payload integration had a couple of options considered before settling on the design described above. A trade matrix summarizing the analysis of the different designs can be seen below in **Table 6.8-1**. The first option that was considered was a rack and pinion gearing system that would see the payload barrel extruded out along a set of rack gears sitting inside of the launch vehicle. The barrel would then be driven along by a motor spinning a pinion gear. This design was tempting because of the reliability in the linear motion of the barrel. However, ultimately the weight of the components that would have to be implemented ended up negating its potential for use. The next system considered to deploy the payload would see springs locked in compression by linear actuators that would disengage and subsequently push the payload out of the launch vehicle. While this proposed design was appealing for its small weight and lack of complexity, the nature of springs providing an impulse force meant that should anything obstruct the nose cone, the PLI system would fail to deploy as the springs can only provide force once. The reliability of the system thus ultimately prevented it from being the leading candidate. The final design option considered saw a Carbon-Dioxide canister opened by a servo arm to suddenly release all the gas and push the payload assembly out with the burst of pressure. This system again was tempting for its weight and lack of complexity, however the fact that the cartridges would have to be replaced paired with concerns in building sufficient pressure to eject the payload ended up weighing down this design.

Table 6.8-1: Payload Ejection Trade Matrix

Utility value (1-10)		Option #1 Rack and Pinion		Option #2 Tensioned Spring Release		Option #3 Sliders with Lead Screw		Option #4 CO2 Burst	
Criteria	**Weight**	**Utility Value**	**Weighted Value**	**Utility Value**	**Weighted Value**	**Utility Value**	**Weighted Value**	**Utility Value**	**Weighted Value**
Strength	**4**	5	20	8	32	7	28	3	12
Weight	**3**	4	12	7	36	6	18	8	24
Cost	**2**	5	10	9	18	8	16	6	12
Manufacturability	**2**	4	8	9	18	8	16	6	12
Reliability	**5**	9	45	3	15	9	45	5	25
Weighted Total		**95**		**119**		**123**		**85**	

6.8.1 PLI Microcontroller Alternatives

The microcontroller board that shall be used for the PLI section shall be the Arduino Nano (see **Figure 6.8.1-1**) due to its flight heritage, the team's familiarity, and its robust form factor. Another option that had the same form factor as the Arduino Nano was the Arduino Nano RP2040 (see **Figure 6.8.1-2**), but due to the lack of EEPROM and increased price because of the Wi-Fi module and lack of a need for IoT for PLI, it was ultimately not chosen. While the Nano ended up being the choice, the team researched other microcontrollers such as the Raspberry Pi 3B+ (see **Figure 6.8.1-3**). This board has a high clock speed, RAM, and built-in incrementally increasing SD card modules. However, it wasn't chosen due to having a greater mass and form factor than the Arduino Nano. While the Raspberry Pi Pico (see **Figure 6.8.1-4**) was a good option, the lack of familiarity with the board and being a 3.3V device didn't meet the team's requirement in terms of output voltage.

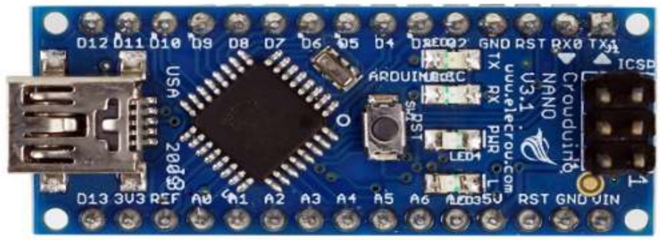

Figure: 6.8.1-1 Arduino Nano

Pros: The Arduino Nano is a familiar board to the team that has flight heritage in similar missions, 5V output, lightweight, and the ideal form factor.

Cons: The Nano has a slower clock speed and SRAM compared to the other boards.

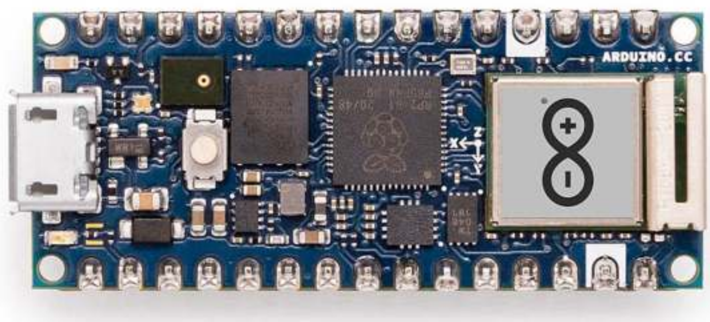

Figure 6.8.1-2: Arduino Nano RP2040

Pros: The Arduino Nano RP2040 offers the same dual core 133MHz as the Raspberry Pi Pico but in the Nano Form Factor and 5V output. Along with the familiarity of the PLI team of Arduino boards.

Cons: The additional cost of the Nano is due to the RP2040 processor.

Figure 6.8.1-3: Raspberry Pi 3B+

Pros: The Raspberry Pi 3B+ offers a 4 core 1.3GHz processor, flashable OS for easy integration, and software-in-the-loop testing along with any COMMs bus or Power bus necessary for the mission.

Cons: The mass of the Raspberry Pi 3B+ is 1.66oz and 3.4 inch x 2.3 inch x 0.7 inch, which shall take a good portion of the PLI system and add unnecessary load.

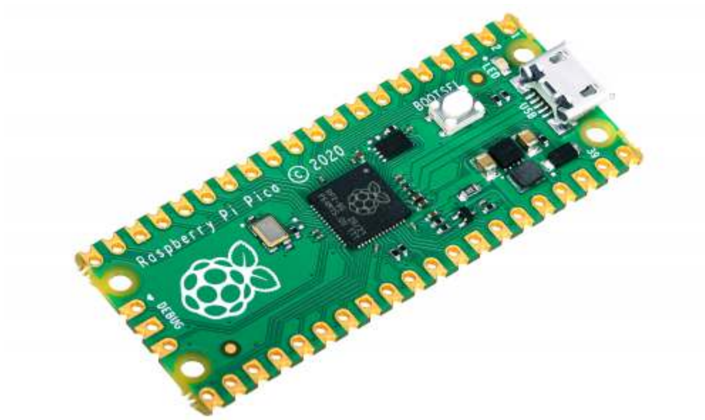

Figure 6.8.1-4: Raspberry Pi Pico

Pros: The Raspberry Pi Pico offers decent processing power with a dual core 133MHz clock speed, compact form factor, lightweight.

Cons: The Raspberry Pi Pico can’t supply the necessary power to the components of the PLI system due to being a 3.3V device and unable to supply 5V.

The pros and cons to each component are summarized below in the trade matrix used to assess the leading component, in **Table 6.8.1-1**

Table 6.8.1-1: Micro Controller Trade Matrix

Utility value (1-10)		Option #1 Arduino Nano		Option #2 Arduino Nano RP2040		Option #3 Raspberry Pi Pico		Option #4 Raspberry Pi 3B+	
Criteria	**Weight**	**Utility Value**	**Weighted Value**	**Utility Value**	**Weighted Value**	**Utility Value**	**Weighted Value**	**Utility Value**	**Weighted Value**
Clock Speed	5	2	10	6	30	8	40	10	50
Memory	4	2	8	6	24	7	28	9	40
Pins Available	3	8	24	6	18	8	27	9	30
Mass	3	9	27	8	24	8	24	5	15
Size	4	9	36	10	40	8	32	3	12
Cost	4	4	16	8	32	9	36	4	16
Required Power	5	9	50	2	10	2	10	8	40
Ease of Use	5	9	50	10	50	5	30	4	20
Weighted Total		**211**		**228**		**219**		**216**	

6.8.2 Stepper Motor Alternatives

The Stepper motor is a key component in the payload integration system, and as such was also evaluated among other competitive models. Before doing so however, some preliminary calculations had to be done to size the stepper motor according to the required holding torque it would need since it would be supporting the nose cone and PLI assembly during flight. The most substantial force it would have to withstand would be during descent when the parachute opens, as there would be a large impulse force combined with the weight of assembly pulling against the lead screw. Using a roughly estimated total force of approximately 16 lb, the minimum required holding torque to support the system based on the dimensions of the selected lead screw is approximately 2.14 lb-in. With this, the three main options considered were the Polulu NEMA 17 stepper motor (see **Figure 6.8.2-1**), the Adafruit NEMA 23 (see **Figure 6.8.2-2**) , and the Redrex NEMA 17, (see **Figure 6.8.2-3**). These were selected trying to stay around the required holding torque without greatly exceeding it, as doing so would mean greater masses and size required which is not ideal for an optimizing.

Figure 6.8.2-1: Polulu NEMA 17 Stepper Motor

Pros: The Polulu brand is a respected source of stepper motors and are well known for their ease of use along with reliability. As a NEMA 17 specification, the dimensions are fairly small at 1.67" x 1.67" X 1.67". It has a low power requirement at 1.2A

Cons: The main con is that this stepper motor only has a maximum holding torque of 2.78 lb-in, which doesn't meet the required holding torque with a comfortable factor of safety.

Figure 6.8.2-2: Adafruit NEMA 23 Stepper Motor

Pros: The Adafruit NEMA 23 stepper motor provides an adequate amount of torque at 8.75 lb-in, which greatly exceeds that of the required value while not exceeding the mass of the other selections by a substantial amount

Cons: The NEMA 23 classification is notably larger than NEMA 17 at 2.3 inch x 2.3 inch x 2 inch which is more complicated to integrate into the system, and the power supply required to run the stepper motor is more demanding at 2.8A.

Figure 6.8.2-3: Redrex NEMA 17 Stepper Motor

Pros: The Redrex NEMA 17 stepper has many of the same pros as the aforementioned Polulu stepper, with similar dimensions due to its NEMA 17 classification at 1.65 inch x 1.65 inch x 1.54 inch. It exceeds the Polulu in holding torque however, at a max value of 3.54 lb-in. It also comes with an integrated lead screw so that a separate one does not need to be purchased.

Cons: The Redrex brand isn't as well-known or familiar as previously mentioned ones and is known to be a little harder to work with though perfectly functional once it does work.

The pros and cons to each component are summarized below in the trade matrix used to assess the leading component, in **Table 6.8.2-1**

Table 6.8.2-1: Stepper Motor Trade Matrix

Utility Value (1-10)		Option 1		Option 2		Option 3	
		Pololu Stepper Motor		Adafruit Stepper Motor		Redrex Stepper Motor	
Criteria	**Weight**	**Utility Value**	**Weighted Value**	**Utility Value**	**Weighted Value**	**Utility Value**	**Weighted Value**
Weight	2	7	14	5	10	7	14
Cost	1	9	9	5	5	8	8
Torque	3	4	12	7	21	6	18
Availability	4	5	20	4	16	8	32
Weighted Total		**55**		**52**		**72**	

6.9 PLI Leading Payload Components

After evaluating each of the alternative components, leading components were selected to be implemented into the actual system. Some components however were not evaluated relative to other options, such as the stepper motor and batteries. This ended up being the case for these components as their specifications were derived based on the requirements coming from the payload integration system itself, with not many competitively viable options for each within those specifications.

6.9.1 PLI Leading Components Microcontroller:

The leading microcontroller for the delivery system is the Arduino Nano, shown below in **Figure 6.9.1-1**. It has dimensions of 0.709 inch x 1.77 inch and weighs 0.015 lb. There are 22 digital I/O pins and 8 analog pins. It has an operating voltage of 5V and consumes power at 19mA.

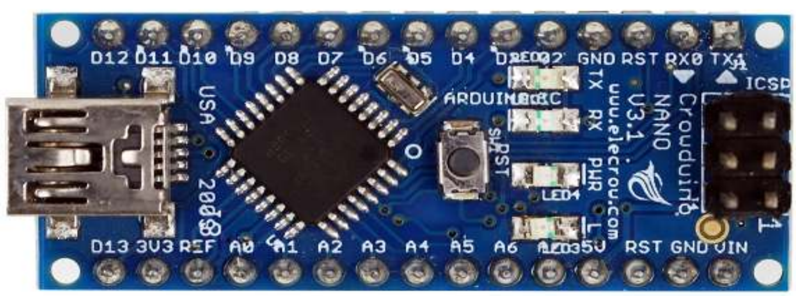

Figure 6.9.1-1: Arduino Nano

Pros:

- Compact size of 10.709 inch x 1.77 inch
- Lightweight at 0.015 lb.
- Has an input voltage of 7-12V, which makes it compatible with our chosen power supply.
- 5V output voltage.
- Proven flight heritage.
- The 22 digital I/O pins are sufficient to interface with the motor, motor driver, and transceiver.

Cons:

- Slower clock speed and SRAM compared to the other boards researched.

6.9.2 PLI Leading Components Stepper Motor

The chosen stepper motor is the Redrex NEMA 17 Bipolar Stepper Motor with an integrated lead screw, shown in **Figure 6.9.2-1**. The motor has 1.65 inch x 1.65 inch faces and is 1.54 inch long. It has a 200 step-per-revolution ratio with each phase drawing 1.5A at 3.3V, which allows for a holding torque of 3.54 lb-in, and a total mass of 1.01 lb. The specifications for the stepper motor were based on the minimum required holding torque the motor would need to have to support the maximum impulse forces it would be subjected to during the deployment of the parachute, paired with the weight of the nose cone and system itself. Doing so revealed a minimum holding torque of 2.14 lb-in, so the Redrex NEMA 17 was chosen for its 3.54 lb-in of holding torque which meets the required value within a comfortable factor of safety, while also not adding too much mass to the system.

Figure 6.9.2-1: Redrex NEMA 17 Stepper motor w/ Integrated Lead Screw

Pros:

- The torque on this model meets or exceeds the values of other motors of the same size at a lower price point.
- Higher torque and efficiency when compared to other motors at a higher price range.

Cons:

- The lead screw is not detachable from the stepper motor assembly.

6.9.3 PLI Leading Components Lead Screw

The lead screw, which is integrated with the motor shown in **Figure 6.9.2-1** above, has a 5/6 inch diameter, 2/25 inch pitch, mm lead, and has a length of 1 ft.

Pros:

- There is no need to purchase and assemble separate lead screw, shaft coupling, and lead nut.
- Being integrated ensures a secure connection between the lead screw and stepper motor.

Cons:

- The lead screw is not detachable from the stepper motor assembly and cannot be changed for another lead screw with different dimensions.

6.9.4 PLI Leading Components Radio Transceiver

The leading component that will enable communication with the PLI is the Adafruit RFM96W LoRa Radio Transceiver (see **Figure 6.9.4-1)**, which works on a frequency of 433MHz. It will interface with the Arduino Nano through the SPI protocol. The module has dimensions of 1.14 inch x 0.984 inch x 0.157 inch and weighs 0.007 lb. This specific component ended up being selected primarily because it was already owned and thus immediately available as well as familiar in use.

Figure 6.9.4-1: LoRa Radio Transceiver

Pros:

- A range of 1.24 miles using a simple wire antenna and up to 12.43 miles with a directional antenna.
- Has the ability to do error correction.
- It can auto-retransmit packets.
- It can be used with the Arduino Nano and has Arduino libraries.
- Although transmissions are slower, the range is much higher in comparison with non-LoRa modules.
- Readily available

Cons:

- Requires a line of sight with the ground station.
- Packet transmissions are slower in comparison with other non-LoRa modules that run on higher frequencies.

6.9.5 PLI Leading Components Battery:

The leading power supply component is the LitePower NiMH rechargeable battery pack, displayed in **Figure 6.9.5-1**. It is rated at 2.2Ah with an output voltage of 12V with a total mass of 0.62 lb.

Figure 6.9.5-1: 12V NiMH Battery Pack

Pros:

- Lighter than other options researched at 0.62 lb.
- Compact with dimensions of 2.8 inch x 1.14 inch x 2.1 inch.

Cons:

- Requires an adapter to integrate with the Arduino Nano.

6.10 PLI Proposed Payload Circuit

The payload integration circuit system, as seen in **Figure 6.10-1**, uses an Arduino Nano to control a Nema 17 stepper motor that powers the lead screws using an A4988 stepper motor driver. A 12 V battery is used to power the driver which then sends power to the Arduino Nano to power the system. To communicate with this system, an RFM96W transceiver is included in this payload electrical design which allows it to be controlled with another receiver of up to 12.43 miles if using an omnidirectional antenna.

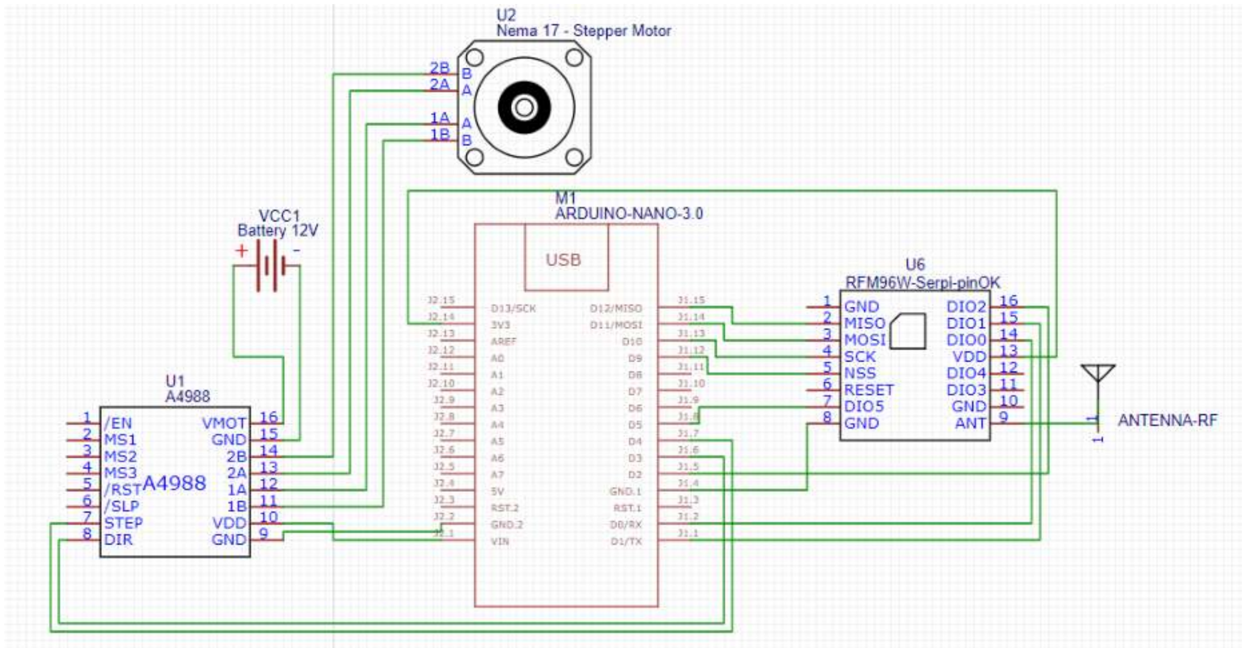

Figure 6.10-1: Payload Electrical Design

6.11 Payload Integration & Deployment Risk Analysis

The payload integration system has a variety of risks associated with it that can be analyzed according to the risk assessment cube presented in the safety section 7.0. Doing so allows the risks posed to be placed in red, yellow, or green zones; thereby providing information on what kinds of risks need to be prioritized and what risk mitigations must be put in place.

The first risk to be looked at is one associated with actual payload deployment. To be able to deploy the payload effectively, the mechanism designed to house it safely must be able to deploy it at the desired time. In so, there are risks involved that can affect the payload and the components holding it together. One of those risks involves the barrel that stores the payload bay. Potential modes of failures exist once the rocket touches the ground. The barrel not being able to be ejected properly is one of the more pressing ones. This would jeopardize the ability of the payload to deploy, while not necessarily jeopardizing the payload mission itself as data can still be reached from within the rocket. In the worst-case scenario were there to be high winds however, the rocket could potentially be dragged out of range of the home base thereby cutting communication between the payload onboard computer and the base station. Failure to communicate would mean the rocket couldn't be located at all resulting in a payload mission failure. As such, in this case, failure to deploy the payload poses a catastrophic risk. One way this could happen is if the rocket lands near a pile of dirt or some obstruction that were to block the exit. Another way this could happen is if any of the key connections in the electronic system are compromised, causing a system failure. The possibility of either of these occurring however is at worst within low likelihood. As if the parachute were to continually drag the launch vehicle along the ground after touchdown, it would be unlikely to get stuck in one place. Additionally, the chances of any connections being compromised remains low so long as they are kept out of the way of moving parts. The only real chance of electronic failure comes from the possibility that the transceiver used to remotely trigger the protocol doesn't work, which is also not likely since a reliable one with an ability to work within the accepted landing radius of the rocket was selected. This combined with the fact that failure to deploy is only an issue if the parachute is being dragged away which itself is unlikely means payload mission failure catastrophic risk is not likely. As such the overall position of payload deployment failure sits comfortably in the green zone at E1 in the risk assessment cube.

The next risk posed by the payload integration system is due to the nose cone being fixed to the lead screw stepper motor in the system. This means that should the payload integration locking mechanism fail, the nose cone risks detaching during launch which would seem to result in mission failure. However, the nose cone is also snugly fit into the body of the launch vehicle for additional redundancy. Additionally, separation of the nose cone would be most catastrophic during takeoff; however, it's unlikely since gravity and air resistance would be pushing the nose cone into the body of the rocket instead of trying to pull it out. Thus, disengagement only becomes a concern during the descent of the rocket, at which point this mode of failure would, while not ideal, it won't pose a catastrophic risk. The risk would move down to critical, as premature disengagement could damage the nose cone which could potentially warrant a repurchase and thus set back mission performance. Since the stepper motor is robust and unlikely to fail unless over-torqued, and the nose cone is also held in place with a friction fit, the chance of failure is in low likelihood. This places the risk in the yellow section of the risk cube sitting at D2, thus warranting mitigation.

6.12 Payload Integration & Deployment Risk Mitigation

The primary risk mitigation that must be implemented is addressing the chance of premature nose cone separation, which was within the yellow zone of the risk cube. To alleviate some of the risk, the main mitigation that can be put in place is properly sizing the stepper motor to meet the loading requirements brought about by holding the nose cone with a margin of safety. The main window of concern comes from the impulse force introduced when the main parachute for the rocket is deployed, as this would put a lot of stress on the lead screw holding the nose cone in place. Pair with this the fact that the launch vehicle is now facing downwards such that gravity will want to pull the nose cone out, and it is now moving at a slower speed meaning that air resistance is no longer aiding the stepper, and this timeframe is where the stepper is most likely to fail. After performing the calculations based on the approximate weight of the system and nose cone held by the stepper, accounting for the frictional force supporting it due to its snug fit, a minimum required holding torque was established based on the dimensions of the lead screw selected. This torque was then used as a reference to select the stepper motor that would hold the system in place, ensuring it met it with a comfortable factor of safety. On top of this, rigorous testing will be performed in different ground conditions to ensure the nose cone cannot easily separate from the launch vehicle with the selected stepper. These mitigations combined mean that this mode of failure moves from a low likelihood to not likely, thus moving the risk into the green zone of the risk assessment cube at position E2.

The next risk introduced in the payload integration system was the potential for failure to deploy the payload. While it's already been established that this risk is in the acceptable green zone, the mitigation that can be put in place is simple enough that it wouldn't warrant any major redesigns or reconsiderations and can therefore be implemented anyways. Specifically, redundancies can be inserted in the code to repeatedly try and disengage the payload after the initial attempt. This increases the chance that it would deploy, thereby decreasing the likelihood of failure. On top of this, the main mode of failure that could occur in the electronics system is an inability to communicate with the onboard transceiver to initiate the deployment protocol. This can be avoided by testing the device well within the range of the launch vehicle landing radius laid out in the mission requirements, as well as outside of this range by a comfortable margin should that end up being the case. A reliable transceiver has already been selected for implementation, so verifying its reliability through testing as well as adding a redundant one to try and trigger should the first one fail can even further reduce the already small significance of this risk.

7.0 Safety

7.1 Safety Plan

The safety officer, Christopher Kinyon, is responsible for creating a safety plan addressing the proper and safe usage of materials and facilities throughout the duration of the NSL competition. As an assigned safety officer, he has become familiar with the safety codes of NAR, FAA, NFPA, and TRA so that he may advise and ensure the safe usage of any possible launch site used by the team. There will also be extensive research on the federal laws and regulations regarding the use of airspace above launch sites. All hazardous materials that will be present during the NSL competition will be researched extensively to ensure they are handled properly and to mitigate the risk of personal injury and project failure. The safety procedures of all additional facilities, such as CPP's testing laboratories, will be read through by the safety officer and any other team members that wish or use the facilities. The safety officer will maintain contact with all team-leads to ensure all members that plan to use a facility or work with hazardous material have reviewed the necessary safety codes and requirements prior to usage. Additionally, as a precaution to the continuing COVID-19 pandemic, the safety officer will follow all state, county, and university safety guidelines prior to any in-person meetings, including requiring a vaccination status or a current negative COVID-19 test.

7.2 Safety Officer

The roles and responsibilities of the safety officer will include, but are not limited to:

- The monitoring of sub-teams and remaining up to date on their build or design progress to further provide safety information at each development stage
- Providing appropriate and sufficient safety briefing meetings
- Composing safety briefings for each team on how to safely operate their respective machinery, tools, and handling of hazardous materials
- Being present if necessary to ensure safety guidelines are being upheld with each team
- Inspecting launch vehicle and payload for any safety liabilities according to NAR trained-safety officer guidelines, and ensuring construction was completed and safety measures are still in place

- Providing an abundance of safety documents, manuals, pamphlets, and any other sources of safety information to the entire NSL team to minimize the hazards of using machinery/equipment and reducing the risk of injuring oneself or others
- Communicating with the team mentor to ensure the safe purchase, handling, transportation, and storage of any hazardous materials

7.3 Risk Assessment and Analysis

Risk assessment will be used to identify any hazards or potential threats to the team and the mission's success. It will serve as a proactive accident-avoidance system and will provide all team members with the briefing they need to stay safe and keep the mission on track to meet all budgetary and time sensitive milestones. Using risk cubes, as shown in **Figure 7.3-1**, all threats and risks to the team's success will be analyzed using levels of likelihood and consequences. Green squares show a low risk, yellow illustrates medium or reduced risk, and red shows a high risk. This risk cube in cohesion with the use of risk waterfalls as shown in **Figure 7.8-2** through **Figure 7.8-7**, will help identify and reduce any risks to team members, the launch vehicle, and all systems required for success in the NSL competition.

Levels of Likelihood:

A. **Near Certainty** (80-100%) Unpreventable failure and requires mission to be modified
B. **Highly Likely** (60-80%) Certain failure of a system but can be avoided
C. **Likely** (40-60%) Will likely occur but can be amended to avoid future setbacks
D. **Low likelihood** (20-40%) Proper risk assessment will negate majority risks
E. **Not likely** (0-20%) Basic safety procedures and protocols will negate risks

Levels of Consequences:

1. **Catastrophic-** Almost guaranteed total mission failure. Unacceptable risk and will not meet key program milestones or deadlines. Budget Increase >10%
2. **Critical**- Significant regression of mission goals and may jeopardize milestones and budget limits. Budget Increase <10%
3. **Significant**- Slight reduction on mission performance, will not affect major deadlines but may serve as a significant schedule slip and budget increase. Budget Increase <5%
4. **Moderate**- Minor impact on mission performance goal and deadline, any setback is recoverable with minor schedule and budget impact. Budget Increase <1%

5. **Minimal**- Minimal or no risk to mission performance, schedule, or cost. Budget Increase ~0%

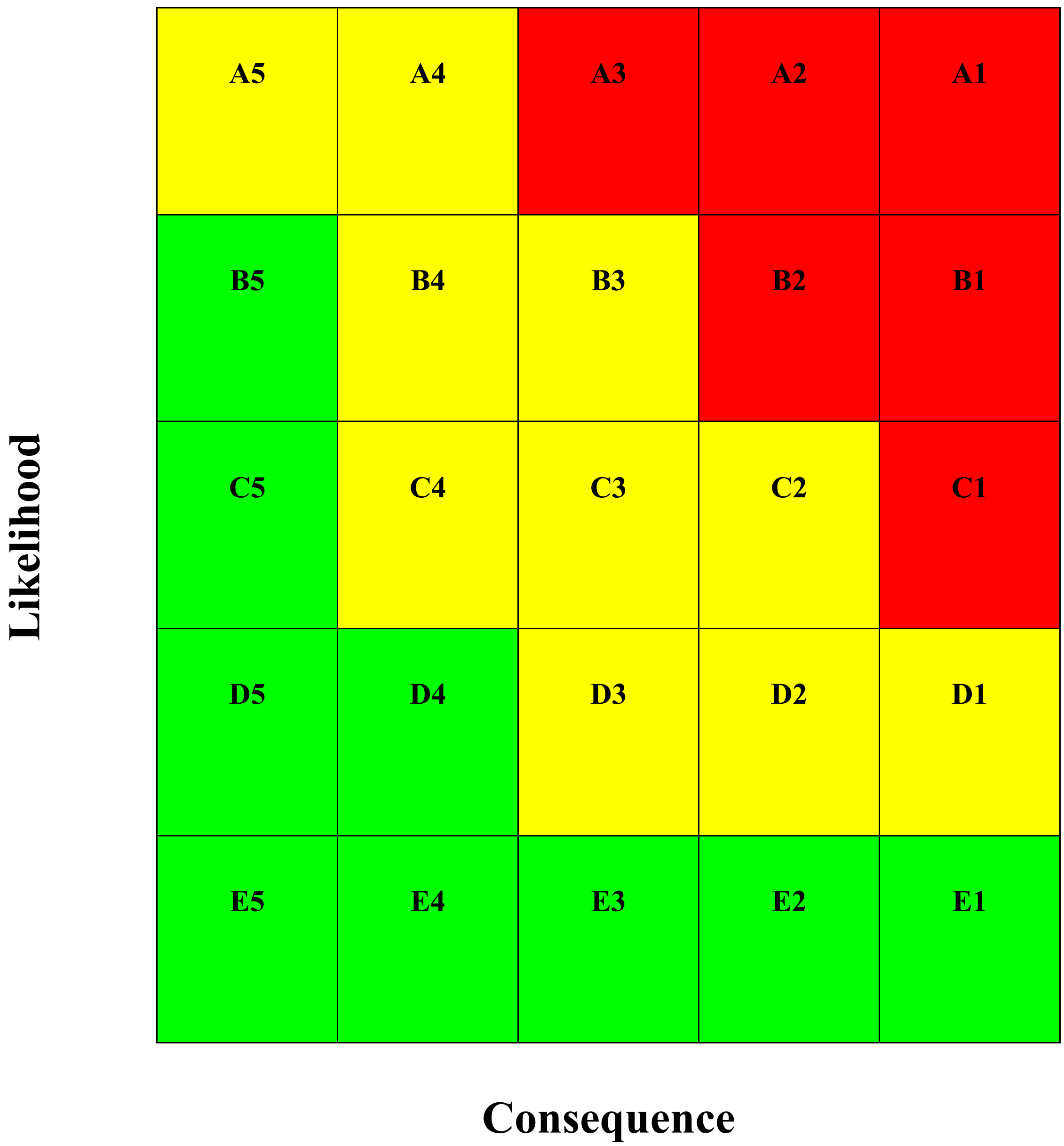

Figure 7.3-1: Risk Cube

7.4 Personnel and Programmatic Hazard Analysis

Table 7.4-1: Personnel Hazard Analysis Matrix

Hazard	Cause	Effect	Risk Rating	Proposed Mitigation
Rocket motor	Accidental ignition	Excessive heat and pressure may cause bodily injury or even death	**D1**	Team mentor must be present for motor assembly, proper PPE must be worn, and NAR high-powered rocketry procedures must be followed
Black powder	Accidental ignition	Excessive heat and pressure may cause bodily injury	**D2**	Team mentor must be present for use of black powder, proper PPE must be worn, and team is not allowed in front or behind rocket in case of ignition
Covid-19 (or other illness)	Infection of team member by virus	Serious illness of team member, planned timeline is setback from inability to maintain work schedule	**C3**	Following university CDC Covid-19 guidelines and having constant communication with team members to plan for delegation of ill team members work
Power Tools	Spinning/moving parts and sharp blades	Bodily injury or amputation	**E2**	Team members must review safety procedures for power tools and wear proper PPE
Electronics	Electrical static discharge	Possible damage to sensitive electronics	**E4**	Team member should wear electrostatic bracelet to prevent buildup of static electricity
Epoxy and Adhesives	Toxic fumes and extremely adhesive material	Respiratory problems, skin irritation, and unintended bonding	**B5**	Team members must use materials in ventilated areas and wear proper PPE

Fiberglass	Dust and splinters from material	Skin irritation and respiratory problems	**C5**	Team members must review safety procedures for fiberglass and wear proper PPE
Heat/Sun	Excessive heat and sun exposure without adequate hydration or nutrition	Possible heat stroke, sunburn, and heat exhaustion	**C5**	Bringing enough water for team to stay hydrated through launch, advising team to eat before going to launch site, and wearing adequate sun protection
Electronics Fracturing	Launch, flight, or landing impact forces break solder joints or pins	Electronics systems break and cannot transmit location data	**D4**	Force damper in payload system to decrease amount of shock on electronics
Recovery system fire	Black powder ejection sets parachute and shroud lines on fire	Parachute loses enough surface area to remain effective or detached completely	**E2**	Fire blanket wrapping to protect parachute and shroud lines from blast, pop test to ensure survivability

Table 7.4-2: Programmatic Hazard Analysis Matrix

Hazard	Cause	Effect	Risk Rating	Proposed Mitigation
Unavailable components	Supplier or manufacturer not having sufficient supply of rocket components	Inability to construct rocket and vital systems	**B4**	Numerous contingency plans for each component needed in the circumstance that the primary component is unavailable
Missing supplies/tools	Team members forget tool or materials necessary to construct launch vehicle at launch site	Inability to construct rocket with components present, might not be able to launch	**B4**	Launch checklist documenting every tool, part, material, and spare equipment needed to launch rocket

Cost overrun	Cost of materials runs over designated budget and funds	Project cannot continue without funds to continue building rocket	**C4**	Sub teams develop bills of materials throughout project to appropriate necessary funds
Travel budget	Fundraising and sponsorships do not meet travel costs for team to go to Huntsville, Alabama	Team cannot participate on site with NASA officials and other competing teams	**A5**	Reach out to friends, families, and possible companies to donate or sponsor the team to raise sufficient funds
Airbrake design project delay	The addition and design of air brakes may strain team and adds to workload	Team has less time to spend on project research and may miss deadlines	**D4**	Setting specific deadlines to have design planned or cutting design to eliminate strain
Report legibility	Non continuous formatting across review reports and presentations	Deduction of points in report grading, degradation of displayed information in presentations	**B5**	Creation of systems engineering team to thoroughly review each review report and presentation before submission

7.5 Failure Modes and Effects Analysis

Table 7.5-1: Failure Modes and Analysis Matrix

Failure Hazard	Cause	Effect	Risk Rating	Proposed Mitigation
Under target apogee	Weight of rocket or insufficient thrust from motor	Rocket doesn't go high enough to meet design and competition requirements	**C1**	Numerous simulations through OpenRocket, Rocksim, RASaero, and hand calculations to ensure rocket is meeting target altitude
Fins	Fin flutter causes structural failure of fins	Loss of fins will lead to instability and catastrophic failure of rocket	**D1**	Continuous analysis of fin flutter to find acceptable fins for rocket that will survive flutter
Recovery Deployment Failure	Recovery black powder charges do not ignite or do not provide sufficient force	Parachutes are not deployed and launch vehicle becomes ballistic	**D1**	Before every launch, pop tests with same amount of black powder as launch are

	for parachute deployment			conducted to ensure parachute is ejected and redundant second charge is onboard
Avionics electronics loss of power	Takeoff flight forces, current limiting circuit, or bad connectors	Recovery electronics will not function, disabling system from deploying parachutes	**D1**	Battery used will not have current limiter and connectors will be checked for continuity before flight
Shroud lines breaking	Flight forces snap shroud lines, disconnects parachutes	Rocket has no parachutes and becomes ballistic projectile	**D1**	Shroud line material will withstand forces of the descending launch vehicle
Premature Recovery Deployment	Recovery black powder charges ignite prior to target parachute deployment time	Premature parachute deployment would increase drag prior to reaching its apogee	**D1**	Redundancy in parachute design and full system vacuum chamber test to ensure parachute is ejected
Air brakes	Premature deployment of air brakes on ascent	Additional drag will cause rocket to miss target altitude	**D2**	Planned numerous tests of brake system or elimination of design with bleak outlook
Tangled shroud lines	Shroud lines of parachute become tangled	Rocket collides with other sections, damages components, or restricts parachutes from deploying	**D2**	Shroud line length testing to find right length for deployment and proper parachute packing procedures
Payload Transmitting Location Data	Rocket body material blocks payload signal transmission or signal is not strong enough	Location data is not able to be sent back to launch site	**C3**	Communication module will be tested extensively to ensure data can be transmitted through a payload capsule and launch vehicle. Launch vehicle will be constructed from fiberglass to allow for signal transmission
Nose Cone	Stepper motor, used to	Untimely ejection of the	**D3**	Calculated required holding

retention	extrude the lead screw, could induce a premature nose cone ejection	nosecone would result in premature payload ejection and thus failure		torque based on accurate estimates of friction the nose cone would experience during descent, to ensure the stepper motor could be set to the correct torque
Payload Electronics Overheating	Outside temperatures overheat electronics	Electronics either shut down or fail and cannot transmit location data	**D4**	Ventilation system to allow for heat to escape payload capsule and cool electronics
Transceiver is unable to pick up on the signal	Transceiver becomes damaged due to the shock experienced from landing	Payload won't be able to deploy	**D4**	Research into the flight heritage of the transceiver and hardware-in-the-loop-testing
Ball bearings become loose during launch or during descent	Depth of the hole that the bearings occupy become hollowed out due to the forces experienced during the mission	Unequal balancing of the payload platform	**D5**	Multiple test prints and FDA analysis on the CAD design to determine weak points along with system-in-the-loop testing
Avionics electronics interference	Electromagnetic and radio frequency interference	Electronics performance is degraded or has total loss of function	**E2**	Copper tape faraday cage around avionics bay to shield recovery electronics
Above target apogee	Miscalculations of rocket weight or design	Rocket goes past competition requirements	**E3**	Target altitude will be designed to be between minimum and maximum apogee to provide margin of failure without affecting competition performance

7.6 Environmental Hazard Analysis

Table 7.6-1: Environmental Hazard Matrix

Hazard	Cause	Effect	Risk Rating	Proposed Mitigation
Wind	Strong wind hitting rocket	Rocket is blown off course on launch or drifts past landing zone on descent	**C3**	Design error margin for mission to succeed with minimal wind and reschedule launch for wind speeds 20+ mph
Flooding	Excessive rain	Launch site is flooded on launch day and deemed inaccessible	**C3**	Research weather forecasts for proposed launch days and designate additional dates for launch
Rough Terrain	Uneven terrain	Terrain blocks payload lead screw from ejecting payload	**C3**	Payload communication signal is not reliant on ejection, increase strength of lead screw ejection
Wildfire	Motor blast, black powder charge, or burning fuselage on landing	Fire at launch site or in landing zone	**D4**	Follow proper NAR, NFPA, and FAR fire codes to prevent fire and extinguish them if possible

7.7 Risk Mitigation Quantification

Table 7.7-1: Risk Mitigation Quantification Matrix

Risk	Mitigation Technique	Likelihood and Impact	Quantification
Fuselage, fins, or nose cone breaking on landing	Ordering spare body parts to replace broken parts	Low impact High probability	Lack of reusability adds to additional budget constraints
Additional flight needed after system failure	Numerous simulations to justify system effectiveness	Medium impact Medium probability	Every launch requires additional purchase of motor
Covid-19 restrictions closing university testing labs	Plan for ordering fuselage parts rather than construction in available labs	Low impact High probability	Forced to pay prices of pre-manufactured parts
Recovery system failure	Including redundant systems to ensure recovery deployment	High impact Medium probability	Additional redundant system adds to budget constraints
Launch site flooded or extreme wind	Research weather patterns on launch day and set multiple launch dates as back up	Low impact Medium probability	Rescheduling launch date decreases time to analyze launch data before deadlines
Black powder charges	Testing black powder charges before each launch in pop tests	Low impact High Probability	Additional usage of black powder for safety assurance adds to budget constraints

7.8 Risk Mitigation Waterfall

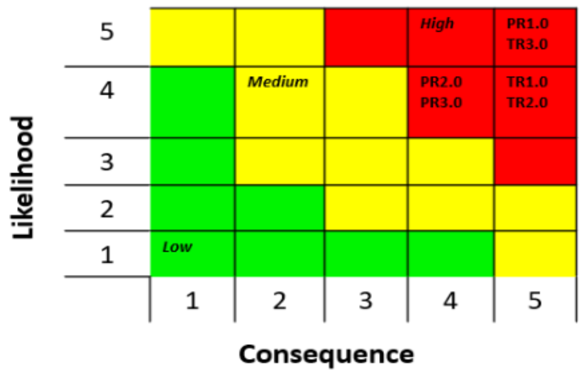

Figure 7.8-1: Risk Waterfall Risk Cube

Table 7.8-2: Risk Waterfall Programmatic and Technical Risks

Programmatic Risks		
Risk #	Related Req	Risk Description
PR1.0	5.3.2	Team member contracting Covid-19 virus
PR2.0	3.2	The SLCF does not arrive on time to perform ground ejection test
PR3.0	1.2	Cost of materials and components runs over designated budget and

Technical Risks		
Risk #	Related Req	Risk Description
PR1.0	5.3.2	Team member contracting Covid-19 virus
PR2.0	3.2	The SLCF does not arrive on time to perform ground ejection test
PR3.0	1.2	Cost of materials and components runs over designated budget and

		allocated funds

		allocated funds

Programmatic Risk 1.0: If a team member is infected with Covid-19, due to the ongoing pandemic then the team member would not be able to help the team and would pose a risk to the health of other team members
Related Requirement 5.3.2: Implement procedures developed by the team for construction, assembly, launch, and recovery activities.

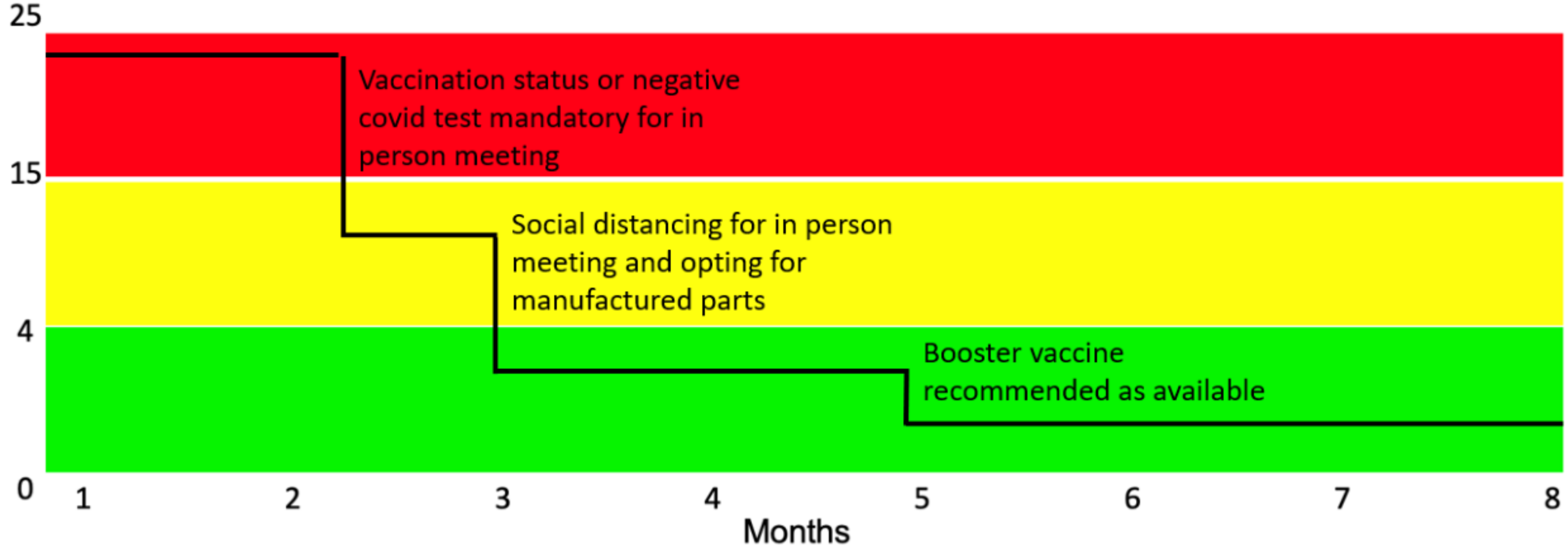

Figure 7.8-2: Covid-19 Programmatic Risk Waterfall

Programmatic Risk 2.0: If the SLCF does not arrive on time to perform ground ejection test, due to the ongoing pandemic or a supply shortage, we will not be able to implement the redundant flight computer
Related Requirement 3.1.2: The Recovery system will contain redundant, commercially available altimeters

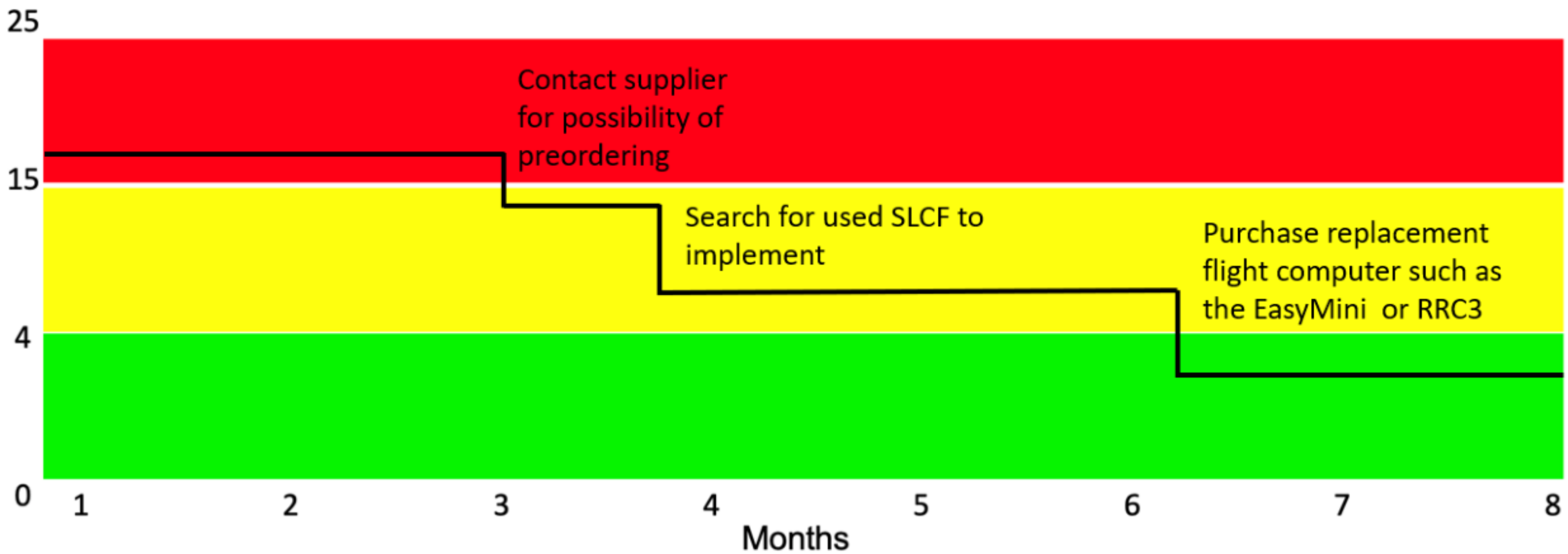

Figure 7.8-3: SLCF Programmatic Risk Waterfall

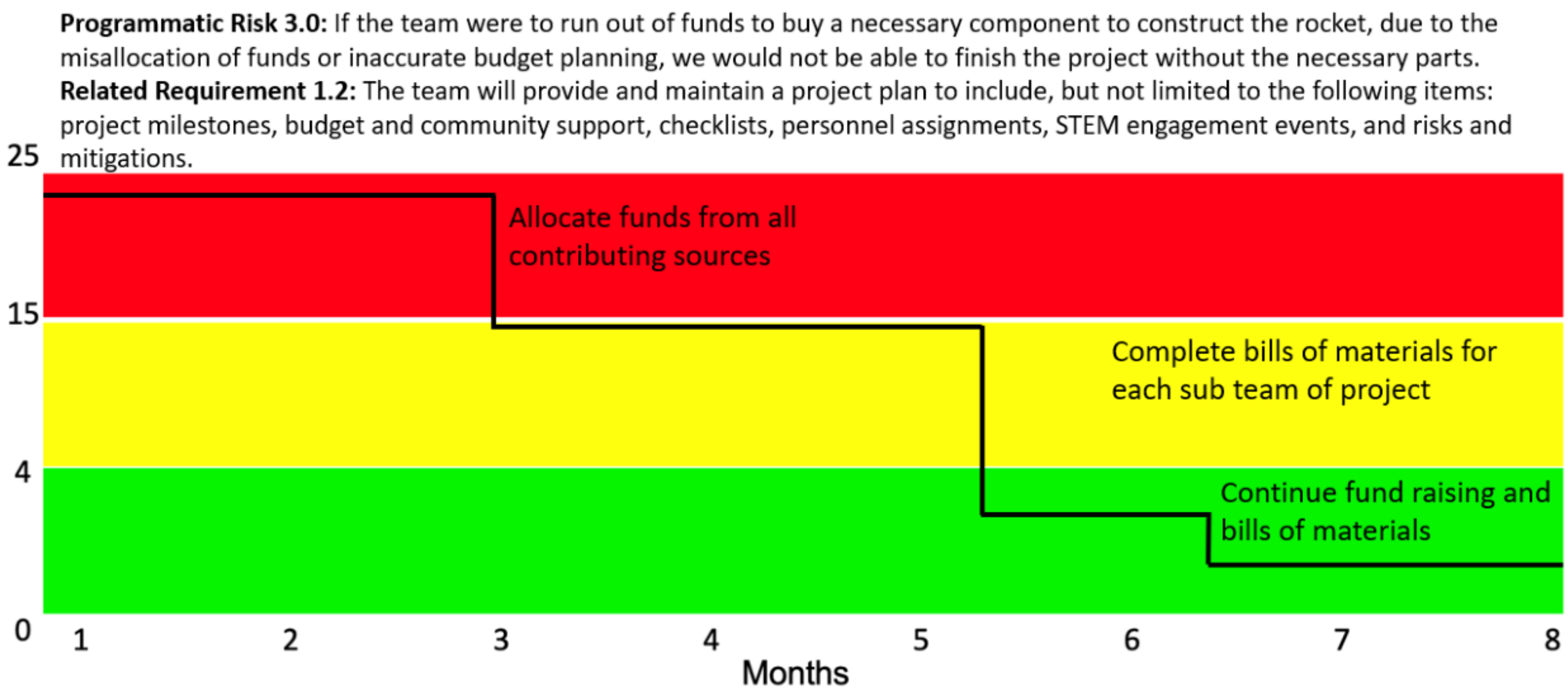

Figure 7.8-4: Budget Overrun Programmatic Risk Waterfall

Technical Risk 1.0: If the TeleMetrum and SLCF do not send signals to deploy black powder charges, launch vehicle recovery will fail and the launch vehicle will no longer be reusable.
Related Requirement: 3.5: The apogee event may contain a delay of no more than 2 seconds

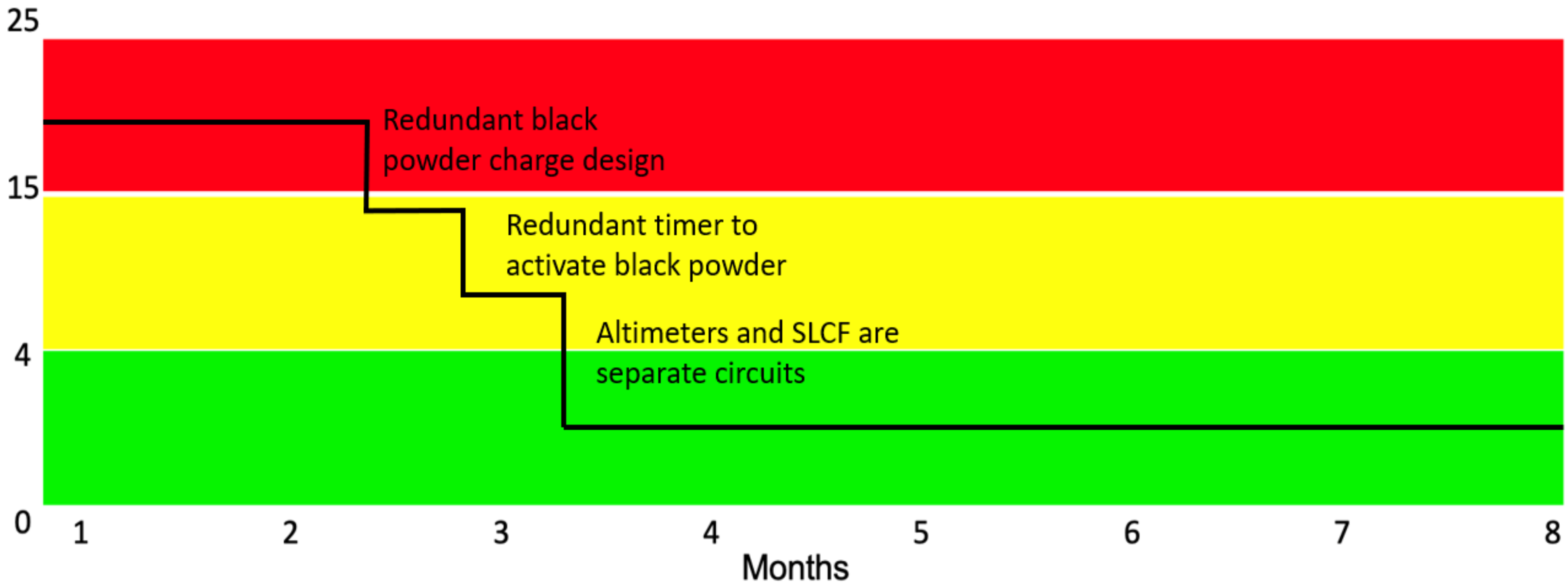

Figure 7.8-5: Black Powder Charge Failure Technical Risk Waterfall

Technical Risk 2.0: If PLI system encounters interference when attempting to deploy payload, then the payload may encounter trouble sending gridded square location
Related Requirement 4.1: Teams shall design a payload capable of autonomously locating the launch vehicle upon landing by identifying the launch vehicle's grid position on an aerial image of the launch site without the use of a global positioning system (GPS).

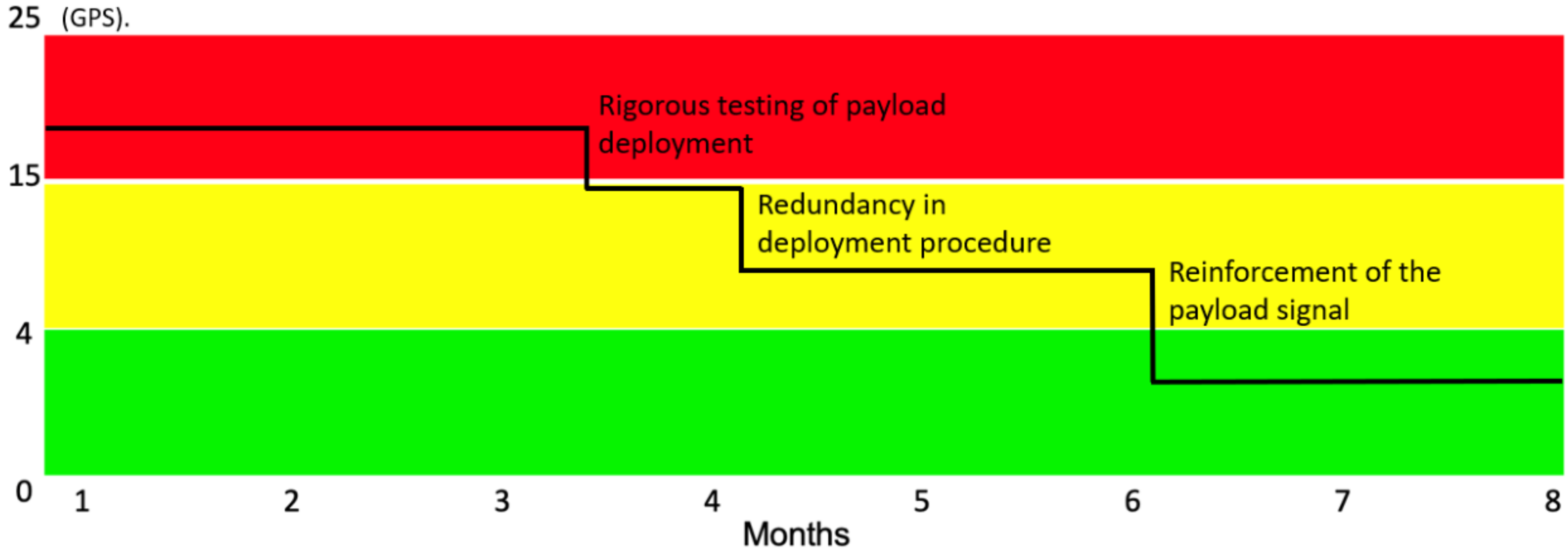

Figure 7.8-6: Payload Deployment Technical Risk Waterfall

Technical Risk 3.0: If the air brake system deploys prematurely during launch, due to a system malfunction, the launch vehicle will experience excessive drag and likely will not reach our target altitude.
Related Requirement 2.2: Teams shall identify their target altitude goal at the PDR milestone. The declared target altitude will be used to determine the team's altitude score.

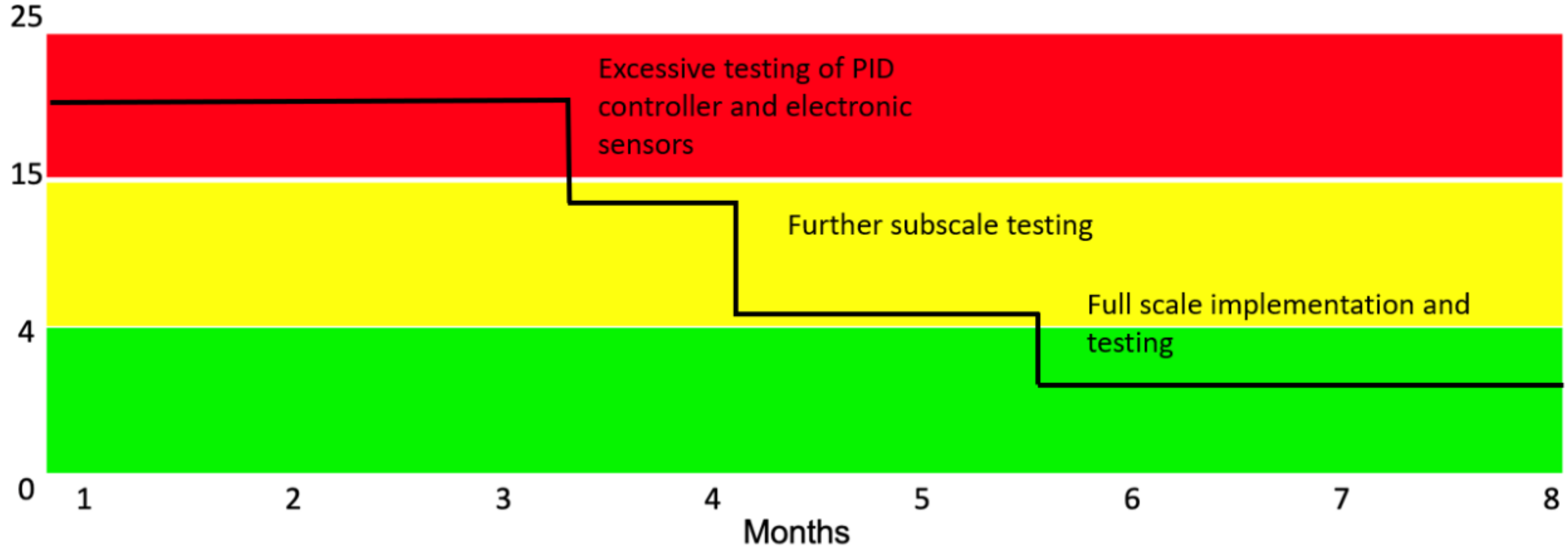

Figure 7.8-7: Air Brake System Technical Risk Waterfall

8.0 Requirement Compliance

8.1 Derived Requirements

The team created derived requirements during the design process to help each sub team understand what is required from the system. Each derived requirement was established with a measurable value or constraint so progress could be checked during the various tests the team plans to carry out for the Critical Design Review. It was essential to make each requirement formatted this way to help finalize the launch vehicle and payload design.

Table 8.1-1: Launch Vehicle Derived Requirements

Derived Req. #	Related Req. #	Statement	Verification Method	Verification Plan	Status
2.5.1	2.5	The team shall produce a full-scale Solidworks Assembly that is accurate and updated completely	Design	A completely updated full-scale model will provide an accurate mass and CG of the final design of the rocket	Completed
2.18.3.1	2.18.3	The team shall conduct stress analysis on critical components including the Airframe, Fins, and brakes using expected loads	Analysis	Chosen component designs must have sufficient analysis proving they will not fail on launch so that rocket will achieve target altitude and successful flight	Completed
6.0.1	6.0	The team shall produce a LV Structure Sheet that displays the masses and dimensions of the overall vehicle	Analysis	A sheet that summarizes key data will allow for easy access to important information for future analysis and allows all team members to be up to date.	Completed
2.1.1	2.1	The team shall continue analysis and refining expected apogee to estimate an accurate target apogee of 5,100 ft	Analysis	Continuously updated simulations will provide an accurate final apogee of the final design of the rocket	Completed
2.10.1.1	2.10.1	The team shall conduct trade studies and further comparison to select subscale and full-scale motors	Analysis	Only acceptable class motors that meet competition guidelines will be used in launch vehicle	Completed

2.14.1	2.14	The team shall perform fin flutter analysis and twist analysis to ensure rockets survival and a stability margin of 2.0	Analysis	Chosen fins must have sufficient analysis proving they will not fail on launch so that rocket will achieve target altitude	Completed
2.17.1	2.17	The team shall perform calculations of the coefficient of drag to remain under 0.8 to ensure target apogee can be reached	Analysis	Drag analysis will help predict a more realistic and accurate target apogee	Completed
2.18.2	2.18.3	The team shall create models of launch vehicle and mission plan using Rocksim and Open Rocket and ensure simulated apogee reached is above 5,100 ft	Analysis	Models and simulations of the launch vehicle will provide accurate data to judge progress and effectiveness of the design and will account for error of weight estimates as project progresses	Completed
2.18.3.2	2.18.3	The team shall perform stress analysis of the motor mounts and bulkheads to ensure flight forces do not exceed 0.58 ksi shear stress on the motor mounts and 1.32 ksi bending stress on any bulkheads	Analysis	Analysis of the strength of motor mount and bulkhead will either prove acceptable to survive launch stresses or call for redesign	Completed
2.14.2	2.14	The launch vehicle shall have main parachute versus drogue parachute situated towards nose cone to maintain stability margin of over 2.0	Design	Full scale model and simulations will account for heavier parachute towards top of rocket and effects of cg position on stability margin and target apogee	Completed
2.19.2.1	2.19.2	The launch vehicle material will not interfere with radio frequencies	Design	Launch vehicle will be constructed out of fiberglass to allow for frequencies to transmit without interference	Completed
2.4.1	2.4	The launch vehicles motor centering rings will not interfere with the attachment of fins	Design	The motor will only use 2 centering rings to allow adequate space for fins to be attached	Completed

2.1.2	2.1	The launch vehicle shall use a 6 in diameter body tube to reach 5,100 ft apogee	Analysis	The chosen launch vehicle size will have analysis and simulations to prove target apogee will be reached	Completed
2.2.1	2.2	The team shall perform stress analysis of the air brakes to ensure flight forces do not exceed 27 ksi on the air brakes when deployed	Analysis	Analysis of the strength of the air brakes will either prove acceptable to survive launch and effectively alter apogee or call for redesign	Completed
2.14.3	2.14	The team shall mount the fins 90 degrees from each other to maintain stability margin of 2.0	Design	The team will design a fin mounting apparatus to accurately position and attach fins to rocket body	Completed

Table 8.1-2: Recovery Derived Requirements

Derived Req. #	Related Req. #	Statement	Verification Method	Verification Plan	Status
2.7.1	2.7	The team shall use Li-po battery supplies to ensure the minimum two hours on the launch pad is reached, and to decrease overall weight of the rocket.	Design	Only Li-po batteries will be purchased during material acquisition and will then be tested on subscale, and full-scale test launches.	Completed
3.13.2.1	3.13.2	All avionics components must be shielded, and this shielding shall consist of lightweight material to meet necessary weights for the launch vehicle.	Observation	Trade matrices of various materials such as copper tape will be conducted to ensure shielding ability, weight, and cost effectiveness.	Completed
3.8.1	3.8	The avionics system will be housed in a separate section of the launch vehicle away from payload and closed using copper tape and bulkheads, to ensure independence and no interference.	Design	Avionics team will work with the structures team to acquire adequate spacing and housing for the avionics bay.	Completed
3.12.2.1	3.12.2	All avionics electrical components will be able to remain fully functional for a duration no less than	Testing	The team will conduct a "shake and bake" test on the avionics systems to	In Progress

		3 hours to ensure all electronic recovery systems including GPS are functional during launch and flight.		simulate in-flight vibrations and the heating of the electronic components to ensure their ability to remain fully functional during flight.	
3.3.1	3.3	Each independent section of the launch vehicle will have a maximum kinetic energy of 75 ft-lbf at landing.	Analysis	Kinetic energy will be calculated based on the mass of each section and verified through MATLAB to not exceed 75 ft-lbf.	Completed
3.11.1	3.11	The descent time of the launch vehicle will be limited to 90 seconds (apogee to touch down).	Analysis	Descent time will be calculated based on the target apogee and verified through MATLAB to not exceed 90 seconds.	Completed

Table 8.1-3: Payload Derived Requirements

Derived Req. #	Related Req. #	Statement	Verification Method	Verification Plan	Status
4.2.1	4.2	The payload shall collect data throughout the mission at a rate of up to 200 Hz.	Analysis	The Raspberry Pi 4 added quad-core processor and higher CPU clock speed fits within payloads mission criteria.	Completed
4.2.2	4.2	The payload shall be capable of pinpointing the location of the launch vehicle with an accuracy of ±50 m.	Analysis	The GPS module BN-880 has a faster satellite lock and will be sufficient to verify the location of the launch vehicle.	Completed
4.2.2.6.1	4.2.2.6	The payload shall transmit data to the receiver with a range of up to 5km.	Design	The chosen microcontroller LoRa can transmit and receive data over great distances.	Completed
4.1.1	4.1	The payload shall collect accurate acceleration and gyroscope data under launch vibration conditions and must	Analysis	The Embedded LX Evaluation Kit using a triaxial gyroscope with acceleration range at ±8g	Completed

		be reliable when reaching ± 4gs.		fitting within the mission's criteria.	
4.2.4.1	4.2.4.	The payload shall collect data at a resolution of at least 16 bits.	Design	The use of the 3-Space Nano Evaluation Kit has advanced processing creating the desired resolution.	In Progress
4.2.2.6.1	4.2.2.6	The payload shall be identified on its location within target altitude of 5,100ft and the Barometric pressure sensor must fall within 84kPa to 101.3kPa to be transmitted to the teams ground station.	Design	The wireless communications will be aided by using Raspberry Pi allowing data connection to be transmitted.	Completed
4.2.3.1	4.2.3	The payload shall contain an IMU and barometric pressure sensors that will act as a simple inertial navigation system and shall identify on its location and not be aided with GPS to ensure payload mission success.	Design	Through sensor component selection the barometric pressure sensors and IMU ensure no use of GPS is necessary for the payload.	In progress
4.3.1.1	4.3.1	Payload shall utilize electronic and/or mechanical deployment mechanisms to ensure that no black powered energetics will be used as a system to deploy the payload.	Design	The components for the payload integration system will primarily consist of linear actuators and bearings.	Completed

9.0 Project Plan

9.1 Bill of Materials

Cal Poly's NASA Student Launch Team is composed of several sub teams, with three main systems that take care of the overall design of the launch vehicle and payload. The Payload Integration and Payload sub teams under the Payload System created separate bills of materials, **Table 9.1-1** and **Table 9.1-2**, that include available shipping and tax information. The same can be said for the Avionics and Parachute Analysis sub teams. **Table 9.1-4** and **Table 9.1-5** summarize their respective bill of materials that include available shipping and tax information for the Recovery System. The Launch Vehicle Team combined their bills of materials for the Structures and Analysis sub teams, which is shown in **Table 9.1-3**.

Table 9.1-1: Payload Integration's Bill of Materials

Product Name	Quantity	Price	Shipping & Taxes	Total
Redrex Nema 17 Stepper Motor with 310mm T8x8 Lead Screw	3	$24.99	$7.68	$82.65
A4988 Stepper Motor Driver Carrier	3	$5.95	$6.24	$24.09
Mini Electric Linear Actuator Stroke 1"	2	$29.99	$6.14	$66.12
Relay board for linear actuator	2	$17.40	$3.56	$38.36
8mm bearing balls (100 pack)	1	$6.90	$0.71	$7.61
Arduino Nano RP2040	2	$25.50	$9.31	$60.31
AA-batteries (4 pack)	1	$14.51	$1.31	$15.82
12 V AA NiMH rechargeable battery	2	$21.98	$4.50	$48.46
PLA Pro Filament (1 kg Spool)	3	$22.99	$7.08	$76.05
			Total	**$419.47**

Table 9.1-2: Payload's Bill of Materials

Product Name	Quantity	Price	Shipping & Taxes	Total
Polypropylene	1	$54.00	$0.00	$54.00
Raspberry Pi	1	$45.00	$0.00	$45.00
IMU	1	$99.00	$13.37	$112.37
BaroMetric Pressure Sensors	2	$9.95	$13.13	$33.03
Li-po Battery	3	$10.99	$2.55	$35.52
GPS Module	1	$20.49	$1.49	$22.08
Voltage Stepper	1	$8.79	$0.68	$9.47
LoRa Modules	2	$34.95	$18.55	$88.45
			Total	**$399.92**

Table 9.1-3: Launch Vehicle's Bill of Materials

Product Name	Quantity	Price	Shipping & Taxes	Total
Standard Servo Plate A	1	$4.99		$5.64
Actobotics Dual Servo Arm	1	$7.99		$9.03
NiMH Battery (6V)	1	$12.99	$12.37	$23.67
HS-645MG Servo-Clockwise (stock)-Stock Rotation	1	$34.99		$39.54
DDP125 Standard Pan	1	$24.99		$28.24
Lead Shot Balls	1	36.99		$41.80
Raspberry Pi 4 Model B (2 GB)	1	$55.98	$25.87	$69.25
TUOFENG 22 awg Solid Wire-Solid Wire Kit-6 Different Colored 30 ft spools 22 Gauge Jumper Wire- Hook up Wire Kit	1	$15.49	$10.04	$25.53

6" OD G12 fiberglass filament wound tube 60" long Airframe	2	$252.00	$63.00	$567.00
D 6.0" - 7.5" diameter Rocket Fins	4	$40.98	$5.13	$46.11
G-10 Fiberglass Centering Ring CR 75MM/6"	3	$19.95	$7.56	$67.41
FNC-6.0 Fiberglass Nose Cone	2	$149.95	$14.95	$314.85
Epoxy	2	$19.99	$6.00	$45.98
Fiberglass Tube Bulkhead Disk 6"	4	$9.80	$10.66	$49.86
Aerotech 29.04" long 75mm Casing w/ forward seal disk	1	$519.06	$14.62	$533.68
Aero tech adapter system (spacer, forward and aft closure)	1	$134.82	$0.90	$135.72
6-in G12 Fiberglass Coupler Tube, 18" long	1	$30.00	$7.50	$37.50
Lead Shot Ballast Weight beads	5	$7.00	$5.25	$40.25
Rail Buttons (2)	1	$11.73	$1.76	$13.49
Aerotech L2200G Motor, 75mm dia.	1	$292.99	$46.03	$339.02
Motor Mount, fits 75mm motor, " long	1	$37.00	$5.55	$42.55
			Total	**$2,476.12**

Table 9.1-4: Avionics' Bill of Materials

Product Name	Quantity	Price	Shipping & Taxes	Total
Telemetrum V3	1	$300.00	$30.75	$330.75
StratologgerCF	2	$54.95	$11.26	$121.16
TeleDongle Starter Kit	1	$100.00	$10.25	$110.25
USB Data Transfer Kit	1	$24.95	$2.56	$36.00

1200 mAh Li-po Battery	2	$9.69	$1.99	$21.37
Copper Foil Tape (2 in X 33 ft)	1	$12.49	$1.28	$13.77
6.0-in Bulkhead	2	$6.89	$14.37	$43.93
Electronics Rotary Switch	2	$6.00	$1.23	$13.23
1/2 in. x 13 tpi x 12 in. Stainless Steel Threaded Rod	2	$5.98	$1.23	$13.19
1/2 in.-13 Stainless Steel Hex Nut (25 pack)	1	$16.15	$1.66	$17.81
3D Printed Sled	1	$5.00	$0.51	$5.51
1/4 in. x 1-1/8 in. x 2 in. Stainless Steel U-Bolt	2	$3.65	$0.75	$8.05
1/2in Copper Tube	1	$5.86	$0.60	$6.46
18 Gauge Stranded Wire	1	$16.99	$1.74	$18.73
Fireworks Firing System Igniter (100 pack)	1	$29.80	$3.05	$32.85
Terminal Block Set	1	$7.29	$0.75	$8.04
4-40 Screws and Standoffs (4 pack)	2	$1.79	$0.37	$3.95
			Total:	**$805.05**

Table 9.1-5: Parachute Recovery's Bill of Materials

Product Name	Quantity	Price	Shipping & Taxes	Total
Gorilla Tape, Black Duct Tape, 1.88 in. x 12 yd., Black, (Pack of 1)	1	$6.81	$0.54	$7.35
hyStik 1 in. x 60 yds. Blue Painters Masking Tape	1	$4.85	$7.32	$12.17
Pre-made e-matches (bundle of 100)	1	$35.50	$14.44	$49.94
1/4" U-Bolt. Stainless Steel	2	$3.00	$7.43	$13.43
SW- 350	2	$1.50	$7.99	$10.99
1/4" QUICK LINK	4	$4.26	$11.06	$28.10
Nylon Shear Pins - 20 pack	1	$5.56	$12.00	$5.56

Jolly Logic Chute Release	2	$129.95	$23.39	$283.29
Jolly Logic Chute Release Protector	2	$9.95	$3.56	$23.46
3-gram Aluminum Charge Wells - 2 pack	1	$14.95	$6.20	$21.15
2 in. Copper Pressure Tube Cap Fitting	2	$10.98	$3.85	$25.81
120" Iris Compact parachute (w/15% disc)	1	$460.68	$57.78	$518.46
Classic Elliptical Compact 24" (w/15% disc)	1	$61.23	$21.14	$82.37
			Total	**$1,082.08**

9.2 Budget

The fundraising goal for the year was set on the initial bill of materials that was created by the individual sub teams. As the design phase progressed, different choices of materials were down selected causing the budget to decrease from its initial value. The allocation amounts can be seen in **Table 9.2-1**. This budget considers the discounts acquired from various companies as well.

Table 9.2-1: Allocation of Budget

System	Amount Allocated
Payload System	$819.39
Launch Vehicle System	$2,476.12
Recovery System	$1,887.13
Outreach	$500.00
Safety	$75.00
Team Merchandise	$600.00
Travel	$8,050.00
Total	**$14,407.64**

If the team decides to not travel, the budget for team merchandise will be increased, which would help advertise NASA Student Launch and affect Outreach. With the increased budget in merchandise, the team plans to buy official Team collared jackets, stickers, and more. The Outreach Team also received a large allocation of the budget to prepare for the STEM Engagement activities.

9.3 Funding Sources

Funding sources, as mentioned in the proposal, will still come from the university, businesses, and donations from individuals. The following table shows funds that have been secured, which come from a variety of sources. The first two sources come entirely from funding supplied by programs overseeing NASA Student Launch. Firstly, most of the funds secured thus far come from the grant supplied by Cal Poly Pomona Associated Students, accounting for over 50% of the funding at $5,315. After that, the next biggest contributor is the project program overseeing the NSL project division at Cal Poly Pomona, the Undergraduate Missiles and Ballistics and Rocketry Association, which initially funded the project $2,500 total. The next main source of funding was secured via sponsorship from Lockheed Martin. After the project mentor spoke with representatives at Lockheed Martin, they agreed to sponsor the project and granted $2,000. The final source of funding to the project thus far is just leftover budget from the previous year's NSL project, which contributed $300 total.

Table 9.3-1: Funding Sources

Funding Source	Support
Cal Poly Pomona Associated Students, Incorporated Grant	$5,315
Undergraduate Missiles and Ballistics and Rocketry Association	$2,500
Lockheed Martin Sponsorship	$2,000
Previous Year NSL Budget (leftover)	$300
Total	**$10,115**

9.3.1 Outreach

The Outreach team continues to do a significant amount of work branching out to the local schools within our community. The team is continuing to contact and offer schools STEM Engagement events. The team is in talks with some schools and is currently awaiting confirmation dates. We are accompanying our offers with a sneak peek providing interested participants an explanation of what they can expect to happen within each STEM engagement event. The outreach team has shared the NSL Team's social media handles to keep our communities updated, interested, and excited about new outreach events. Our team is looking into new STEM topics and ideas to share and spark as much interest within STEM as possible.

9.4 Timeline

Figures 9.4-1,2,3,4,5, describe the current project plan that the team is following. Our ideal date for subscale launch is on the 13th of December and we have begun ordering a few parts for sub-scale assembly. The team is doing their best given the current circumstances, but as school labs are opening and most classes are being converted back to in-person we are very confident in our manufacturing abilities.

The outreach team has missing events in the Gantt Charts due to the pandemic and trouble contacting schools. The Outreach Lead has been working hard to contact as many schools as she can, and we are currently awaiting confirmation from some schools for specific dates and what type of event they can accommodate.

TASK ID	TASK TITLE	TASK OWNER	START DATE	DUE DATE	DURATION (Weeks)	PCT OF TASK COMPLETE	Proposal							
							August					Septembe		
							1	2	3	4	5	6	7	8
1	Proposal													
1.1	Proposal Writing	General	8/19/2021	9/20/2021	4.5	100%								
1.2	Initial Electronics/Software Recovery Research and AV Bay Design Finalized	Recovery	8/19/2021	9/7/2021	4	100%								
1.2.1	Planned Parachute System Design Finalized	Recovery	8/19/2021	9/10/2021	3	100%								
1.3	Proposal Research (requirements, air brake design and feasability, materials)	Structures	8/19/2021	9/4/2021	2	100%								
1.3.1	CAD Launch Vehicle Components	Structures	9/4/2021	9/13/2021	1.5	100%								
1.4	Preliminary Research on Rocket Body and Fins (trade matrices)	Analysis	8/24/2021	9/10/2021	2.5	100%								
1.4.1	Projected Altitude Simulations and Calculations (including hand calculations)	Analysis	8/24/2021	9/10/2021	2.5	100%								
1.5	Initial Research/Design and Finalizing Chosen Payload design/ ejection system	Payload	8/19/2021	9/9/2021	3.0	100%								
1.5.1	Completion of CAD of Possible Designs for Payload and Ejection System	Payload	9/3/2021	9/13/2021	1.5	100%								
1.6	Sub-Team WBS	Systems	8/27/2021	9/10/2021	2	100%								
1.7	Verification/Tracebility Matrix	Systems	8/19/2021	9/15/2021	4.0	100%								
1.8	Initial Risk assessment and possible solutions	General	9/3/2021	9/13/2021	1.5	100%								
1.9	Initial Detailed Budget for hardware, software, travel, and miscellaneous	General	9/7/2021	9/14/2021	1	100%								

Figure 9.4-1: Gantt Chart-Proposal

TASK ID	TASK TITLE	TASK OWNER	START DATE	DUE DATE	DURATION (Weeks)	PCT OF TASK COMPLETE	PDR October 11	12	13	14	15	16
2	Preliminary Design Report											
2.1	Preliminary Design Report Writing	General	10/7/2021	11/1/2021	3.5	100%						
2.2	Recovery Electronics/ Software & AV Bay Design Revised and Finalized	Recovery	10/8/2021	10/22/2021	2	100%						
2.2.1	Parachute System Design Revised with Supporting Calculations	Recovery	10/8/2021	10/22/2021	2	100%						
2.3	Launch Vehicle System Design Revised with structural analysis	Structures	10/8/2021	10/22/2021	2	100%						
2.3.1	Downselect air brakes, materials, and overall vehicle	Structures	10/8/2021	10/22/2021	2	100%						
2.4	Revise payload design, components and payload integration then finalize	Payload	10/8/2021	10/23/2021	2	100%						
2.4.1	Payload electronics, safety switches/indicators discussion with supporting drawings, diagrams	Payload	10/15/2021	10/29/2021	2	100%						
2.5	Determine official launch target altitude and preliminary motor selection	Analysis	10/8/2021	10/22/2021	2	100%						
2.5.1	Mission performance predictions with vehicle criteria changes since proposal	Analysis	10/8/2021	10/22/2021	2	100%						
2.6	System Level and Derived Requirements	Systems	10/8/2021	10/25/2021	2.5	100%						
2.7	PDR Updates since Proposal	Systems	10/8/2021	10/25/2021	2.5	100%						
2.8	Test Equipment Procurement and Lab Scheduling	Systems	10/11/2021	10/25/2021	2	100%						
2.9	Revised Detailed Budget	General	10/8/2021	10/29/2021	3	100%						

Figure 9.4-2: Gantt Chart-Preliminary Design Report

							R			CDR									
							ber				November				December				
TASK ID	TASK TITLE	TASK OWNER	START DATE	DUE DATE	DURATION (Weeks)	PCT OF TASK COMPLETE	14	15	16	17	18	19	20	21	22	23	24	25	26
3	Critical Design Report																		
3.1	Critical Design Report Writing	General	11/30/2021	1/3/2022	4.5	0%													
3.1.2	Subscale Test Flight	General	12/13/2021	12/29/2021	3	0%													
3.2	Design avionics and parachutes systems for subscale launch	Recovery	12/1/2021	12/29/2021	2.5	0%													
3.2.1	Mock AV Bay and Avionics system assembled	Recovery	12/13/2021	12/29/2021	2.5	0%													
3.3	CAD all Subscale Rocket components	Structures	11/30/2021	12/10/2021	1.5	0%													
3.3.1	Determine all subscale rocket materials	Structures	11/30/2021	12/10/2021	1.5	0%													
3.4	Complete Gridded Map w/ proper scale	Payload	10/25/2021	1/3/2022	9	0%													
3.4.1	Finalize CAD design for payload delivery according to NASA revisions from PDR	Payload	12/1/2021	12/27/2021	4	0%													
3.4.2	Finalize flight reliablity and results of flight/planned flights, all aspects of payload system performance.	Payload	12/10/2021	1/3/2022	3	0%													
3.5	Perform subscale flight analysis (with comaprisons to full-scale estimations)	Analysis	11/30/2021	12/20/2021	3	0%													
3.5.1	Final motor choice with thrust to weight ratio and estimated rail exit velocity	Analysis	11/30/2021	12/20/2021	3	0%													
3.6	CDR Updates since PDR	Systems	12/2/2021	12/30/2021	4	0%													
3.7	Additional Derived Requirements according to PDR	Systems	12/2/2021	12/30/2021	4	0%													

Figure 9.4-3: Gantt Chart-Critical Design Review

TASK ID	TASK TITLE	TASK OWNER	START DATE	DUE DATE	DURATION (Weeks)	PCT OF TASK COMPLETE
4	Flight Readiness Review					
4.1	Flight Readiness Review Writing	General	1/27/2022	3/7/2022	5	0%
4.1.1	Vehicle Demonstration Flight Test	General	2/10/2022	3/5/2022	3	0%
4.1.2	Payload Demonstration Flight	General	3/19/2022	4/2/2022	2	0%
4.2	Avionics Bay and Components Assembled/Vaccuum Test Completed	Recovery	2/10/2022	2/25/2022	2	0%
4.2.1	Parachute System Deployment Test	Recovery	2/10/2022	3/5/2022	3	0%
4.3	Testing: Vibration, Stress, and Wind Tunnel	Structures	2/1/2022	2/18/2022	2.5	0%
4.3.1	Revisions Based on Strucural Integrity Testing	Structures	2/18/2022	2/28/2022	2	0%
4.4	Payload and Payload integration completed designs, dimensions, retention systems and flight plans/ flight test results	Payload	2/25/2022	3/26/2022	4	0%
4.4.1	Test payload delivery system in various positions	Payload	2/25/2022	3/26/2022	4	0%
4.4.2	Finalize summaries of payload mission sequence, retention systems and addressing failures encountered.	Payload	3/12/2022	3/25/2022	2	0%
4.5	Updated target altitude and selection of competition launch motor with Flight profile simulations using simulated vehicle data	Analysis	1/27/2022	2/28/2022	4	0%
4.5.1	Analyze demonstration flight data from recorded alitmeter data	Analysis	1/27/2022	2/28/2022	4	0%
4.6	Validate and Organize Testing for Subteams	Systems	1/28/2022	2/11/2022	2	0%
4.7	Develop Launch day Procedures for Subteams	Systems	2/18/2022	3/7/2022	3	0%
4.8	Travel to Huntsville,AL	General	4/17/2022	4/20/2022	0.5	0%
4.9	Competition Launch Day	General	4/23/2022	4/24/2022	0.0	0%

Figure 9.4-4: Gantt Chart-Flight Readiness Review

TASK ID	TASK TITLE	TASK OWNER	START DATE	DUE DATE	DURATION (Weeks)	PCT OF TASK COMPLETE	Launch Week and PLAR			
							May			
							45	46	47	W
5	Post Launch									
5.1	Travel back Home	General	4/24/2022	4/25/2022	1	0%				
5.2	Post Launch Assesment Report	General	4/26/2023	5/9/2022	2	0%				

Figure 9.4-5: Gantt Chart-Post Launch Assessment Review

Appendix A: Team Hour Log Sheet

FALL - Week 5 — **September 19 - September 25**

Team Hour Log	Major	Hours	Description
Alex Djansezian	Aerospace Eng.	5	General, Leads Meeting, proposal review and submission, Edberg update
Alton Lo	Aerospace Eng.		
Andre Perez	Mechanical Eng.	6	Meetings, Proposal
Andrew Alday	Aerospace Eng.	1	Proposal review
Angela Velazquez	Aerospace Eng.	1	General meeting, ideas for outreach opportunities
Anthony Rodrgiez	Aerospace Eng.	6	General Meeting, Sub Team Leads meeting, Proposal review
Ashif Ahmed	Aerospace Eng.	1	General/Sub meeting
Ashley Schiller	Aerospace Eng.	0.5	general meeting attendance
Ashley Taylor Perez	Aerospace Eng.	3	General meeting, leads meeting, parachutes meeting
Ben Tran	Aerospace Eng.	1	General Meeting/ Avionics Meeting
Bulamro Sanchez	Aerospace Eng.	1	General Meeting, Leads meeting
Caleb Padilla	Mechanical Eng.	5	General Meeting, Sub Team Leads meeting, Solidworks Payload CAD
Christopher Kinyon	Aerospace Eng.	5	General Meeting, Systems meeting, Proposal edits
Daniella Nicomedes	Aerospace Eng.	10	Proofreading & Editing Proposal
David Hernandez	Mechanical Eng.	1	General Meeting
Garrett Arian	Aerospace Eng.		
Giovanni Mejia	Aerospace Eng.	1.5	General Meeting, parachutes meeting
Jessica Margala	Comp. Sci.	1	General Meeting
Jesus Antonio Rebolledo	Aerospace Eng.	1	Attended General Meeting, submitted new headshot.
Joelle Vargas	Aerospace Eng.	1	General Meeting
Jon-Michael Brown	Electrical Eng.	2	General and Avionics Meetings/Read PDR Requirements
Joshua Duque	Aerospace Eng.	2	
Lachlan Maccarthy	Aerospace Eng.		
Luis Andrade	Aerospace Eng.		
Luke Kohler	Mechanical Eng.	4	General meeting, proposal writing
Michael Quach	Aerospace Eng.	1.5	General Meeting, Sub-team Meeting
Nathan Castanon	Aerospace Eng.	0.5	General meeting
Nathan Lara	Aerospace Eng.	5	General meeting, leads meeting, Proposal review and submission, Dr. Edberg update
Nick Hall	Aerospace Eng.	1.5	General meeting, PDR Planning
Rogelio S Perez	Aerospace Eng.	2	Attended General Meeting, Sub-Team Leading (Assigned tasks for PDR)
Samy Ousman	Aerospace Eng.	3	general and sub-team meetings, editing proposal and slides
Sebastian Londono	Aerospace Eng.	1	Team Meeting
Stephen Jimenez	Aerospace Eng.	3	Attended general meeting, Systems Team Meeting, and Payload meeting for being the (Liaison)
Yosuf Mayar	Mechanical Eng.	1.5	Sub-Team Meeting & General
Ashley Kim	Mechanical Eng.		
Rene J. Holmes	Aerospace Eng.	1	General meeting, parachutes meeting
Ali Moulvi	Mechanical Eng.		
Ernesto Montes	Aerospace Eng.	1	Team Meeting, general meeting
Anthony Martinez	Mechanical Eng.	1.5	Sub-Team Meeting & General
Edward Hernandez	Aerospace Eng.	1	Team Meeting

Figure A-1: Week 5 Hour Log Sheet for the Team

FALL - Week 6 **September 26 - October 2**

Team Hour Log	Major	Hours	Description
Alex Djansezian	Aerospace Eng.	5	General, Leads Meeting, set up gofundme and grabcad, Edberg and Rick update
Alton Lo	Aerospace Eng.	12	CAD, extend design to 10 inches, general meeting, subteam meeting, research, learn how to use easyEDA
Andre Perez	Mechanical Eng.	7	CAD,meetings, redesign considerations and research
Andrew Alday	Aerospace Eng.	1	Analysis meeting and general team meeting
Angela Velazquez	Aerospace Eng.	4	Geneal meeting, updates for Outreach, Creating Email format
Anthony Rodrgiez	Aerospace Eng.	2	General Meetings, subteam meetings
Ashif Ahmed	Aerospace Eng.	1.5	General/Sub meeting
Ashley Schiller	Aerospace Eng.	1	Attended General and Subteam Meetings
Ashley Taylor Perez	Aerospace Eng.	3	General meeting, leads meeting, parachutes meeting
Ben Tran	Aerospace Eng.	2	General Meeting, Avionics Meeting, Research
Bulamro Sanchez	Aerospace Eng.	3	General meeting, subteam meeting.
Caleb Padilla	Mechanical Eng.	7	General Meeting, Sub Team Leads meeting, Solidworks Payload CAD
Christopher Kinyon	Aerospace Eng.	2	General meeting, failure modes research
Daniella Nicomedes	Aerospace Eng.	3	General Meeting, Subteam Meetings (Systems & Parachutes), Task Delegation to Parachutes Subteam
David Hernandez	Mechanical Eng.	3	General Meeting, Sub Team Meeting, Further Research on Component Selection
Garrett Arian	Aerospace Eng.		
Giovanni Mejia	Aerospace Eng.	1.5	General meeting, PDR work, parachutes meeting
Jessica Margala	Comp. Sci.	3	General Meeting, Sub-team Meeting, Individual research for component selection of sensors
Jesus Antonio Rebolledo	Aerospace Eng.	3	Attended General and Subteam Meetings and worked on individual tasks.
Joelle Vargas	Aerospace Eng.	1.5	General Meeting, Parachute's Meeting for PDR, individual PDR work
Jon-Michael Brown	Electrical Eng.	3	General, Meeting, Avionics Meeting, Electrical Schematics
Joshua Duque	Aerospace Eng.	4	
Lachlan Maccarthy	Aerospace Eng.	3	General and team meetings with material research
Luis Andrade	Aerospace Eng.		
Luke Kohler	Mechanical Eng.	3	General meeting, filament material research
Michael Quach	Aerospace Eng.	2	General Meeting, Sub-team Meeting, Nose cone ejection research
Nathan Castanon	Aerospace Eng.	3	General Meeting, Sub-team Meeting, Cp Research
Nathan Lara	Aerospace Eng.	6	General meeting, leads meeting, Set up GoFundMe, GrabCad, Dr. Edberg update and Rick update
Nick Hall	Aerospace Eng.	2	General meeting, sub team meeting, leads meeting, building drone
Rogelio S Perez	Aerospace Eng.	1	General meeting
Samy Ousman	Aerospace Eng.	2	general and sub-team meetings
Sebastian Londono	Aerospace Eng.	4	General Meeting, Sub-team Meeting, CAD Modeling
Stephen Jimenez	Aerospace Eng.	4	Attended general meeting, Systems Team Meeting, and Payload meeting for being the (Liaison)
Yosuf Mayar	Mechanical Eng.	2	general and sub team meeting
Ashley Kim	Mechanical Eng.	3	General meeting and subteam meeting, research
Rene J. Holmes	Aerospace Eng.	1.5	General meeting, draft PDR sections
Ali Moulvi	Mechanical Eng.		
Ernesto Montes	Aerospace Eng.	1	Team Meeting, general meeting
Anthony Martinez	Mechanical Eng.	2.5	Team Meeting, 3D Print Considerations
Edward Hernandez	Aerospace Eng.	1.5	Team Meeting, General Meeting

Figure A-2: Week 6 Hour Log Sheet for the Team

FALL - Week 7 — **October 3 - October 9**

Team Hour Log	Major	Hours	Description
Alex Djansezian	Aerospace Eng.	6.5	General, Leads meeting. Email Edberg, Rick,
Alton Lo	Aerospace Eng.	8	General Meeting, Subteam meeting, pros/cons, think of ideas for sled orientation, CAD, added copper tubes and fixed design
Andre Perez	Mechanical Eng.	15	Meetings, PLI redesign, CAD, research, PDR
Andrew Alday	Aerospace Eng.	7.5	Analysis spin research, modeling, and general meeting
Angela Velazquez	Aerospace Eng.	8	Contacting schools , presentations for outreach, creating emails, General meetings
Anthony Rodrgiez	Aerospace Eng.	7	Developing PDR Draft, Leads Meeting, Subteam Systems meeting.
Ashif Ahmed	Aerospace Eng.	4	General/Sub meeting, wiring schematic, transceiver research
Ashley Schiller	Aerospace Eng.	1	Attended General and Subteam Meetings
Ashley Taylor Perez	Aerospace Eng.	5	General meeting, leads meeting, parachutes meeting, began PDR writing, research
Ben Tran	Aerospace Eng.	3	General Meeting, Avionics Meeting, PDR Writing and research
Bulamro Sanchez	Aerospace Eng.	10	General Meeting, Subteam meeting, OpenRocket Model edits, Analysis Research, Fin Shape, Sizing and Orientation
Caleb Padilla	Mechanical Eng.	5	General Meeting, Payload team meeting, Research
Christopher Kinyon	Aerospace Eng.	3	Hazard and failure mode research, systems engineering method research
Daniella Nicomedes	Aerospace Eng.	3	General Meeting, Subteam Meetings
David Hernandez	Mechanical Eng.	4	General Meeting, Payload team meeting, Research
Garrett Arian	Aerospace Eng.		
Giovanni Mejia	Aerospace Eng.	3	PDR writing, research on Shroud lines, General Body meeting
Jessica Margala	Comp. Sci.		
Jesus Antonio Rebolledo	Aerospace Eng.	2	Attended Analysis Sub Team meeting and reviewed tasks.
Joelle Vargas	Aerospace Eng.	1	General meeting
Jon-Michael Brown	Electrical Eng.	5.5	General Meeting, Subteam meeting, pros/cons for GPS options, update avionics bill of materials and weights, proving redundancy exists within the system
Joshua Duque	Aerospace Eng.	2	
Lachlan Maccarthy	Aerospace Eng.	2	Full scale source research, and analysis of drag coeffecients
Luis Andrade	Aerospace Eng.		
Luke Kohler	Mechanical Eng.	2	General meeting, sub-team meeting
Michael Quach	Aerospace Eng.	4	General Meeting, Sub-team Meeting, Preliminary FMEA (Failure Modes)
Nathan Castanon	Aerospace Eng.	5	General meeting, Sub-team meeting, Cp Calculations
Nathan Lara	Aerospace Eng.	7	General meeting, Sub-team Leads meeting, Emailed edberg & rick,
Nick Hall	Aerospace Eng.	5	General meeting, leads meeting, PDB/battery/flight controller research,
Rogelio S Perez	Aerospace Eng.	1	General meeting
Samy Ousman	Aerospace Eng.	2	General and sub-team meetings
Sebastian Londono	Aerospace Eng.	12	General Meeting, Sub-team Meeting, CAD Modeling, 1-on-1 Meeting with Andre, Design change/brainstorming
Stephen Jimenez	Aerospace Eng.	5	Attended general meeting, Systems Team Meeting, and Payload meeting for being the (Liaison) ,PDR writing.
Yosuf Mayar	Mechanical Eng.	2	general meeting, subteam meeting, research
Ashley Kim	Mechanical Eng.	6	General meeting, analysis meeting, research, contacting schools for outreach
Rene J. Holmes	Aerospace Eng.		
Ali Moulvi	Mechanical Eng.		
Ernesto Montes	Aerospace Eng.	3.5	PLI Schematics, Transceiver Research, Meetings
Anthony Martinez	Mechanical Eng.	4	3D Print Research, Material Considerations, Pros Vs Cons consideration, team and general meeting
Edward Hernandez	Aerospace Eng.	2	Team Meeting, PDR Writing

Figure A-3: Week 7 Hour Log Sheet for the Team

FALL - Week 8 — **October 10 - October 16**

Team Hour Log	Major	Hours	Description
Alex Djansezian	Aerospace Eng.	8	General, Leads meeting, payload redesign, update rick
Alton Lo	Aerospace Eng.	12	Meetings, PDR writing, research, matricies, CAD
Andre Perez	Mechanical Eng.	7	Meetings, PLI redesign, CAD
Andrew Alday	Aerospace Eng.	5	General meeting and Cd calculations
Angela Velazquez	Aerospace Eng.	6	Graphics for STEM engagement, Powerpoint for STEM Engagement, Emailing/ Calling schools for STEM Engagement, Working on Social media Handles, Team Meeting
Anthony Rodrgiez	Aerospace Eng.	4	General, subteam, and lead meetings.
Ashif Ahmed	Aerospace Eng.	5.5	General/Sub meeting, wiring schematic
Ashley Schiller	Aerospace Eng.	1	Attended General and Subteam Meetings
Ashley Taylor Perez	Aerospace Eng.	7	General meeting, leads meeting, parachutes meeting, continue PDR writing, MATLAB: main deployment time, decent time, drift calcs.
Ben Tran	Aerospace Eng.	3	General Meeting, Avionics Meeting, PDR Writing
Bulamro Sanchez	Aerospace Eng.	9	General meeting, subteam meeting, leads meeting, launch vehicle resizing to
Caleb Padilla	Mechanical Eng.	6	General Meeting, Payload team meeting, Research, CAD Drawings
Christopher Kinyon	Aerospace Eng.	3	General meeting, systems meeting, Safety PDR writing
Daniella Nicomedes	Aerospace Eng.	2	General Meeting, Subteam Meeting
David Hernandez	Mechanical Eng.	5.5	General Meeting, Payload team meeting, Pitot Tube Research
Garrett Arian	Aerospace Eng.		
Giovanni Mejia	Aerospace Eng.	5	General Meeting, PDR, verification of Calcs, research
Jessica Margala	Comp. Sci.		
Jesus Antonio Rebolledo	Aerospace Eng.	8	Attended Sub Team and General Meetings. Conducted Fin Flutter Analysis.
Joelle Vargas	Aerospace Eng.	4	General meeting, PDR writing, parachutes research
Jon-Michael Brown	Electrical Eng.	5	General Meeting, Subteam meeting, PDR writing
Joshua Duque	Aerospace Eng.	12	
Lachlan Maccarthy	Aerospace Eng.	5	Airbrake redesign, full scale cad
Luis Andrade	Aerospace Eng.		
Luke Kohler	Mechanical Eng.	5	general meeting, sub-team meeting, 3D printing reseach
Michael Quach	Aerospace Eng.	8.5	General Meeting, Sub-team Meeting, Wrapping and altering failure modes
Nathan Castanon	Aerospace Eng.	5	General Meeting, Subteam Meeting, Cd Calculations
Nathan Lara	Aerospace Eng.	12	General meeting, leads meeting, Team member help, mass Analysis, Team design meeting, update to rick
Nick Hall	Aerospace Eng.	8	Payload team meeting, leads meeting, general meeting, Payload redesign analysis, meeting with PLI
Rogelio S Perez	Aerospace Eng.		
Samy Ousman	Aerospace Eng.	10	Meetings, Airframe Load Analysis, Bill of Material Review, CAD airframe/airbrake drawings
Sebastian Londono	Aerospace Eng.	10	General Meeting, Sub-team Meeting, CAD Modeling, Design change/brainstorming
Stephen Jimenez	Aerospace Eng.	9	Attended general meeting, Systems Team Meeting, and Payload meeting for being the (Liaison) PDR derived requirements start
Yosuf Mayar	Mechanical Eng.	2	general meeting, subteam meeting, research
Ashley Kim	Mechanical Eng.	6	General meeting, analysis meeting, analysis calculations
Rene J. Holmes	Aerospace Eng.	2	PDR sections, general meeting slide
Ali Moulvi	Mechanical Eng.		
Ernesto Montes	Aerospace Eng.	4	Meetings, PLI Schematics,
Anthony Martinez	Mechanical Eng.	8	Drone Arm Test Prints, New Extruder Install along w/ E-Step Calibrations for Experimental Filaments, TPU Print Research & Testing, General Meeting, Payload Meeting
Edward Hernandez	Aerospace Eng.	3	Team Meeting, PDR Writing

Figure A-4: Week 8 Hour Log Sheet for the Team

FALL - Week 9 **October 17 - October 23**

Team Hour Log	Major	Hours	Description
Alex Djansezian	Aerospace Eng.	6	General Meeting, Leads Meeting, LM slide prep
Alton Lo	Aerospace Eng.	11	CAD, meetings, PDR writing, more research into redesign
Andre Perez	Mechanical Eng.	12	CAD, meetings, PDR writing, more research into redesign
Andrew Alday	Aerospace Eng.	8.5	Bulkhead stress analysis and fin analysis in openrocket
Angela Velazquez	Aerospace Eng.	6	Creation of Sneek peek, contacting schools, general and team lead meeeting
Anthony Rodrgiez	Aerospace Eng.	10	General, sub, lead meetings, PDR writing, Budget development.
Ashif Ahmed	Aerospace Eng.	1	General/Sub meeting
Ashley Schiller	Aerospace Eng.	3.5	Attended General and Subteam Meetings, worked on PDR writing
Ashley Taylor Perez	Aerospace Eng.	6	General meeting, leads meeting, shock cord research, shroud line research, MATLAB: main deployment time, decent time, drift calcs.
Ben Tran	Aerospace Eng.	4	General Meeting, Subteam Meeting, PDR Writing
Bulamro Sanchez	Aerospace Eng.	10	General meeting, subteam meeting, pdr writing, leads meeting, updating launch vehicle model, apogee calculations
Caleb Padilla	Mechanical Eng.	6	General Meeting, Payload team meeting, Research, CAD Drawings, PDR Write Up
Christopher Kinyon	Aerospace Eng.	12	General meeting, hazard research, systems PDR writing, Safety PDR matrix writing
Daniella Nicomedes	Aerospace Eng.	5	General Meeting, Subteam Meetings, Budget Calculations, PDR writing
David Hernandez	Mechanical Eng.	6	General Meeting, Payload team meeting, Research, PDR Writing
Garrett Arian	Aerospace Eng.		
Giovanni Mejia	Aerospace Eng.	4	General Meeting, PDR, parachutes meeting, research
Jessica Margala	Comp. Sci.		
Jesus Antonio Rebolledo	Aerospace Eng.	5	General Meeting, Subteam meeting and Cd calcs.
Joelle Vargas	Aerospace Eng.	2	General meeting, PDR for parachutes
Jon-Michael Brown	Electrical Eng.	5.5	General Meeting, Subteam meeting, PDR writing, CAD rendering
Joshua Duque	Aerospace Eng.	10	
Lachlan Maccarthy	Aerospace Eng.	3	Sourcing and Airbrake redesign
Luis Andrade	Aerospace Eng.		
Luke Kohler	Mechanical Eng.	6	General meeting, sub-team meeting, LoRa research
Michael Quach	Aerospace Eng.	4	General Meeting, Sub-team Meeting, Preliminary PDR Writing for PLI
Nathan Castanon	Aerospace Eng.	6	General Meeting, Subteam Meeting, Bulkhead stress analysis
Nathan Lara	Aerospace Eng.	7	General meeting, leads meeting, Dr.edberg update, PDR template slides, dr.bandari emails
Nick Hall	Aerospace Eng.	9.5	Payload redesign research, Inertial navigation research, payload meeting, leads meeting, general meeting
Rogelio S Perez	Aerospace Eng.		
Samy Ousman	Aerospace Eng.	8	General Meeting, Sub-team meeting, airframe analysis continued work, pdr writing
Sebastian Londono	Aerospace Eng.	13	General Meeting, Sub-team Meeting, CAD Modeling
Stephen Jimenez	Aerospace Eng.	10	Attended general meeting, Systems Team Meeting, and Payload meeting for being the (Liaison) updated B.O.M for payload
Yosuf Mayar	Mechanical Eng.	2	general meeting, subteam meeting, research
Ashley Kim	Mechanical Eng.	3	general meeting, sub meeting, research
Rene J. Holmes	Aerospace Eng.	2	lockheed slides, PDR section
Ali Moulvi	Mechanical Eng.		
Ernesto Montes	Aerospace Eng.	1	General meeting, sub-team meeting
Anthony Martinez	Mechanical Eng.	12	Microcontroller/SBC research, Pitot Tube + Dead Reckoning Research, General Meeting, Payload Meeting
Edward Hernandez	Aerospace Eng.	4	Team Meeting, PDR Writing, Liaison Meeting

Figure A-5: Week 9 Hour Log Sheet for the Team

FALL - Week 10 **October 24 - October 30**

Team Hour Log	Major	Hours	Description
Alex Djansezian	Aerospace Eng.	32	General,leads meeting, LM slides, LM presentation + practice, PDR writing
Alton Lo	Aerospace Eng.	10	Meetings, PDR writing + proofreading, PDR formatting, CAD
Andre Perez	Mechanical Eng.	15	Meetings, PDR writing, Lockheed presentation, CAD for post PDR
Andrew Alday	Aerospace Eng.	16	Bulkhead stress analysis, descent time and drift calculations, CD fin calculations, CG calculations, PDR writing, General Meeting, Analysis Meeting
Angela Velazquez	Aerospace Eng.	11	Outreach presentations, social Media updated post, Lockheed Presentation, PDR presentation, PDR writing
Anthony Rodrgiez	Aerospace Eng.	15	General,sub,leads meetings, LM slides and presentation/presentation practice, PDR writing.
Ashif Ahmed	Aerospace Eng.	4	General/Sub meeting, wiring schematic, PDR writing
Ashley Schiller	Aerospace Eng.	3.5	Attended General and Subteam Meetings, worked on PDR writing
Ashley Taylor Perez	Aerospace Eng.	15	General/leads/parachute meetings, PDR writing, PDR presentation slides, PDR proofreading, Lockheed Martin slides, Lockheed Martin presentation and practice, edited MATLAB code.
Ben Tran	Aerospace Eng.	4	General/Sub Meetings, PDR Proofing
Bulamro Sanchez	Aerospace Eng.	25	general meeting, subteam meeting, leads meeting, pdr writing and editing, pdr slides, proofreading, mototr mount stress calculations
Caleb Padilla	Mechanical Eng.		
Christopher Kinyon	Aerospace Eng.	25	Gen mtg, systems mtg, risk analysis, LM presentation, PDR work and hazard mitigations
Daniella Nicomedes	Aerospace Eng.	6	General Meeting, Subteam Meetings, PDR writing/review, PDR slides
David Hernandez	Mechanical Eng.	18	General Meeting, Payload Meeting, Lockheed Martin Slides, GPS Module/BMP/Comms Module Research, PDR Writing/Proofread, Wire Diagram
Garrett Arian	Aerospace Eng.		
Giovanni Mejia	Aerospace Eng.	7.5	PDR slides/presentation, proofreading/ PDR writing
Jessica Margala	Comp. Sci.		
Jesus Antonio Rebolledo	Aerospace Eng.	15	General Meeting, Subteam Meeting worked on Cd Calcs of Fins, PDR writing and PDR slides, along with proofreading.
Joelle Vargas	Aerospace Eng.	6.5	PDR work and General meeting
Jon-Michael Brown	Electrical Eng.	16	General Meeting, Subteam meeting, PDR writing, PDR slides, PDR Flysheet, LockHeed Martin Presentation
Joshua Duque	Aerospace Eng.	10	
Lachlan Maccarthy	Aerospace Eng.	4	CAD airbrakes Full scale model
Luis Andrade	Aerospace Eng.		
Luke Kohler	Mechanical Eng.	10	general meeting, LoRa and XBee research, material testing, PDR writing
Michael Quach	Aerospace Eng.	7	General Meeting, Sub-team Meeting, Proposal Writing
Nathan Castanon	Aerospace Eng.	9	General meeting, PDR writing, subteam meeting
Nathan Lara	Aerospace Eng.	42	Leads meeting, general meeting, Lockheed martin slides, Lockheed martin Practice, lockheed martin presentation, PDR assembly, PDR proofreading
Nick Hall	Aerospace Eng.		
Rogelio S Perez	Aerospace Eng.		
Samy Ousman	Aerospace Eng.	10	General meeting, sub-team meeting, airframe analysis completion w/ Garrett, pdr writing, pdr slides
Sebastian Londono	Aerospace Eng.	7	CAD Modeling, PDR Writing and Proofing
Stephen Jimenez	Aerospace Eng.	15	Attended general meeting, Systems Team Meeting, and Payload meeting for being the (Liaison) PDR proofreading, Lockheed Martin slides, Flysheet
Yosuf Mayar	Mechanical Eng.		
Ashley Kim	Mechanical Eng.	6	general meeting, submeeting, pdr writing
Rene J. Holmes	Aerospace Eng.	5.5	PDR section finalization, flysheetinfo
Ali Moulvi	Mechanical Eng.		
Ernesto Montes	Aerospace Eng.	4.5	PDR writing, meetings
Anthony Martinez	Mechanical Eng.	15	Payload SBC/Microcontroller PDR Writing, Research, General Meeting, Payload Meeting
Edward Hernandez	Aerospace Eng.		

Figure A-6: Week 10 Hour Log Sheet for the Team

Appendix B: MATLAB Code

```
clc
clear
```

Inputs

```
section_1 = 8.66769; % lbs to kg , motor
section_2 = 9.0901; % lbs to kg , payload + avionics
section_3 = 2.5401; % lbs to kg , nosecone
apogee = 5100; %ft
main_deployment = 500; %ft
```

Velocity

```
KE_max = 101.686; % Joules (75 lbf)
s1_V = sqrt((2*KE_max)/section_1) * 3.281; % m/s to ft/s
s2_V = sqrt((2*KE_max)/section_2) * 3.281; % m/s to ft/s
s3_V = sqrt((2*KE_max)/section_3) * 3.281; % m/s to ft/s
V = [s1_V s2_V s3_V];  % put values in an array to find max velocity of each section
Vmax = min(V); %Highest acceptable velocity to descend at
```

Kinetic Energy After Drogue Ejection

```
DKE1 = ((1/2) * section_1 * (80/3.28084)^2)/1.356;
DKE2 = ((1/2) * section_2 * (80/3.28084)^2)/1.356;
DKE3 = ((1/2) * section_3 * (80/3.28084)^2)/1.356;
```

Kinetic Energy After Main Ejection

```
KE1 = ((1/2) * section_1 * (Vmax/3.28084)^2)/1.356;
KE2 = ((1/2) * section_2 * (Vmax/3.28084)^2)/1.356;
KE3 = ((1/2) * section_3 * (Vmax/3.28084)^2)/1.356;
```

Descent Time

```
%after drogue
drogue_time = (apogee - main_deployment)/80;  % 80 ft/s is highest acceptable descent velocity
for a drogue chute
%after main deployment
main_time = main_deployment/Vmax;  %in seconds
total_time = main_time + drogue_time; % in seconds
```

Parachute Sizing

```
%inputs
total_weight = section_1 + section_2 + section_3; % lbs to kg, including ONLY dry mass of motor

%Drogue Chute
Co_Dd = 1.6;
rho = 1.185; %kg/m^3
mass_d = total_weight; %kg
velocity_drogue = 80*0.3048; %ft/s to m/s, 80 ft/s is a widely accepted descent drogue rate
gravity = 9.81; %m/s
Surface_Area_drogue = ((2*gravity*mass_d)/(rho*Co_Dd*(velocity_drogue^2)))*10.76391; %surface
area calculation m^2 to ft^2
Ddrogue = sqrt((4*Surface_Area_drogue)/pi()) %in feet
D_spillholed = Ddrogue*0.2 %in feet
Ddrogue_accounting_spillhole_d = Ddrogue - D_spillholed %in feet
Ddrogue_inches = Ddrogue_accounting_spillhole_d*12

%Main Chute
Co_Dm = 2.2;
mass_m = total_weight; %kg
velocity_main = 15.49*0.3048; %ft/s to m/s, 80 ft/s is a widely accepted descent drogue rate
Surface_Area_main = ((2*gravity*mass_d)/(rho*Co_Dm*(velocity_main^2)))*10.76391; %surface area
calculation m^2 to ft^2
Dmain = sqrt((4*Surface_Area_main)/pi()) %in feet
D_spillholem = Dmain*0.2 %in feet
Dmain_accounting_spillhole_m = Dmain - D_spillholem %in feet
Dmain_inches = Dmain_accounting_spillhole_m*12
```

Drift

```
drift0 = ((0/3600)*total_time)*5280; % ft
drift5 = ((5/3600)*total_time)*5280; %ft
drift10 = ((10/3600)*total_time)*5280; %ft
drift15 = ((15/3600)*total_time)*5280; %ft
drift20 = ((20/3600)*total_time)*5280; %ft
```

Displays

```
disp("                                    CALCULATED VALUES                                    ")
disp("-----------------------------------------------------------------------------------------")
disp("                                    KINETIC ENERGY                                    ")
disp("Highest Acceptable Velocity to descend: " + Vmax + "ft/s")
disp("~~~~~~~~~~")
disp("Drogue Descent Time: " + drogue_time + " seconds")
disp("Main Descent Time: " + main_time + " seconds")
disp("Total Descent Time: " + total_time + " seconds")
disp("~~~~~~~~~~")
disp("KE Section 1 after drogue: " + DKE1 + " lbf" )
disp("KE Section 2 after drogue: " + DKE2 + " lbf")
disp("KE Section 3 after drogue: " + DKE3 + " lbf")
disp("~~~~~~~~~~")
disp("KE Section 1 after main: " + KE1 + " lbf" )
disp("KE Section 2 after main: " + KE2 + " lbf")
disp("KE Section 3 after main: " + KE3 + " lbf")
disp("~~~~~~~~~~")

if total_time <= 90
    disp("You met the requirements! Descent time is: " + total_time +" seconds")
else
    disp("try again! you didnt meet the requirements!")
end


disp("__________________________________________________________________________________________
_______")
disp("                                    PARACHUTE SIZING (DROGUE)
")
disp("Drogue Surface Area: " + Surface_Area_drogue + " in^2")
disp("Drogue Reccomended Diameter(round chute): " +  Ddrogue_accounting_spillhole_d + " feet, " +
Ddrogue_inches + " inches")
%disp("Keep in mind that if you are using a toroidal chute, you have to take into account the
spill hole")
%disp("use Drogue diameter for reference but make sure the surface areas match")
disp("Accounting for spill hole!")
disp("__________________________________________________________________________________________
_______")

disp("                                    PARACHUTE SIZING (MAIN)
")
disp("Main Surface Area: " + Surface_Area_main + " in^2")
disp("Main Reccomended Diameter(round chute): " +  Dmain_accounting_spillhole_m + " feet, " +
Dmain_inches + " inches, ")
%disp("Keep in mind that if you are using a toroidal chute, you have to take into account the
spill hole")
%disp("use Main diameter for reference but make sure the surface areas match")
disp("Accounting for spill hole!")
disp("__________________________________________________________________________________________
```

```
_______")


disp("                                        PARACHUTE DRIFT
")
disp("Drift at 0 mph winds: " + drift0 + " ft")
disp("Drift at 5 mph winds: " + drift5 + " ft")
disp("Drift at 10 mph winds: " + drift10 + " ft")
disp("Drift at 15 mph winds: " + drift15 + " ft")
disp("Drift at 20 mph winds: " + drift20 + " ft")
```

```
                                    CALCULATED VALUES
------------------------------------------------------------------------------------------
                                    KINETIC ENERGY
Highest Acceptable Velocity to descend: 15.5191ft/s
~~~~~~~~~~
Drogue Descent Time: 57.4375 seconds
Main Descent Time: 32.5405 seconds
Total Descent Time: 89.978 seconds
~~~~~~~~~~
KE Section 1 after drogue: 1900.3061 lbf
KE Section 2 after drogue: 1992.9153 lbf
KE Section 3 after drogue: 556.892 lbf
~~~~~~~~~~
KE Section 1 after main: 71.5119 lbf
KE Section 2 after main: 74.997 lbf
KE Section 3 after main: 20.9568 lbf
~~~~~~~~~~
You met the requirements! Descent time is: 89.978 seconds
______________________________________________________________________________________________
_
                                    PARACHUTE SIZING (DROGUE)
Drogue Surface Area: 10.764 ft^2
Drogue Reccomended Diameter(round chute): 3.702 ft, 44.4246 inches
Keep in mind that if you are using a toroidal chute, you have to take into account the spill hole
use Drogue diameter for reference but make sure the surface areas match
______________________________________________________________________________________________
_
                                    PARACHUTE SIZING (MAIN)
Main Surface Area: 73.7643 ft^2
Main Reccomended Diameter(round chute): 9.6912ft, 116.2946 inches
Keep in mind that if you are using a toroidal chute, you have to take into account the spill hole
use Main diameter for reference but make sure the surface areas match
______________________________________________________________________________________________
_
                                      PARACHUTE DRIFT
Drift at 0 mph winds: 0 ft
Drift at 5 mph winds: 659.8385 ft
Drift at 10 mph winds: 1319.677 ft
Drift at 15 mph winds: 1979.5155 ft
Drift at 20 mph winds: 2639.354 ft
```

Published with MATLAB® R2021a

Appendix C: Stress Calculations

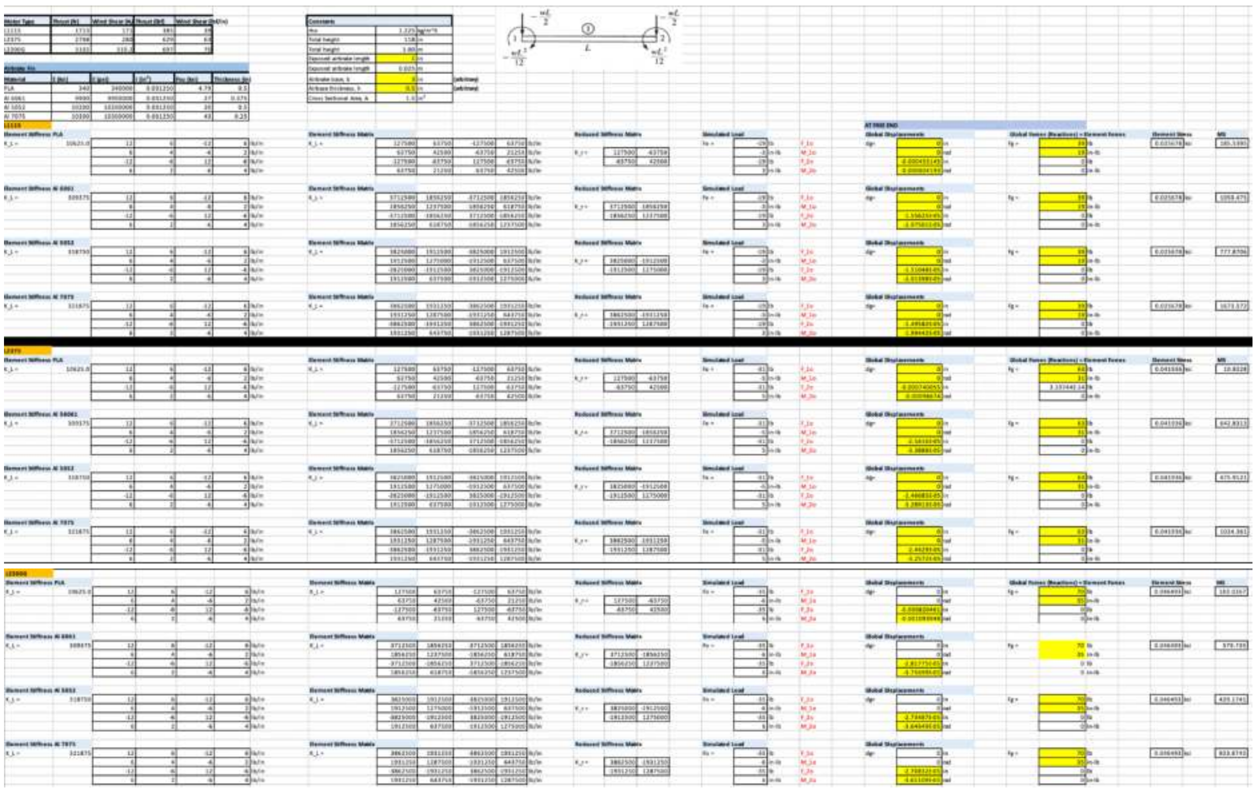

Motor Type	Thrust (lbf)	Wind Shear (lbf)
L1115	385.1540193	38.51540193
L2375	629.015582	62.9015582
L2200G	696.9079	69.69079

Constants		
rho (density)	4.25594E-05	lb/in^3
Total height	118	in
Total height	118.00	in

				L1115				L2375				L2200G			
Item	Height (in)	Height (m)	ight from base (	Axial Loading (lbf	w (lbf/in)	ansverse Shear (lb	Moment (lbf-in	Axial Loading (lbf	w(lbf/in)	ansverse Shear (l	Moment (lbf-in)	Axial Loading (lbf	w(lbf/in)	ansverse Shear (lb	Moment (lbf-in)
Cone	34.5	0.88	112.00	366	38.5	38.52	693	597	62.90	63	1132	661	69.69	69.69	1254
Payload Bay	19	0.48	77.50	253	1.12	38.52	916	413	1.82	63	1495	458	2.02	69.69	1657
Avionics/Drouge	19	0.48	58.50	191	0.72	38.52	1274	312	1.18	63	2081	346	1.30	69.69	2306
Motor/Airbrake Bay	39	0.99	39.50	129	0.53	38.52	1637	211	0.87	63	2673	233	0.96	69.69	2962
XXXX	0.5	0.01	0.50	2	0.35	38.52	2385	3	0.56	63	3894	3	0.63	69.69	4315
Total	112	2.84													

Airframe Thickness	0.085	in
Airframe Radius	6	in
Fcu	224800	psi

Item	Peak Stress (psi)	Running Load (l	Eq. Axial Load (lbf	Peak Stress (psi)	Running Load (lb	. Axial Load (l	Peak Stress (psi)	k Running Load (lb	Eq. Axial Load (lbf)
Cone	186.1995272	15.82695982	596.6623282	304.0923841	25.84785265	974.441088	336.9143641	28.63772095	1079.616645
Payload Bay	174.1822973	14.80549527	558.154022	284.4664046	24.17964439	911.551118	315.1700694	26.7894559	1009.938694
Avionics/Drouge	192.1481653	16.33259405	615.7242898	313.8074224	26.67363091	1005.57219	347.6779877	29.55262895	1114.107864
Motor/Airbrake Ba	210.503134	17.89276639	674.5414013	343.7839013	29.22163161	1101.62956	380.889955	32.37564617	1220.533106
XXXX	248.5563136	21.12728666	796.4799426	405.9305795	34.50409926	1300.7739	449.7443876	38.22827295	1441.171937
Total									

MS Peak Stress	MS Peak Stress	MS Peak Stress
1206.30704	738.24903	666.2318664
1289.601878	789.2514897	712.2656994
1168.930505	715.3629154	645.5753024
1066.917592	652.8991476	589.1967145
903.4228116	552.7892717	498.8394781

Appendix D: Bulkhead & Fasteners Analysis

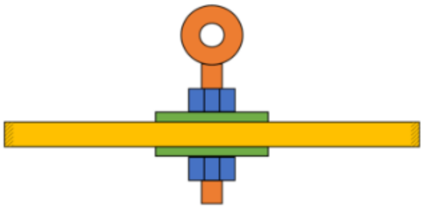

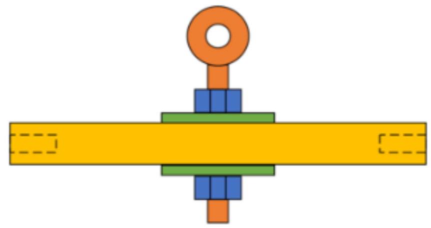

Payload Bulkhead			
Applied Forces & Moments			
Parameter	**Value**	**Units**	**Notes**
Normal Force	200.000	lbf	*x4 loaded weight of the LV
Shear Force	6.969	lbf	*10% Max Thrust
Moment	600	in-lb	
Bulkhead Properties			
Parameter	**Value**	**Units**	**Notes**
Material	Fiberglass	-	
Diameter	6	in	
Thickness	0.125	in	
Epoxied Surface Area	2	in²	
Tensile Strength (F_{tu})	9000	psi	*Fiberglass-AFI
Yield Strength (F_{ty})	30000	psi	*Performance Composites
Bending Allowable (F	16000	psi	*Fiberglass-AFI
Shear Strength (F_{su})	5193	psi	
Epoxy Shear Modulus	4800	psi	
UNC Bolt Properties			
Parameter	**Value**	**Units**	**Notes**
Material	Stainless Steel	-	*Table 5.5.1: Non-Aerospace Fastener (Ref. [Shig] Table
Diameter	0.25	in	
Threads/Inch	20	-	
Tensile Stress Area	0.0318	in²	
Modulus	10000	ksi	
ASTM Nut-Fastener Properties			
Parameter	**Value**	**Units**	**Notes**
Tensile Strength (F_{tu})	150	ksi	*Table 5.5.3 ASTM Fastener Strength Data(Ref. [Shig] T
Washer Properties			
Parameter	**Value**	**Units**	**Notes**
Thickness	0.055	in	*McMaster-Carr 316 Stainless Steel Washer
Outer Diameter	0.625	in	
Inner Diameter	0.281	in	
Material	Stainless Steel	-	
Modulus	10000	ksi	
Moment of Inertia	63.62	in⁴	
Bearing Strength (F_{bru})	162000	psi	*MMPDS-13, Table 2.7.1.0
Bulkhead Stress Analysis			
Parameter	**Value**	**Units**	**Notes**
Shear Stress	84.883	psi	
Bending Stress	1.179	psi	
Bearing Stress	223.008	psi	
Shear Tearout Stress	9.292	psi	
MS_{epoxy}	55.549	-	
$MS_{bending}$	13570.639	-	
$MS_{bearing}$	725.431	-	
$MS_{tearout}$	557.868	-	

AV Bay Bulkheads (I-Bolt Analysis)			
Applied Forces & Moments			
Parameter	**Value**	**Units**	**Notes**
Normal Force	200.000	lbf	*x4 loaded weight of the LV
Shear Force	6.969	lbf	*10% Max Thrust
Moment	600	in-lb	
Bulkhead Properties			
Parameter	**Value**	**Units**	**Notes**
Material	Birch Plywood	-	
Diameter	6	in	
Thickness	0.500	in	
Epoxied Surface Area	-	in²	
Tensile Strength (F_{tu})	5030	psi	
Yield Strength (F_{ty})	2000	psi	*FreeHostia
Bending Allowable (F	1320	psi	
Shear Strength (F_{su})	89923	psi	*FreeHostia
Epoxy Shear Modulus	-	psi	
UNC Bolt Properties			
Parameter	**Value**	**Units**	**Notes**
Material	Stainless Steel	-	*Table 5.5.1: Non-Aerospace Fastener (Ref. [Shig] Table 8-2
Diameter	0.25	in	
Threads/Inch	20	-	
Tensile Stress Area	0.0318	in²	
Modulus	10000	ksi	
ASTM Nut-Fastener Properties			
Parameter	**Value**	**Units**	**Notes**
Tensile Strength (F_{tu})	150	ksi	*Table 5.5.3 ASTM Fastener Strength Data(Ref. [Shig] Tabl
Washer Properties			
Parameter	**Value**	**Units**	**Notes**
Thickness	0.055	in	*McMaster-Carr 316 Stainless Steel Washer
Outer Diameter	0.625	in	
Inner Diameter	0.281	in	
Material	Stainless Steel	-	
Modulus	10000	ksi	
Moment of Inertia	63.62	in⁴	
Bearing Strength (F_{bru})	162000	psi	*MMPDS-13, Table 2.7.1.0
Bulkhead Stress Analysis			
Parameter	**Value**	**Units**	**Notes**
Shear Stress	-	psi	
Bending Stress	4.716	psi	
Bearing Stress	55.752	psi	
Shear Tearout Stress	2.323	psi	
MS_{epoxy}	-	-	
$MS_{bending}$	278.915	-	
$MS_{bearing}$	2904.725	-	
$MS_{tearout}$	38708.858	-	

AV Bay Bulkheads (Fastener Analysis)

Forces on Plate						
P_x =		lbs		Px =	3.000	in
P_y =	0.000	lbs		P_y Location =	3.000	in
P_z =	200.000	lbs		P_z Location	0	in
Chamber Pressure	200.000	psi	Plate Thickness =		0.5	in
EA of Bulkhead	7.069	in²	Aluminum Bulk Outer Radius		3.000	in

Birch Plywood Plate		
F_{tu} =	5.030	ksi
F_{su} =	2.902	ksi
F_{bru} of plate =	16.389	ksi

Bolt		
F_{tu} =	74.694	ksi
F_{su} =	43.099	ksi
Bolt Size		

NO	θ	D_i	x_i	y_i	z_i	A_i	Ax_i	Ay_i	Az_i	J_{xyi}	J_{xzi}	J_{yzi}	τ_{xi}	τ_{yi}	τ_{zi}	τ_{Bi}	S_i	f_b	f_{STD}	MS_{shear}	$MS_{shear\ TD}$	MS_{bear}
	deg	in	in	in	in	in²	in³	in³	in³	in⁴	in⁴	in⁴	ksi	ksi	ksi	ksi	Kips	ksi	ksi	-	-	-
1	45	0.23622	2.1213	2.1213	0.0000	0.0438	0.0930	0.0930	0.0000	0.3944	0.1972	0.1972	0.00E+00	0.00E+00	0.8067	4.8390	0.2121	1.1402	0.5387	7.9065	4.3880	13.3743
2	90	0.23622	0.0000	3.0000	0.0000	0.0438	0.0000	0.1315	0.0000	0.3944	0.0000	0.3944	0.00E+00	0.00E+00	1.1409	5.1732	0.2267	1.2189	0.5759	7.3312	4.0400	12.4458
3	135	0.23622	-2.1213	2.1213	0.0000	0.0438	-0.0930	0.0930	0.0000	0.3944	0.1972	0.1972	0.00E+00	0.00E+00	0.8067	4.8390	0.2121	1.1402	0.5387	7.9065	4.3880	13.3743
4	180	0.23622	-3.0000	0.0000	0.0000	0.0438	-0.1315	0.0000	0.0000	0.3944	0.3944	0.0000	0.00E+00	0.00E+00	0.0000	4.0323	0.1767	0.9501	0.4489	9.6884	5.4660	16.2502
5	225	0.23622	-2.1213	-2.1213	0.0000	0.0438	-0.0930	-0.0930	0.0000	0.3944	0.1972	0.1972	0.00E+00	0.00E+00	-0.8067	4.8390	0.2121	1.1402	0.5387	7.9065	4.3880	13.3743
6	270	0.23622	0.0000	-3.0000	0.0000	0.0438	0.0000	-0.1315	0.0000	0.3944	0.0000	0.3944	0.00E+00	0.00E+00	-1.1409	5.1732	0.2267	1.2189	0.5759	7.3312	4.0400	12.4458
7	315	0.23622	2.1213	-2.1213	0.0000	0.0438	0.0930	-0.0930	0.0000	0.3944	0.1972	0.1972	0.00E+00	0.00E+00	-0.8067	4.8390	0.2121	1.1402	0.5387	7.9065	4.3880	13.3743
8	360	0.23622	3.0000	0.0000	0.0000	0.0438	0.1315	0.0000	0.0000	0.3944	0.3944	0.0000	0.00E+00	0.00E+00	0.0000	4.0323	0.1767	0.9501	0.4489	9.6884	5.4660	16.2502
9						0.0000	0.0000	0.0000	0.0000	0.0000	0.0000	0.0000	0.00E+00	0.00E+00	0.0000	4.0323	0.0000	#DIV/0!	0.0000	9.6884	#DIV/0!	#DIV/0!
10						0.0000	0.0000	0.0000	0.0000	0.0000	0.0000	0.0000	0.00E+00	0.00E+00	0.0000	4.0323	0.0000	#DIV/0!	0.0000	9.6884	#DIV/0!	#DIV/0!
11						0.0000	0.0000	0.0000	0.0000	0.0000	0.0000	0.0000	0.00E+00	0.00E+00	0.0000	4.0323	0.0000	#DIV/0!	0.0000	9.6884	#DIV/0!	#DIV/0!
12						0.0000	0.0000	0.0000	0.0000	0.0000	0.0000	0.0000	0.00E+00	0.00E+00	0.0000	4.0323	0.0000	#DIV/0!	0.0000	9.6884	#DIV/0!	#DIV/0!
13						0.0000	0.0000	0.0000	0.0000	0.0000	0.0000	0.0000	0.00E+00	0.00E+00	0.0000	4.0323	0.0000	#DIV/0!	0.0000	9.6884	#DIV/0!	#DIV/0!
14						0.0000	0.0000	0.0000	0.0000	0.0000	0.0000	0.0000	0.00E+00	0.00E+00	0.0000	4.0323	0.0000	#DIV/0!	0.0000	9.6884	#DIV/0!	#DIV/0!
15						0.0000	0.0000	0.0000	0.0000	0.0000	0.0000	0.0000	0.00E+00	0.00E+00	0.0000	4.0323	0.0000	#DIV/0!	0.0000	9.6884	#DIV/0!	#DIV/0!
16						0.0000	0.0000	0.0000	0.0000	0.0000	0.0000	0.0000	0.00E+00	0.00E+00	0.0000	4.0323	0.0000	#DIV/0!	0.0000	9.6884	#DIV/0!	#DIV/0!
17						0.0000	0.0000	0.0000	0.0000	0.0000	0.0000	0.0000	0.00E+00	0.00E+00	0.0000	4.0323	0.0000	#DIV/0!	0.0000	9.6884	#DIV/0!	#DIV/0!
18						0.0000	0.0000	0.0000	0.0000	0.0000	0.0000	0.0000	0.00E+00	0.00E+00	0.0000	4.0323	0.0000	#DIV/0!	0.0000	9.6884	#DIV/0!	#DIV/0!
19						0.0000	0.0000	0.0000	0.0000	0.0000	0.0000	0.0000	0.00E+00	0.00E+00	0.0000	4.0323	0.0000	#DIV/0!	0.0000	9.6884	#DIV/0!	#DIV/0!
20						0.0000	0.0000	0.0000	0.0000	0.0000	0.0000	0.0000	0.00E+00	0.00E+00	0.0000	4.0323	0.0000	#DIV/0!	0.0000	9.6884	#DIV/0!	#DIV/0!
Σ					0	0.3506	0.0000	0.0000	0.0000	3.1554	1.5777	1.5777										

$\bar{x}$	$\bar{y}$	$\bar{z}$	M_x	M_y	M_z
0.0000	0.0000	0.0000	600	0	0

t set screws go into	Edge Dist	Number of screws	inertial concerned weight	Max G's	Concerned Drag	$f_{t,pressure}$	
in	in		lbs	G's	lbs	ksi	
0.787402	0.25	8	0	0	0	4.032266	0

Air Brakes Bulkheads

Forces on Plate						
P_x =	0.000	lbs		Px =	3.000	in
P_y =	0.000	lbs		Py Location =	3.000	in
P_z =	35.000	lbs		P_z Location	0	in
Chamber Pressure		psi	Plate Thickness =		0.75	in
EA of Bulkhead		in^2				

Birch Plywood Plate		
F_{tu} =	5.030	ksi
F_{su} =	2.902	ksi
F_{bru} of wood =	16.389	ksi

Bolt		
F_{tu} =	74.694	ksi
F_{su} =	43.099	ksi
Bolt Size		

NO	θ	D_i	x_i	y_i	z_i	A_i	Ax_i	Ay_i	Az_i	J_{xyi}	J_{xxi}	J_{yyi}	τ_{xi}	τ_{yi}	τ_{zi}	τ_{Ri}	S_i	f_b	f_{bTO}	MS_{shear}	$MS_{shear\ TO}$	MS_{bear}
	deg	in	in	in	in	in^2	in^3	in^3	in^3	in^4	in^4	in^4	ksi	ksi	ksi	ksi	Kips	ksi	ksi			
1	45	0.23622	1.9445	1.9445	0.0000	0.0438	0.0852	0.0852	0.0000	0.3314	0.1657	0.1657	0.0000	0.0000	0.4079	0.4079	0.0179	0.0961	0.0303	104.6715	94.8898	169.5439
2	90	0.23622	0.0000	2.7500	0.0000	0.0438	0.0000	0.1205	0.0000	0.3314	0.0000	0.3314	0.0000	0.0000	0.3176	0.3176	0.0139	0.0748	0.0236	134.6856	122.1255	217.9839
3	135	0.23622	-1.9445	1.9445	0.0000	0.0438	-0.0852	0.0852	0.0000	0.3314	0.1657	0.1657	0.0000	0.0000	0.0998	0.0998	0.0044	0.0235	0.0074	430.7268	390.7631	695.7670
4	180	0.23622	-2.7500	0.0000	0.0000	0.0438	-0.1205	0.0000	0.0000	0.3314	0.3314	0.0000	0.0000	0.0000	-0.1180	0.1180	0.0052	0.0278	0.0088	364.3073	330.4918	588.5721
5	225	0.23622	-1.9445	-1.9445	0.0000	0.0438	-0.0852	-0.0852	0.0000	0.3314	0.1657	0.1657	0.0000	0.0000	-0.2082	0.2082	0.0091	0.0491	0.0155	206.0079	186.8458	333.0916
6	270	0.23622	0.0000	-2.7500	0.0000	0.0438	0.0000	-0.1205	0.0000	0.3314	0.0000	0.3314	0.0000	0.0000	-0.1180	0.1180	0.0052	0.0278	0.0088	364.3073	330.4918	588.5721
7	315	0.23622	1.9445	-1.9445	0.0000	0.0438	0.0852	-0.0852	0.0000	0.3314	0.1657	0.1657	0.0000	0.0000	0.0998	0.0998	0.0044	0.0235	0.0074	430.7268	390.7631	695.7670
8	360	0.23622	2.7500	0.0000	0.0000	0.0438	0.1205	0.0000	0.0000	0.3314	0.3314	0.0000	0.0000	0.0000	0.3176	0.3176	0.0139	0.0748	0.0236	134.6856	122.1255	217.9839
9						0.0000	0.0000	0.0000	0.0000	0.0000	0.0000	0.0000	0.0000	0.0000	0.0998	0.0998	0.0000	#DIV/0!	0.0000	430.7268	#DIV/0!	#DIV/0!
10						0.0000	0.0000	0.0000	0.0000	0.0000	0.0000	0.0000	0.0000	0.0000	0.0998	0.0998	0.0000	#DIV/0!	0.0000	430.7268	#DIV/0!	#DIV/0!
11						0.0000	0.0000	0.0000	0.0000	0.0000	0.0000	0.0000	0.0000	0.0000	0.0998	0.0998	0.0000	#DIV/0!	0.0000	430.7268	#DIV/0!	#DIV/0!
12						0.0000	0.0000	0.0000	0.0000	0.0000	0.0000	0.0000	0.0000	0.0000	0.0998	0.0998	0.0000	#DIV/0!	0.0000	430.7268	#DIV/0!	#DIV/0!
13						0.0000	0.0000	0.0000	0.0000	0.0000	0.0000	0.0000	0.0000	0.0000	0.0998	0.0998	0.0000	#DIV/0!	0.0000	430.7268	#DIV/0!	#DIV/0!
14						0.0000	0.0000	0.0000	0.0000	0.0000	0.0000	0.0000	0.0000	0.0000	0.0998	0.0998	0.0000	#DIV/0!	0.0000	430.7268	#DIV/0!	#DIV/0!
15						0.0000	0.0000	0.0000	0.0000	0.0000	0.0000	0.0000	0.0000	0.0000	0.0998	0.0998	0.0000	#DIV/0!	0.0000	430.7268	#DIV/0!	#DIV/0!
16						0.0000	0.0000	0.0000	0.0000	0.0000	0.0000	0.0000	0.0000	0.0000	0.0998	0.0998	0.0000	#DIV/0!	0.0000	430.7268	#DIV/0!	#DIV/0!
17						0.0000	0.0000	0.0000	0.0000	0.0000	0.0000	0.0000	0.0000	0.0000	0.0998	0.0998	0.0000	#DIV/0!	0.0000	430.7268	#DIV/0!	#DIV/0!
18						0.0000	0.0000	0.0000	0.0000	0.0000	0.0000	0.0000	0.0000	0.0000	0.0998	0.0998	0.0000	#DIV/0!	0.0000	430.7268	#DIV/0!	#DIV/0!
19						0.0000	0.0000	0.0000	0.0000	0.0000	0.0000	0.0000	0.0000	0.0000	0.0998	0.0998	0.0000	#DIV/0!	0.0000	430.7268	#DIV/0!	#DIV/0!
20						0.0000	0.0000	0.0000	0.0000	0.0000	0.0000	0.0000	0.0000	0.0000	0.0998	0.0998	0.0000	#DIV/0!	0.0000	430.7268	#DIV/0!	#DIV/0!
Σ					0.0000	0.3506	0.0000	0.0000	0.0000	2.6514	1.3257	1.3257										

$\bar{x}$	$\bar{y}$	$\bar{z}$	M_x	M_y	M_z
0.0000	0.0000	0.0000	105	-105	0

t set screws go into	Edge Dist	Number of screws	Inertial concerned weight	Max G's	Concerned Drag	$f_{t\ pressure}$
in	in		lbs	G's	lbs	ksi
0.787402	0.375	8	0	0	0	0

Appendix E: Launch Vehicle Drift Results

Wind Speed: 5 mph Direction: Downwind			Wind Speed: 10 mph Direction: Downwind			Wind Speed: 15 mph Direction: Downwind			Wind Speed: 20 mph Direction: Downwind		
Time (s)	Altitude (ft)	Lateral distance (ft)	Time (s)	Altitude (ft)	Lateral distance (ft)	Time (s)	Altitude (ft)	Lateral distance (ft)	Time (s)	Altitude (ft)	Lateral distance (ft)
0	0	0	0	0	0	0	0	0	0	0	0
0.01	0.0024419	2.14E-04	0.01	0.0024419	2.14E-04	0.01	0.0024419	2.14E-04	0.01	0.0024419	2.14E-04
0.02	0.016505	0.001444	0.02	0.016505	0.001444	0.02	0.016505	0.001444	0.02	0.016505	0.001444
0.03	0.053223	0.0046564	0.03	0.053223	0.0046564	0.03	0.053223	0.0046564	0.03	0.053223	0.0046564
0.04	0.11908	0.010418	0.04	0.11908	0.010418	0.04	0.11908	0.010418	0.04	0.11908	0.010418
0.05	0.21746	0.019025	0.05	0.21746	0.019025	0.05	0.21746	0.019025	0.05	0.21746	0.019025
0.06	0.35005	0.030626	0.06	0.35006	0.030626	0.06	0.35006	0.030626	0.06	0.35006	0.030626
0.07	0.51741	0.045268	0.07	0.51741	0.045268	0.07	0.51742	0.045268	0.07	0.51742	0.045268
0.08	0.71963	0.06296	0.08	0.71964	0.06296	0.08	0.71964	0.062961	0.08	0.71964	0.062961
0.09	0.95683	0.083712	0.09	0.95683	0.083712	0.09	0.95684	0.083713	0.09	0.95685	0.083713
0.1	1.2291	0.10753	0.1	1.2291	0.10753	0.1	1.2291	0.10753	0.1	1.2291	0.10753
0.11	1.5365	0.13443	0.11	1.5365	0.13443	0.11	1.5366	0.13443	0.11	1.5366	0.13443
0.12	1.8791	0.1644	0.12	1.8791	0.1644	0.12	1.8792	0.1644	0.12	1.8792	0.16441
0.13	2.2569	0.19745	0.13	2.2569	0.19745	0.13	2.2569	0.19746	0.13	2.2569	0.19746
0.14	2.6698	0.23358	0.14	2.6698	0.23358	0.14	2.6699	0.23358	0.14	2.6699	0.23358
0.15	3.1179	0.27278	0.15	3.1179	0.27278	0.15	3.1179	0.27278	0.15	3.118	0.27279
0.16	3.6011	0.31506	0.16	3.601	0.31505	0.16	3.6011	0.31506	0.16	3.6012	0.31506
0.17	4.1193	0.3604	0.17	4.1193	0.36039	0.17	4.1194	0.3604	0.17	4.1194	0.3604
0.18	4.6725	0.40879	0.18	4.6724	0.40879	0.18	4.6725	0.40879	0.18	4.6726	0.4088
0.19	5.2606	0.46024	0.19	5.2605	0.46023	0.19	5.2606	0.46024	0.19	5.2606	0.46024
0.2	5.8834	0.51473	0.2	5.8833	0.51472	0.2	5.8834	0.51473	0.2	5.8834	0.51473
0.21	6.5409	0.57226	0.21	6.5407	0.57224	0.21	6.5408	0.57225	0.21	6.5408	0.57225
0.22	7.233	0.6328	0.22	7.2327	0.63278	0.22	7.2328	0.63279	0.22	7.2329	0.63279
0.23	7.9595	0.69637	0.23	7.9592	0.69634	0.23	7.9593	0.69635	0.23	7.9593	0.69635
0.24	8.7204	0.76294	0.24	8.7201	0.76291	0.24	8.7201	0.76291	0.24	8.7202	0.76291
0.25	9.5156	0.83251	0.25	9.5152	0.83247	0.25	9.5152	0.83247	0.25	9.5153	0.83248
0.26	10.345	0.90507	0.26	10.345	0.90503	0.26	10.345	0.90503	0.26	10.345	0.90503
0.275	11.654	1.02	0.275	11.653	1.02	0.275	11.653	1.0204	0.275	11.653	1.0204
0.2975	13.762	1.2065	0.2975	13.761	1.207	0.2975	13.761	1.2095	0.2975	13.761	1.2095
0.33125	17.255	1.5188	0.33125	17.254	1.5204	0.33125	17.253	1.5293	0.33125	17.253	1.5302
0.38125	23.174	2.0542	0.38125	23.172	2.0592	0.38125	23.168	2.0835	0.38125	23.167	2.0874
0.43125	30.009	2.6793	0.43125	30.006	2.6903	0.43125	29.998	2.7374	0.43125	29.998	2.7448
0.48125	37.806	3.3971	0.48125	37.801	3.4178	0.48125	37.789	3.494	0.48125	37.787	3.5065
0.53125	46.609	4.2111	0.53125	46.602	4.245	0.53125	46.585	4.3544	0.53125	46.583	4.3747
0.58125	56.46	5.1235	0.58125	56.45	5.1736	0.58125	56.428	5.3157	0.58125	56.423	5.3491
0.63125	67.388	6.1352	0.63125	67.375	6.2027	0.63125	67.348	6.3717	0.63125	67.341	6.4274
0.68125	79.41	7.2448	0.68125	79.394	7.3283	0.68125	79.362	7.5152	0.68125	79.35	7.6062
0.73125	92.529	8.4497	0.73125	92.51	8.5438	0.73125	92.476	8.7352	0.73125	92.458	8.8738
0.78125	106.75	9.7467	0.78125	106.73	9.8422	0.78125	106.69	10.021	0.78125	106.67	10.212
0.83125	122.08	11.132	0.83125	122.06	11.214	0.83125	122.02	11.364	0.83125	121.99	11.6
0.88125	138.53	12.599	0.88125	138.51	12.646	0.88125	138.47	12.75	0.88125	138.43	13.015
0.93125	156.09	14.144	0.93125	156.07	14.125	0.93125	156.03	14.162	0.93125	155.98	14.43
0.98125	174.76	15.761	0.98125	174.74	15.638	0.98125	174.71	15.586	0.98125	174.65	15.822
1.0313	194.54	17.442	1.0313	194.53	17.171	1.0313	194.5	17.009	1.0313	194.44	17.169
1.0813	215.43	19.184	1.0813	215.42	18.715	1.0813	215.39	18.419	1.0813	215.32	18.448